Surprises in High-Energy Astroparticle Physics

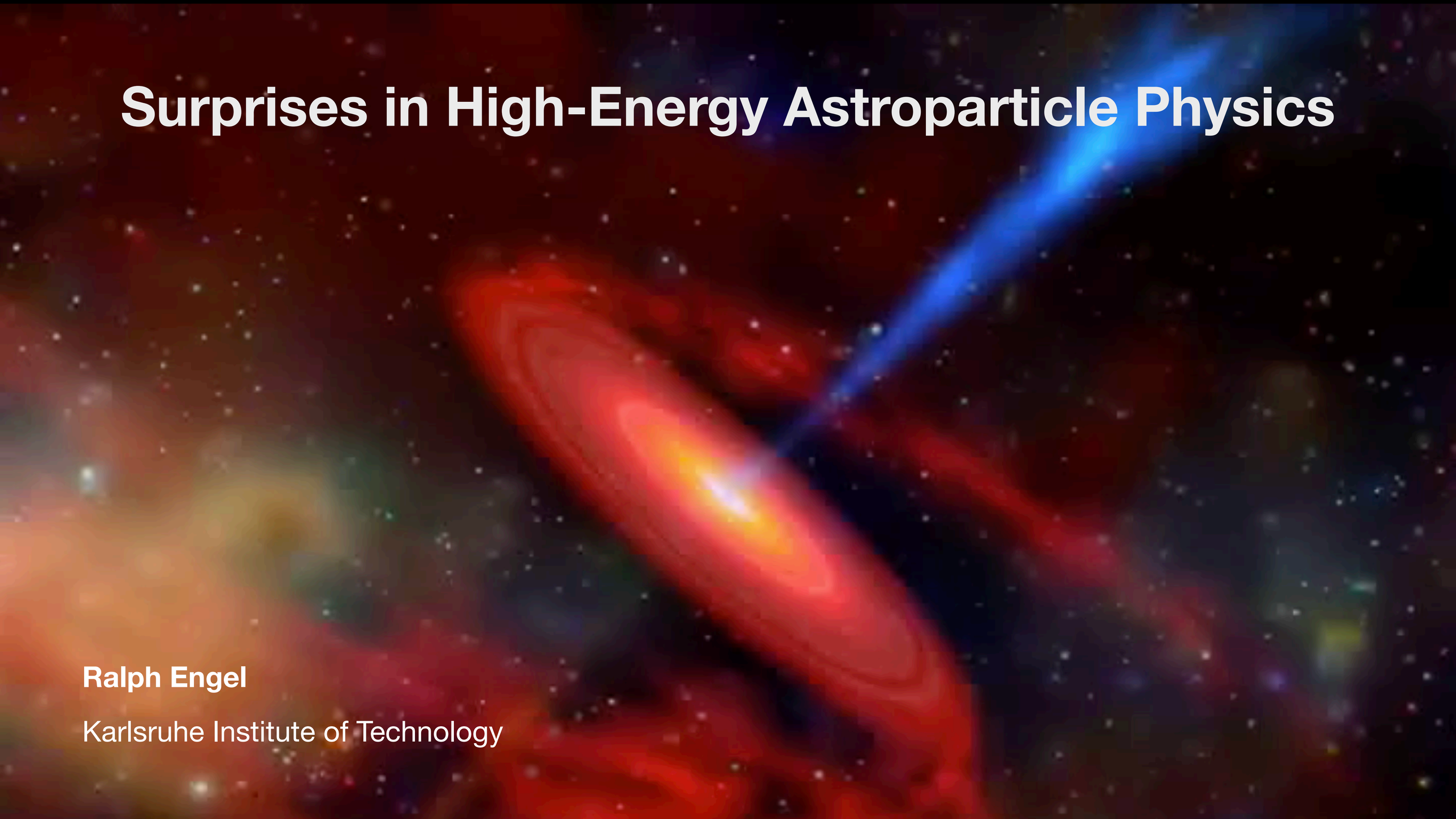

Ralph Engel

Karlsruhe Institute of Technology

Flux of cosmic rays

Mainly nuclei p, He, … Fe

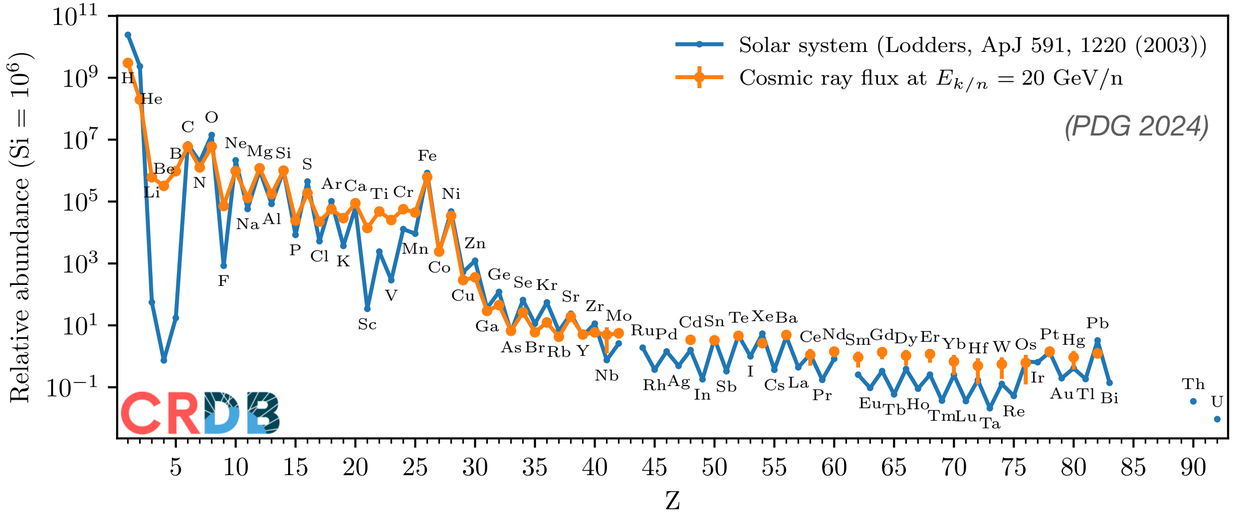

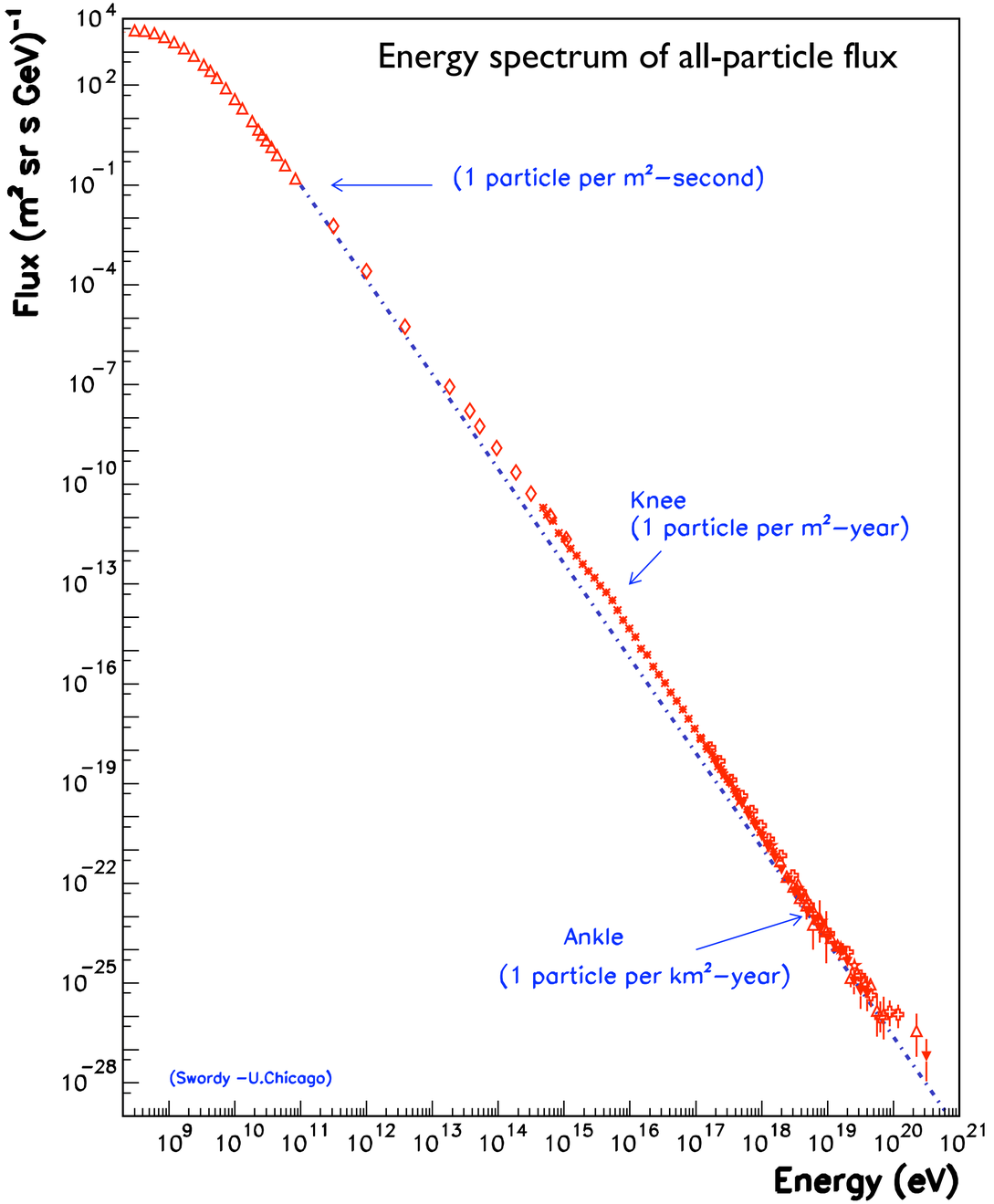

Cosmic ray flux and interaction energies

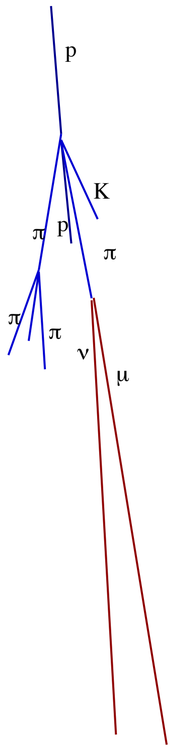

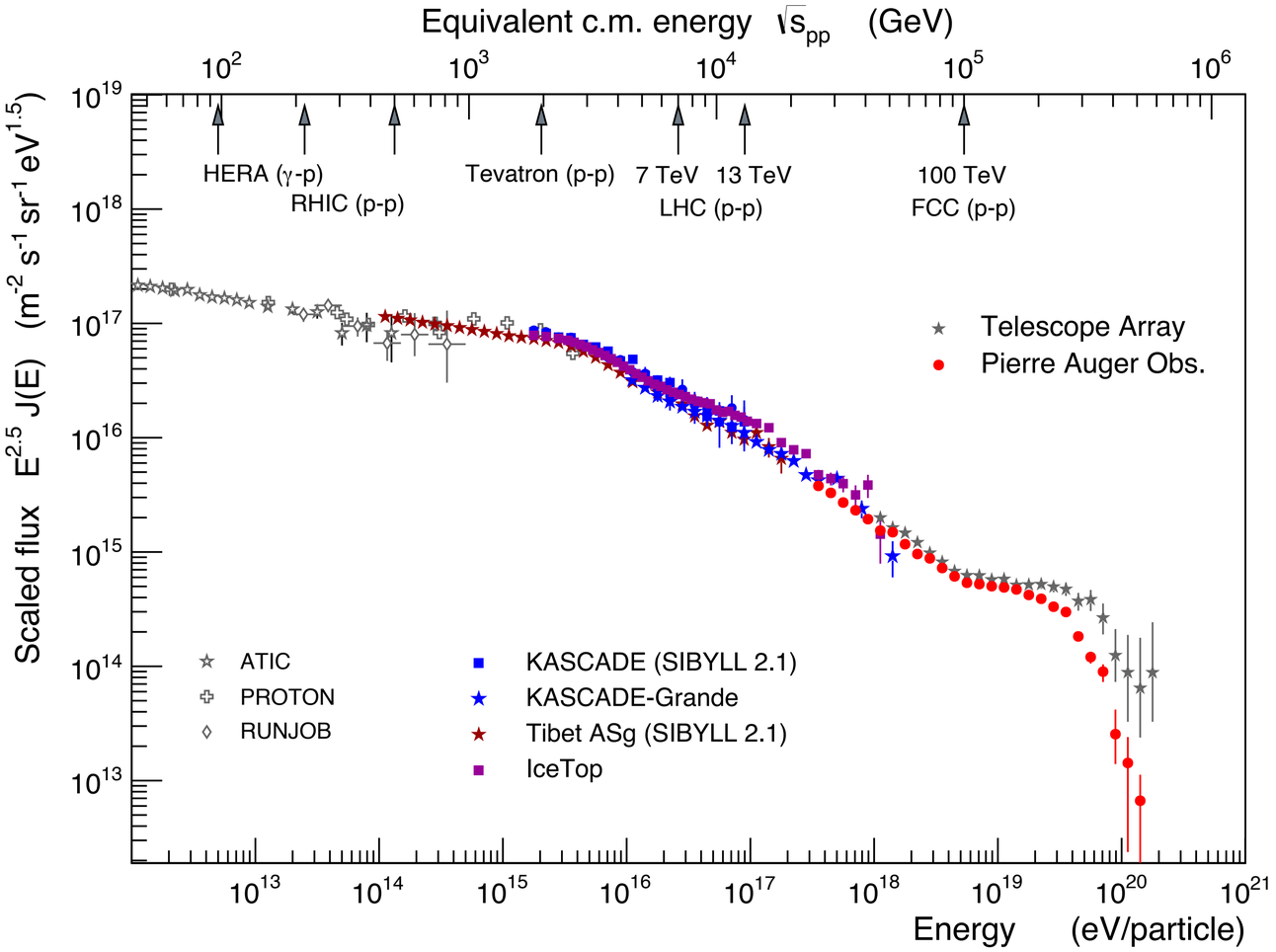

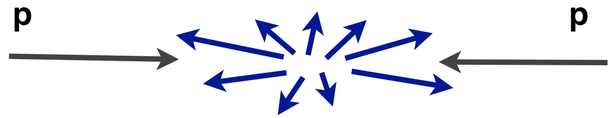

Center-of-mass energy

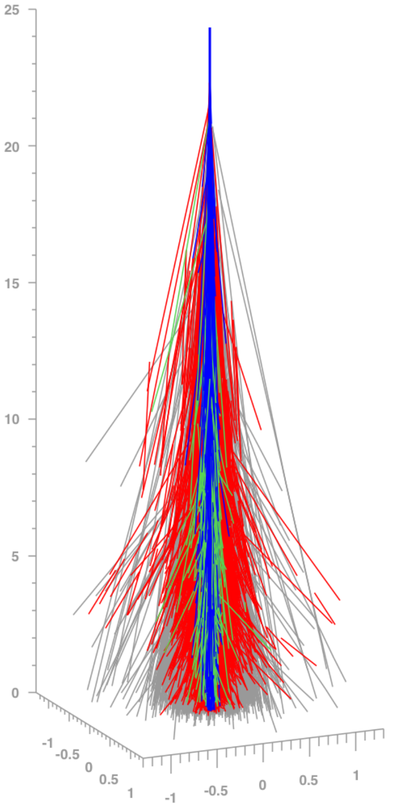

Laboratory energy

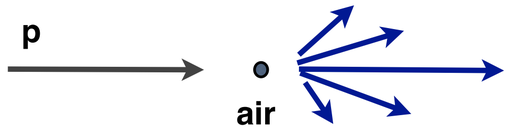

Galactic vs. extragalactic sources

- Galactic magnetic field: ~ 3 μG (3.10^{-10} T)
- Gyroradius:

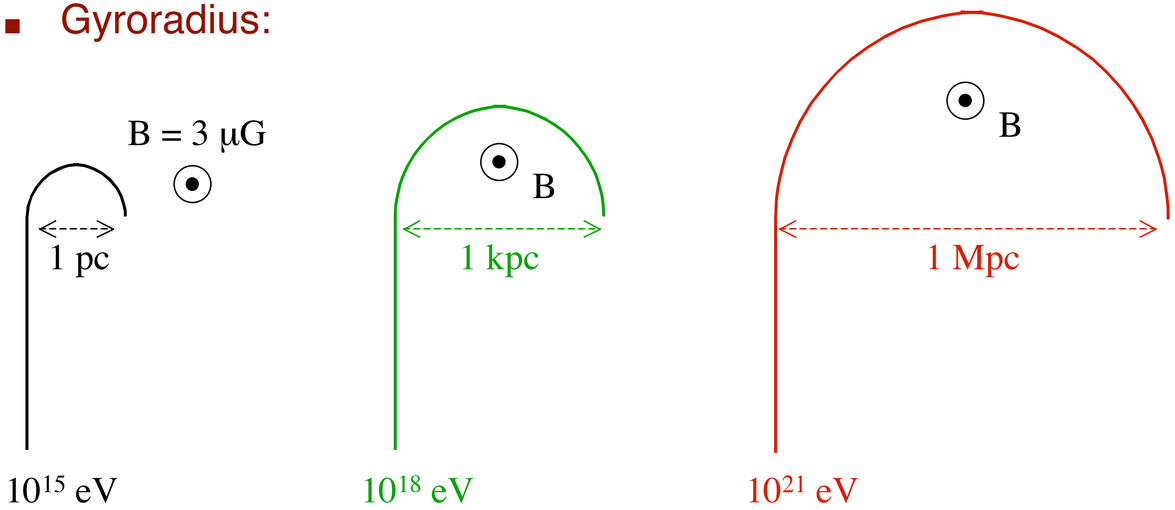

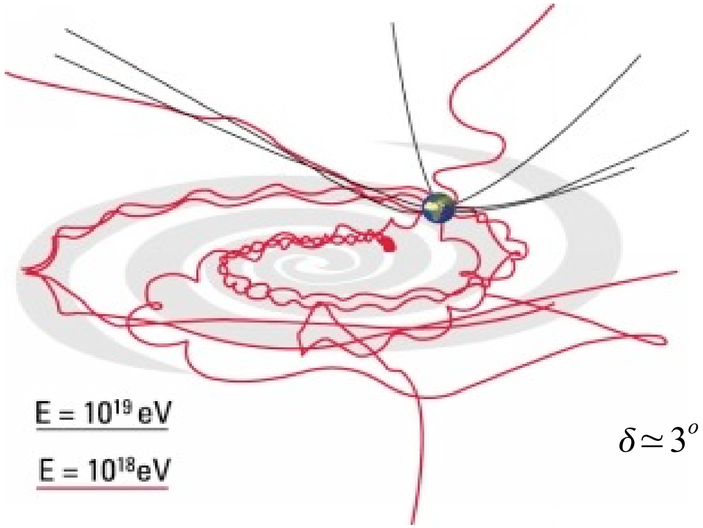

$$\delta \simeq 3^o \frac{B}{3\,\mu G}\frac{L}{kpc}\frac{6\times10^{19}eV}{E/Z}$$

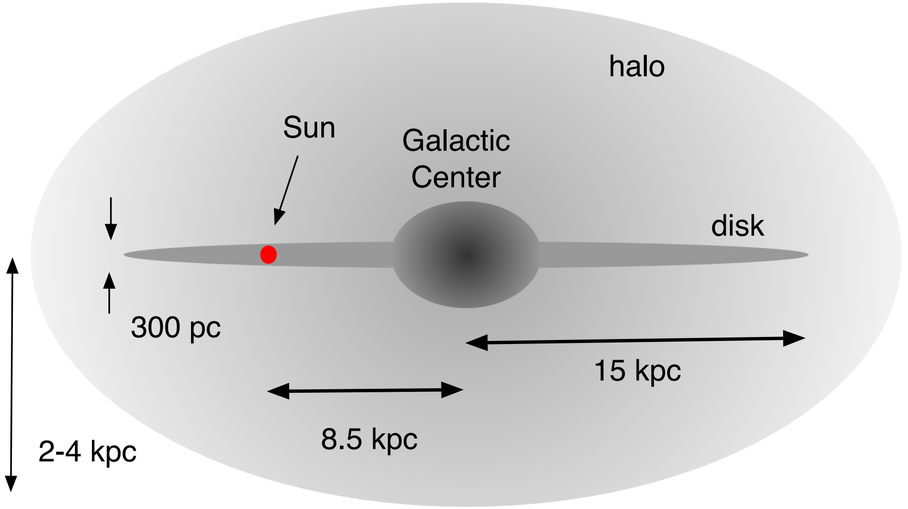

1 pc = 3.26 ly = 3.08 10^{16} m

Ankle as transition region from galactic to extragalactic particles

Over-density of Galactic cosmic rays due to magnetic confinement

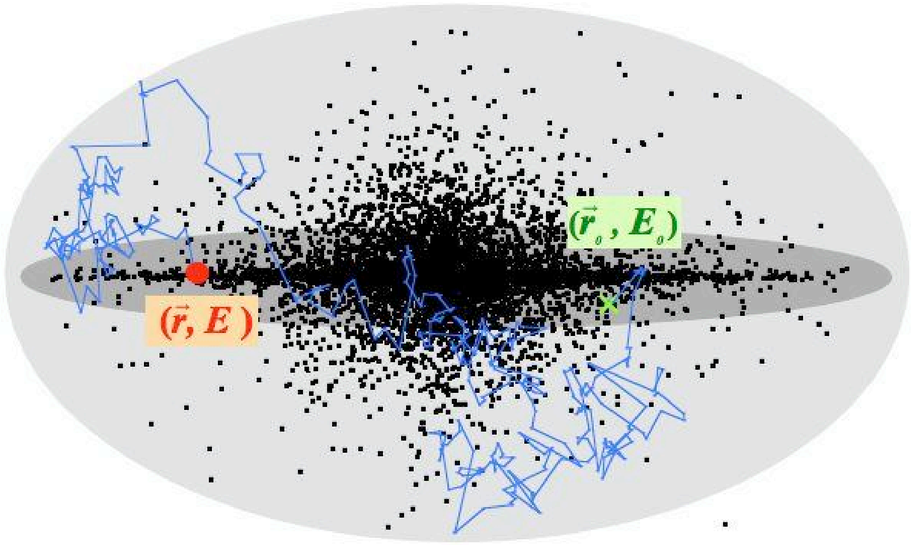

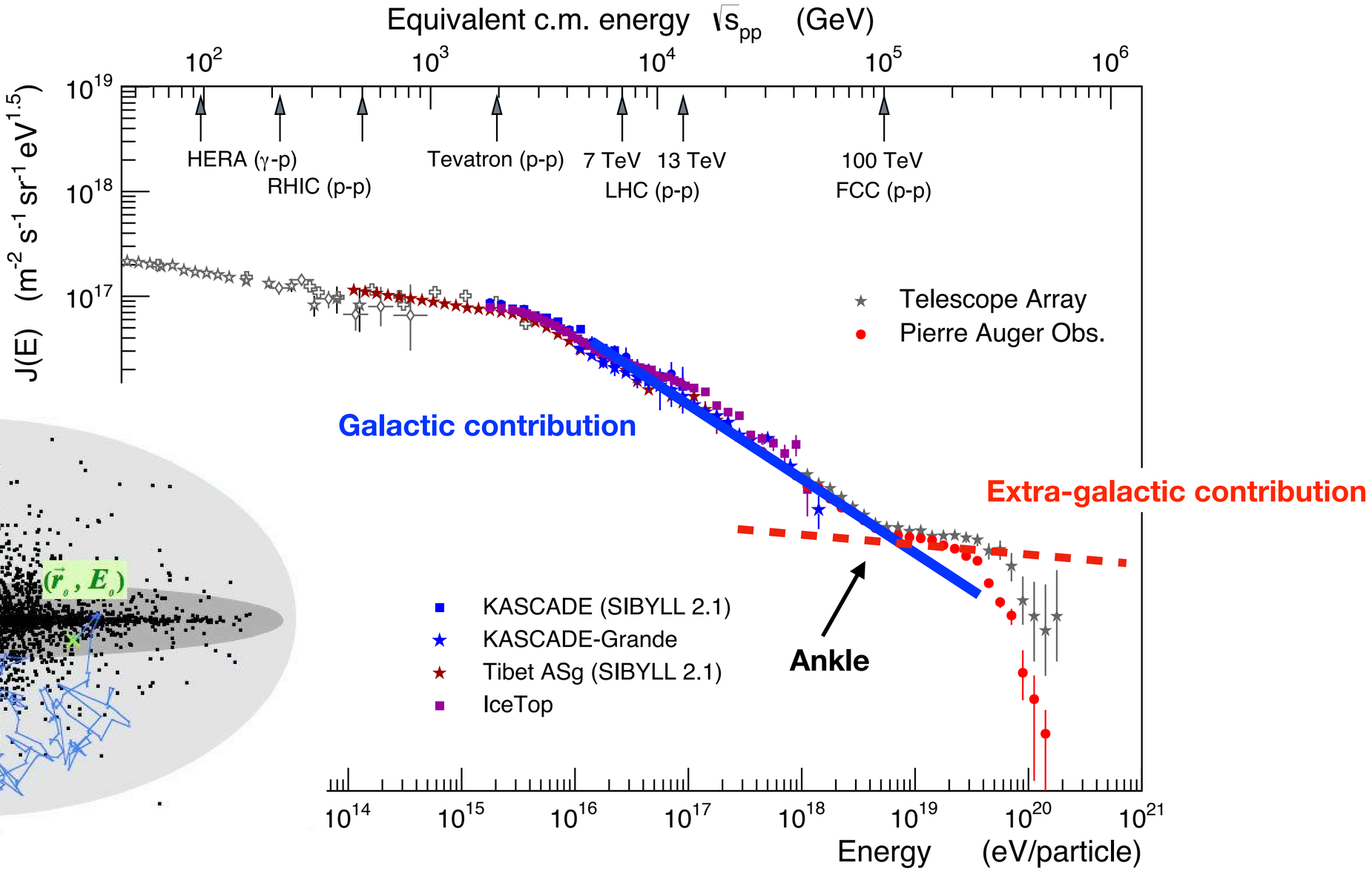

Galactic cosmic ray sources

Fermi's original work: second order acceleration

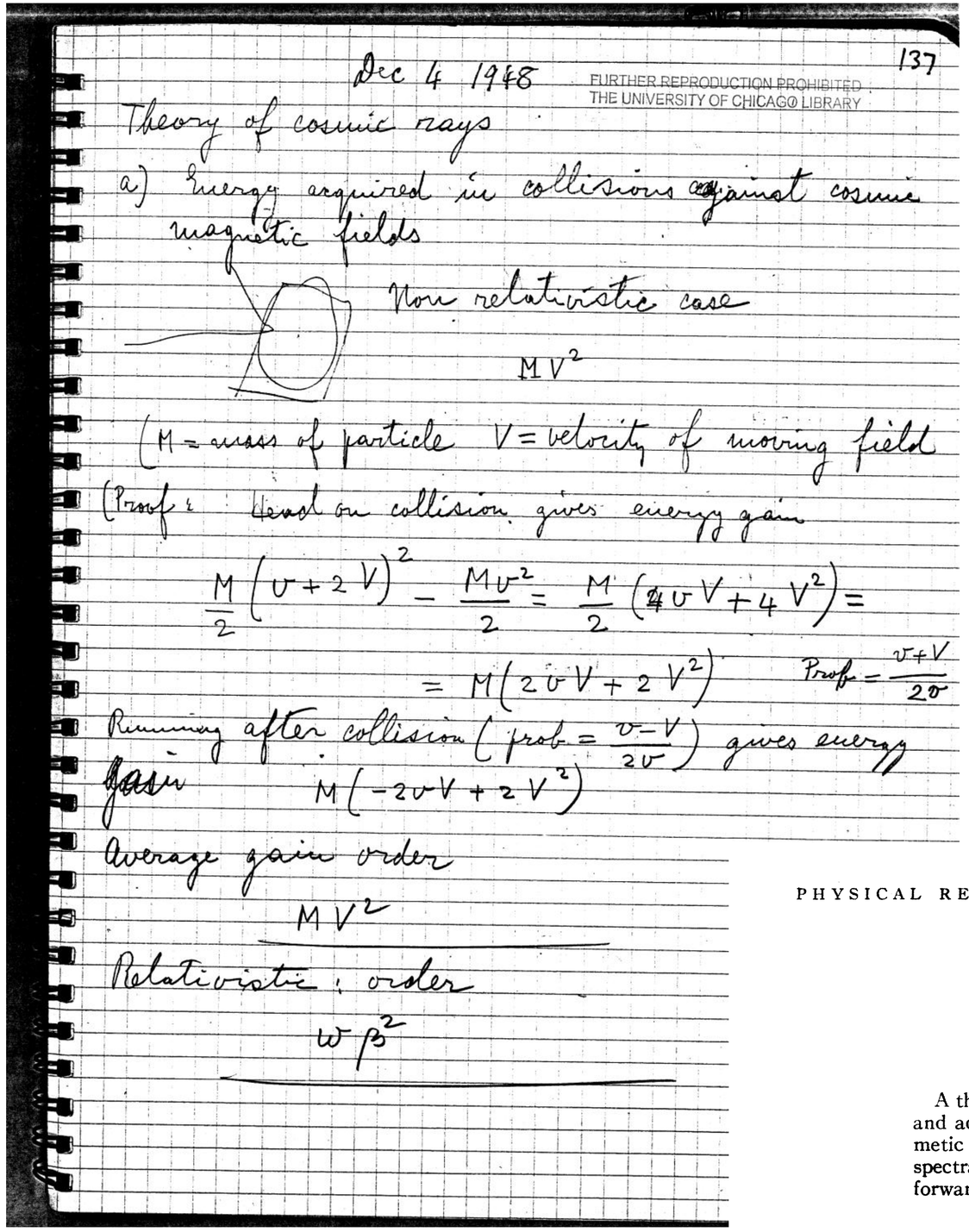
Dec 4 1948 137

FURTHER REPRODUCTION PROHIBITED
THE UNIVERSITY OF CHICAGO LIBRARY

Theory of cosmic rays

a) Energy acquired in collisions against cosmic magnetic fields

Non relativistic case

MV^2

(M = mass of particle V = velocity of moving field

(Proof: Head on collision gives energy gain

$$\frac{M}{2}(v+2V)^2 - \frac{Mv^2}{2} = \frac{M}{2}(4vV+4V^2) =$$

$$= M(2vV+2V^2) \qquad Prob. = \frac{v+V}{2v}$$

Running after collision $(prob. = \frac{v-V}{2v})$ gives energy gain $M(-2vV+2V^2)$

Average gain order

MV^2

Relativistic: order

$w\beta^2$

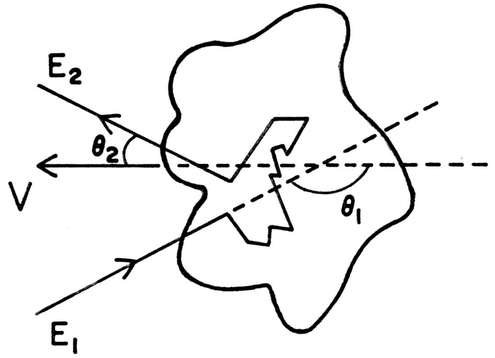

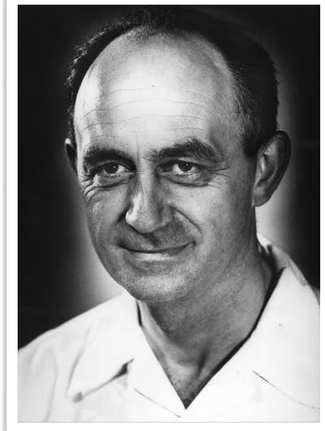

Particles scatter on moving magnetic clouds

PHYSICAL REVIEW VOLUME 75, NUMBER 8 APRIL 15, 1949

On the Origin of the Cosmic Radiation

ENRICO FERMI
Institute for Nuclear Studies, University of Chicago, Chicago, Illinois
(Received January 3, 1949)

A theory of the origin of cosmic radiation is proposed according to which cosmic rays are originated and accelerated primarily in the interstellar space of the galaxy by collisions against moving magnetic fields. One of the features of the theory is that it yields naturally an inverse power law for the spectral distribution of the cosmic rays. The chief difficulty is that it fails to explain in a straightforward way the heavy nuclei observed in the primary radiation.

Fermi acceleration – a simplified view

First order Fermi acceleration at large-scale shock fronts

(shown is second order Fermi acceleration)

$$\frac{\mathrm{d}N_{\mathrm{inj}}}{\mathrm{d}E} \sim E^{-2}$$

Many known accelerators in our Galaxy

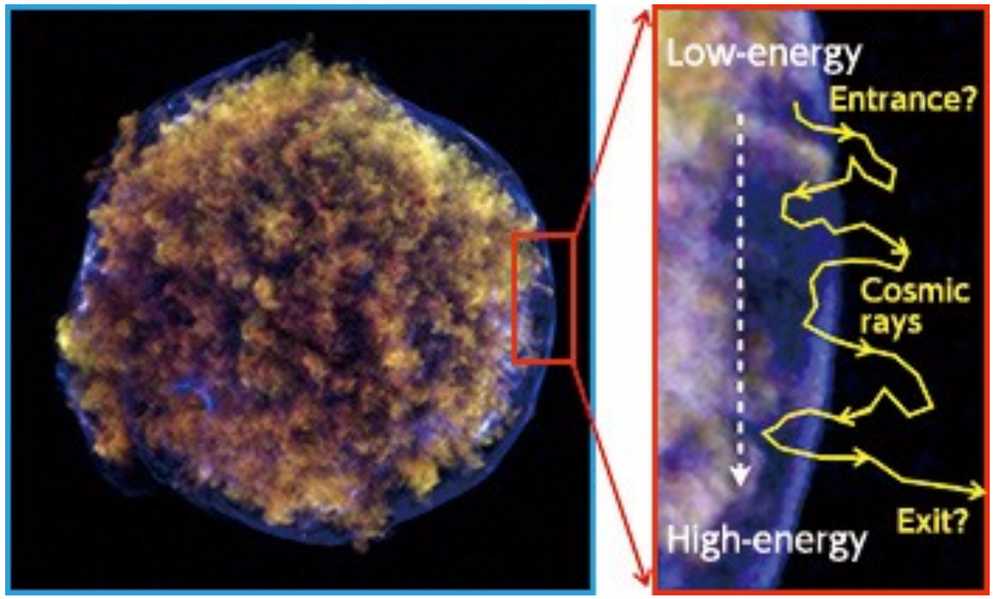

Supernove remnants: Tychos SN 1573

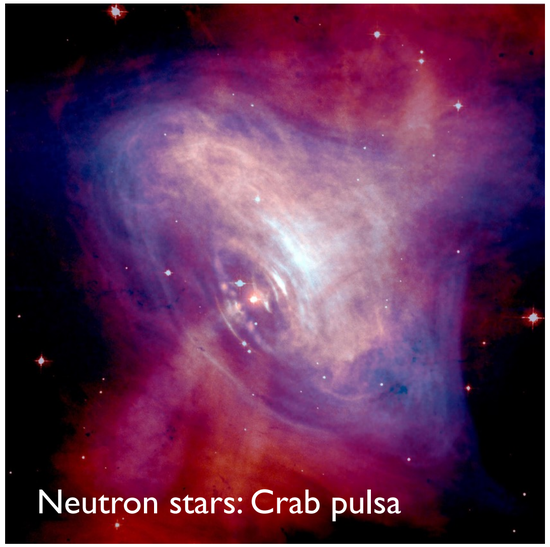

Neutron stars: Crab pulsa

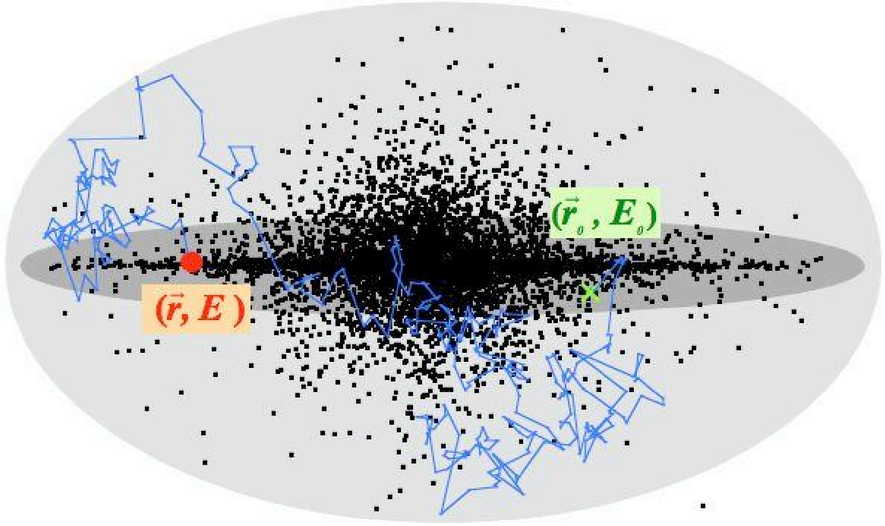

Magnetic confinement in Galaxy

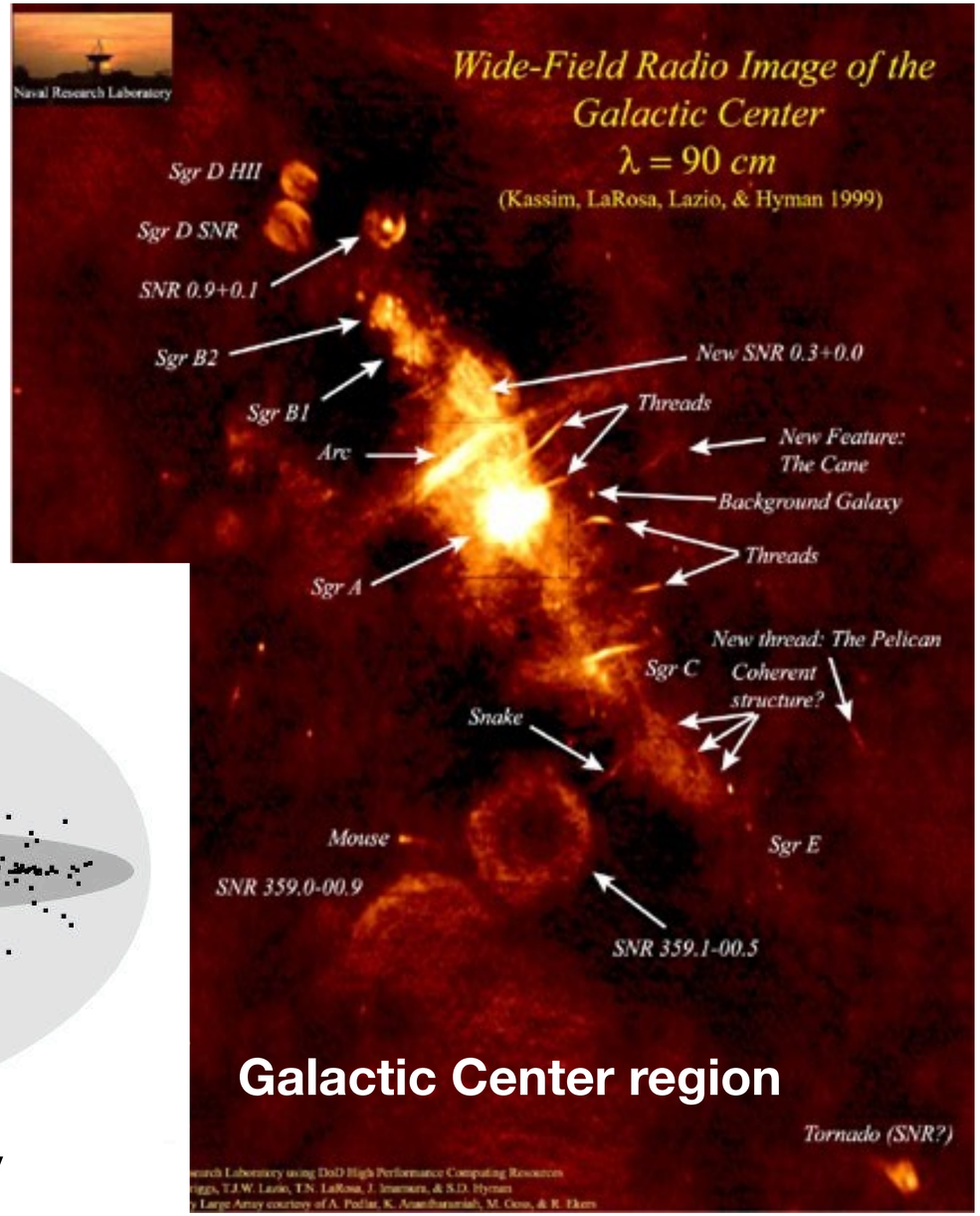

Galactic Center region

Cosmic rays from supernova remnants

COSMIC RAYS FROM SUPER-NOVAE

By W. Baade and F. Zwicky

Mount Wilson Observatory, Carnegie Institution of Washington and California Institute of Technology, Pasadena

Communicated March 19, 1934

A. Introduction.—Two important facts support the view that cosmic rays are of extragalactic origin, if, for the moment, we disregard the possibility that the earth may possess a very high and self-renewing electrostatic potential with respect to interstellar space.

If interest in these questions still prevails at that future time, science will therefore be able to test the correctness of our hypothesis some time during the next thousand years or so, as the occurrence of a super-nova in our own system would multiply the intensity of the cosmic rays by a factor one thousand or more. It also seems quite possible to observe with cosmic-ray electroscopes the flare-up of a super-nova in one of the nearer extragalactic nebulae, as for them $r = 1000\,n$, and

$$\Delta\sigma = 0.01/n^2 \text{ ergs/cm.}^2 \text{ sec.}, \qquad (10)$$

where n is a number of the order one. It might in this connection be of interest to follow up the causes for Regener's[4] curious balloon observation of March 29, 1933.

20 pc

Distance ~ 2.2 kpc

Observed galactic SN explosions:

1604 (Kepler)
1572 (Tycho)
1181 (Chinese astronomers)
1054 (Crab nebula)
1006 (Chinese and Arabian records)

Estimates:

~3 SN explosions / 100 yrs
Kinetic energy of ejecta: ~10^{51} erg

$$P_{\mathrm{SNR}} \approx 10^{42}\mathrm{erg/s}$$

Kinetic energy released in SN explosions

Only 10% of this energy needed for cosmic rays

Possible interpretation of knee in spectrum

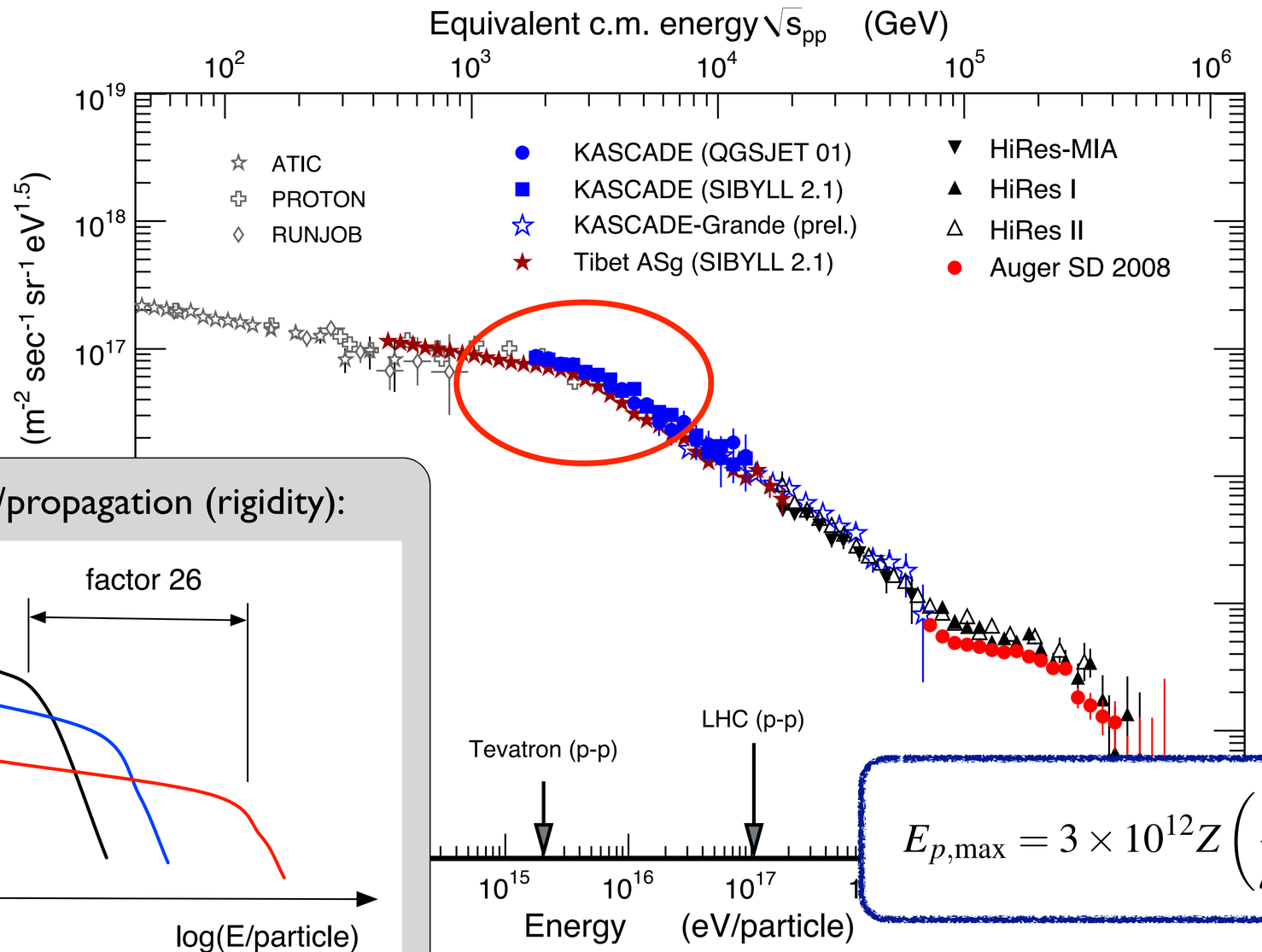

SN remnant 1006

Distance ~ 2.2 kpc

20 pc

Acceleration/propagation (rigidity):

$$E_{p,\max} = 3 \times 10^{12} Z \left(\frac{B}{\mu\mathrm{G}}\right)\left(\frac{u}{1000\,\mathrm{km/s}}\right)\left(\frac{L}{\mathrm{pc}}\right)\ \mathrm{eV}$$

(Lagage & Cesarsky, 1983)

Classic air shower measurement in knee energy region

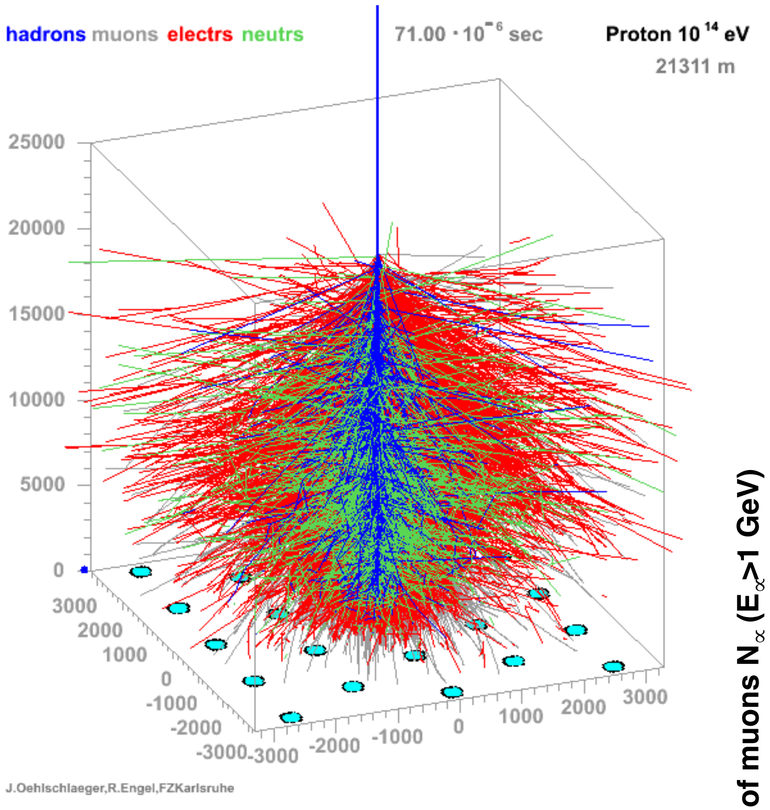

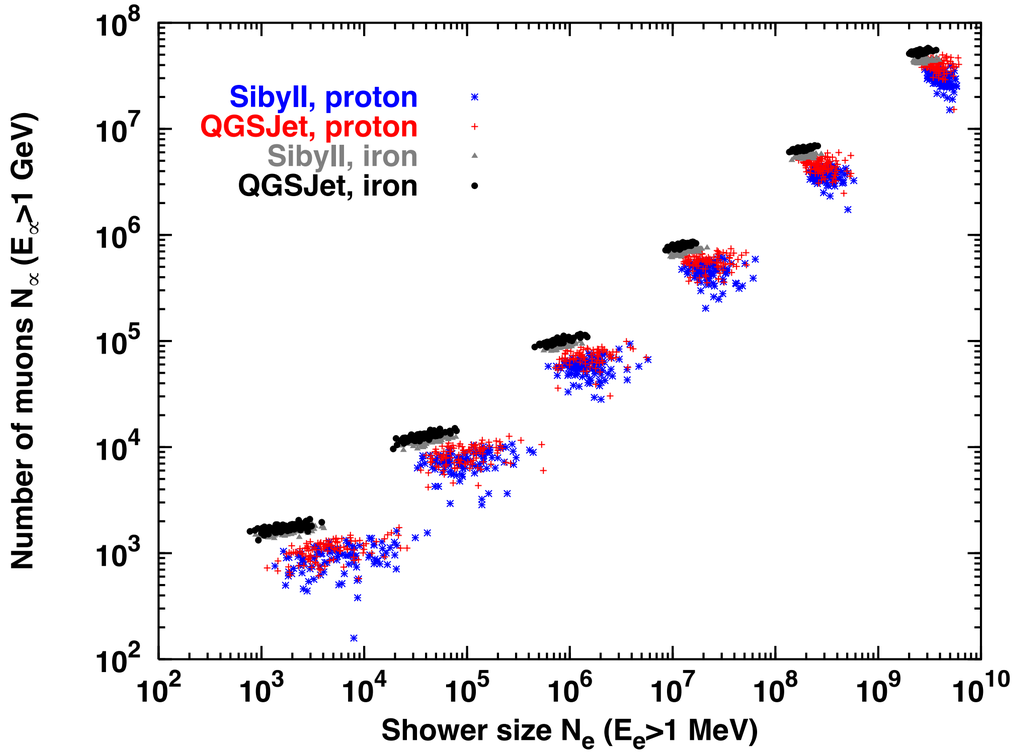

Mass estimate: dependence hadronic interaction model

$$\ln E = a \cdot \ln N_e + b \cdot \ln N_\mu$$

Energy estimate very robust

Mass composition at the knee: KASCADE data

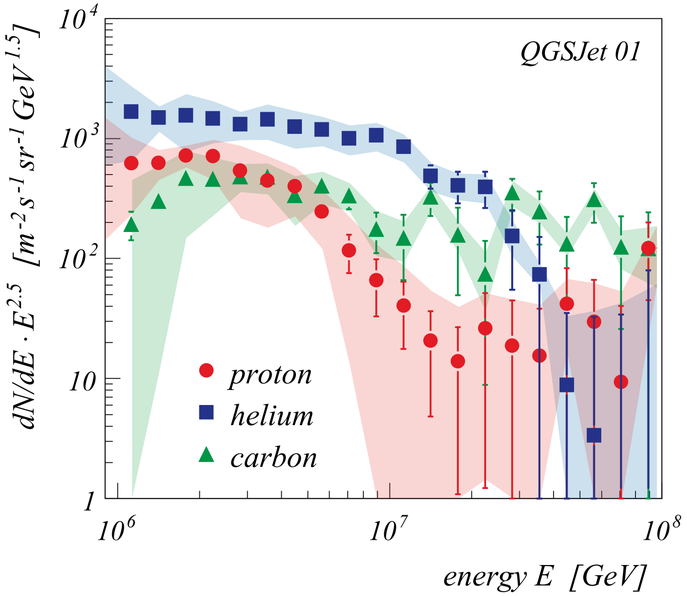

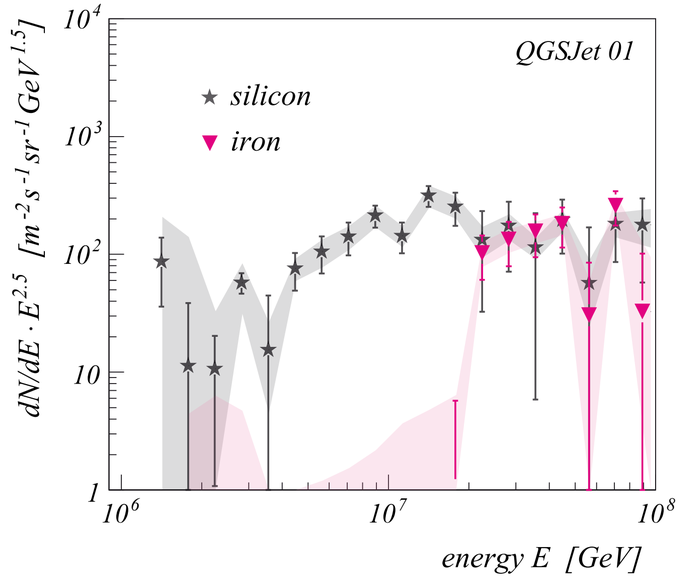

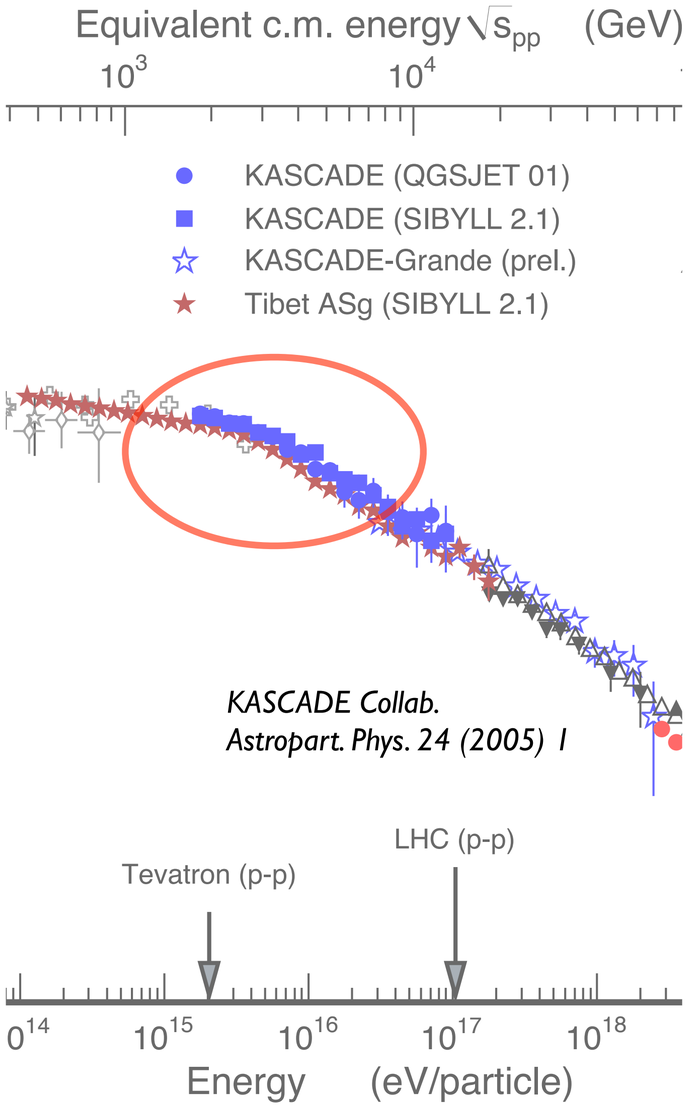

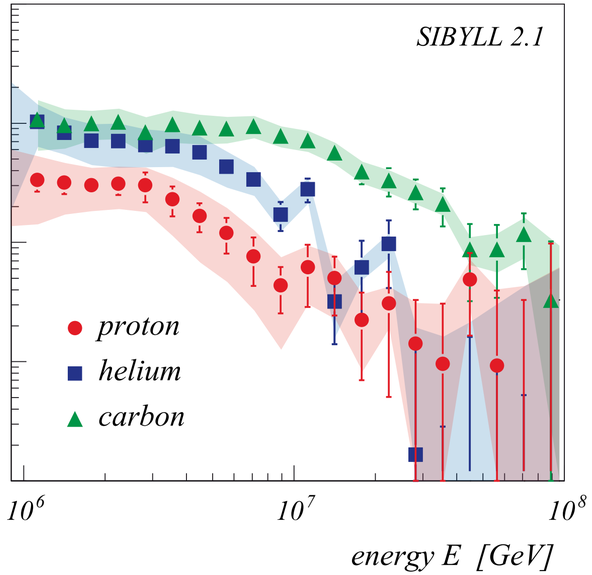

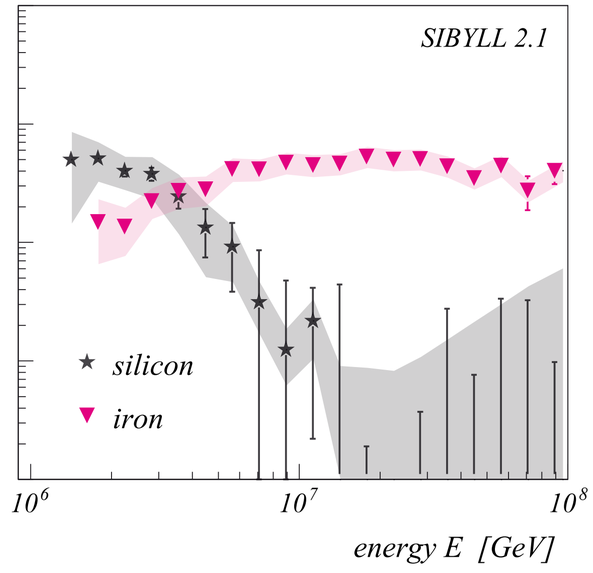

Multi-messenger test of source model

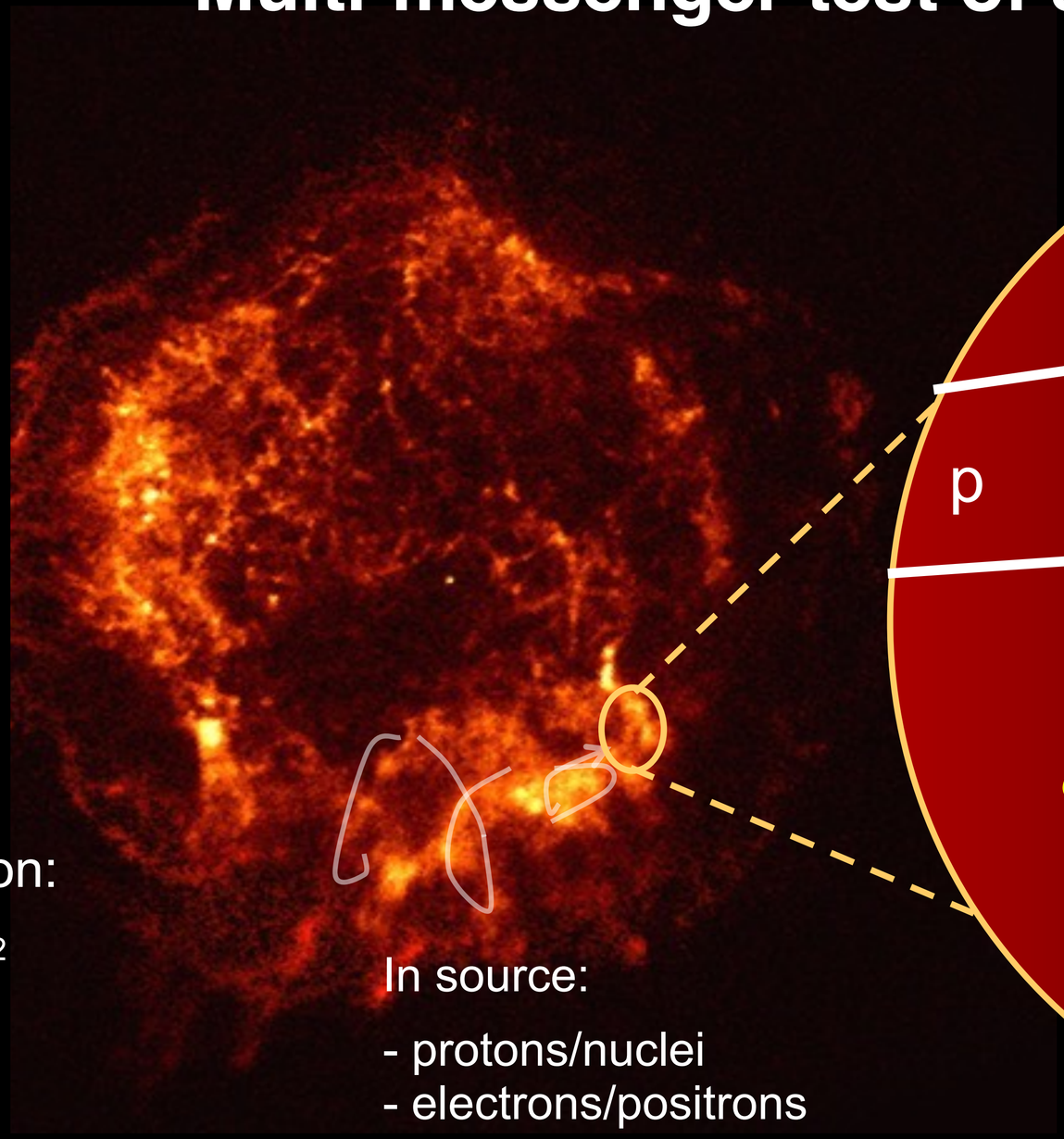

Fermi acceleration:

d*N*/d*E* ~ *E*$^{-2}$

In source:

- protons/nuclei
- electrons/positrons

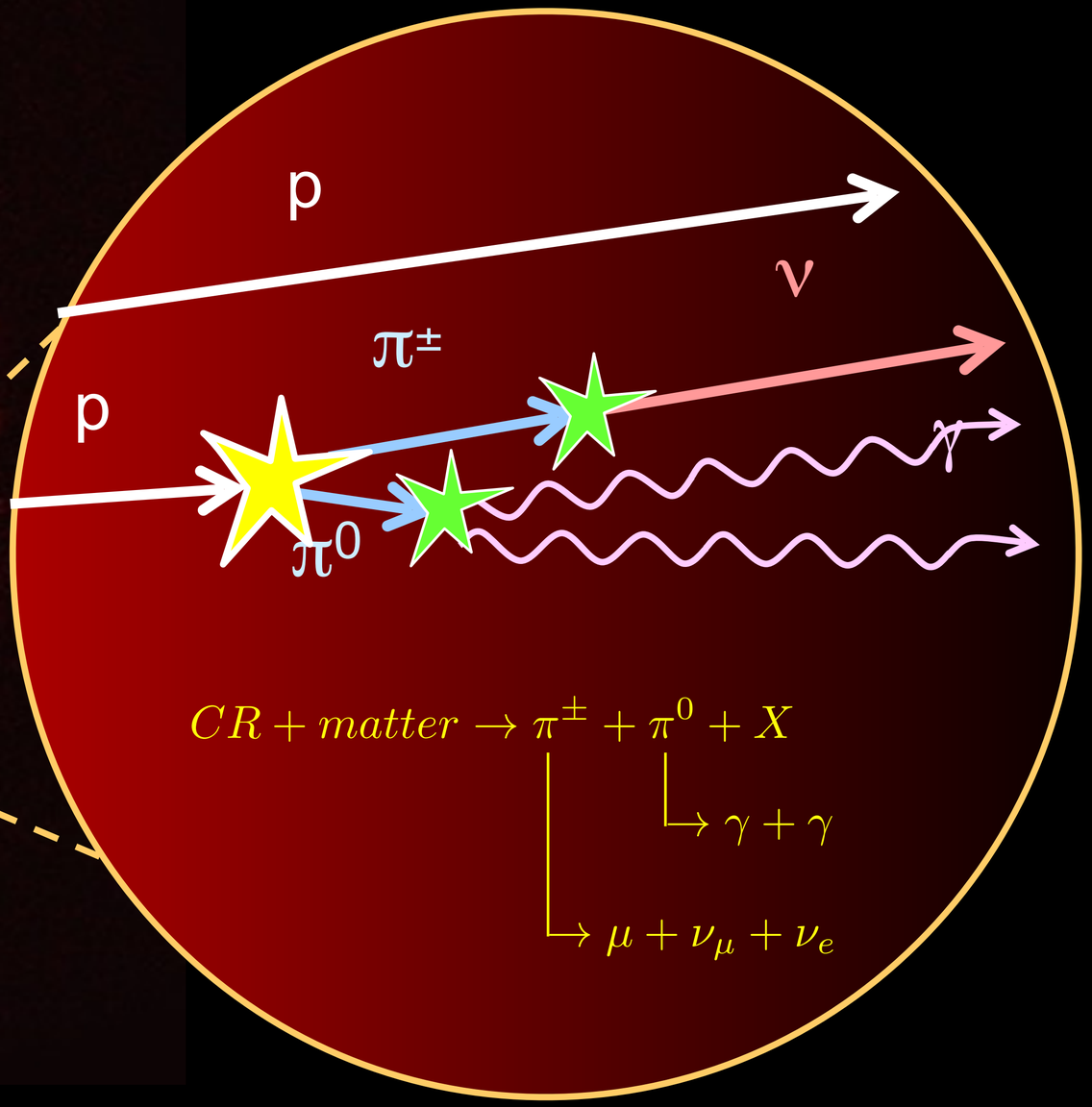

Detection methods

Satellite

Primary particle of

low energy high energy

Extensive Air Shower (EAS) arrays

Cherenkov Telescopes

(slide by Ruben Conceição)


H.E.S.S.


HAWC


MAGIC

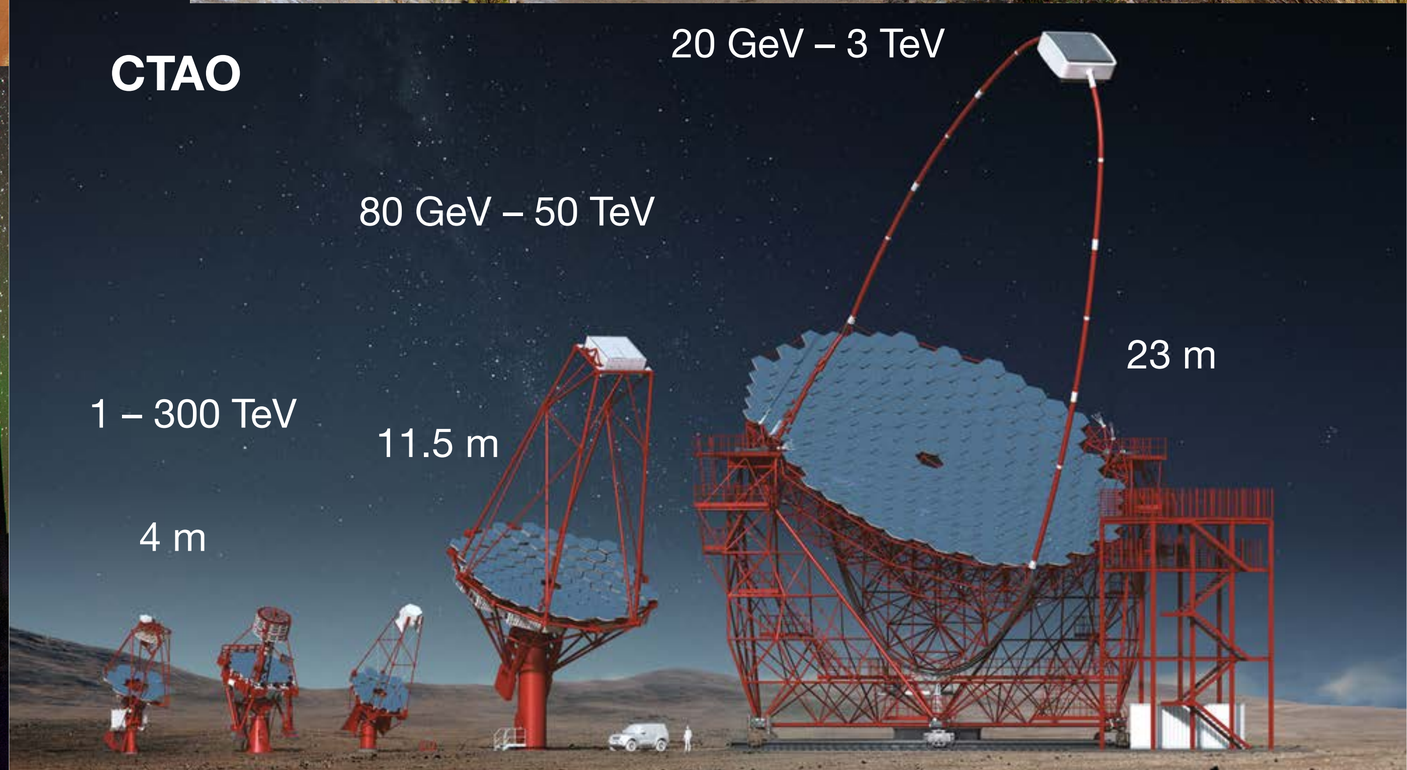
CTAO
20 GeV – 3 TeV
80 GeV – 50 TeV
1 – 300 TeV
23 m
11.5 m
4 m

Gamma-ray observations (i)

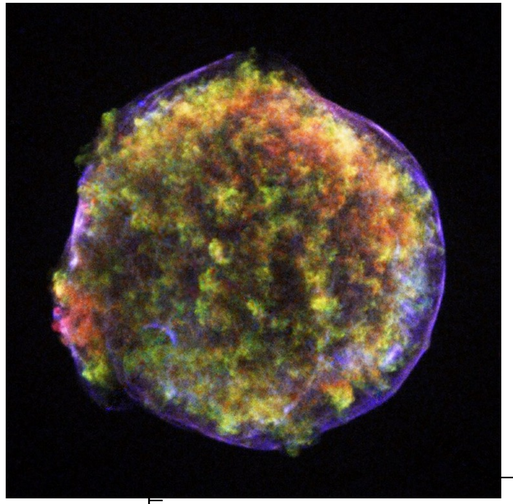

Tycho SNR (SN 1572)

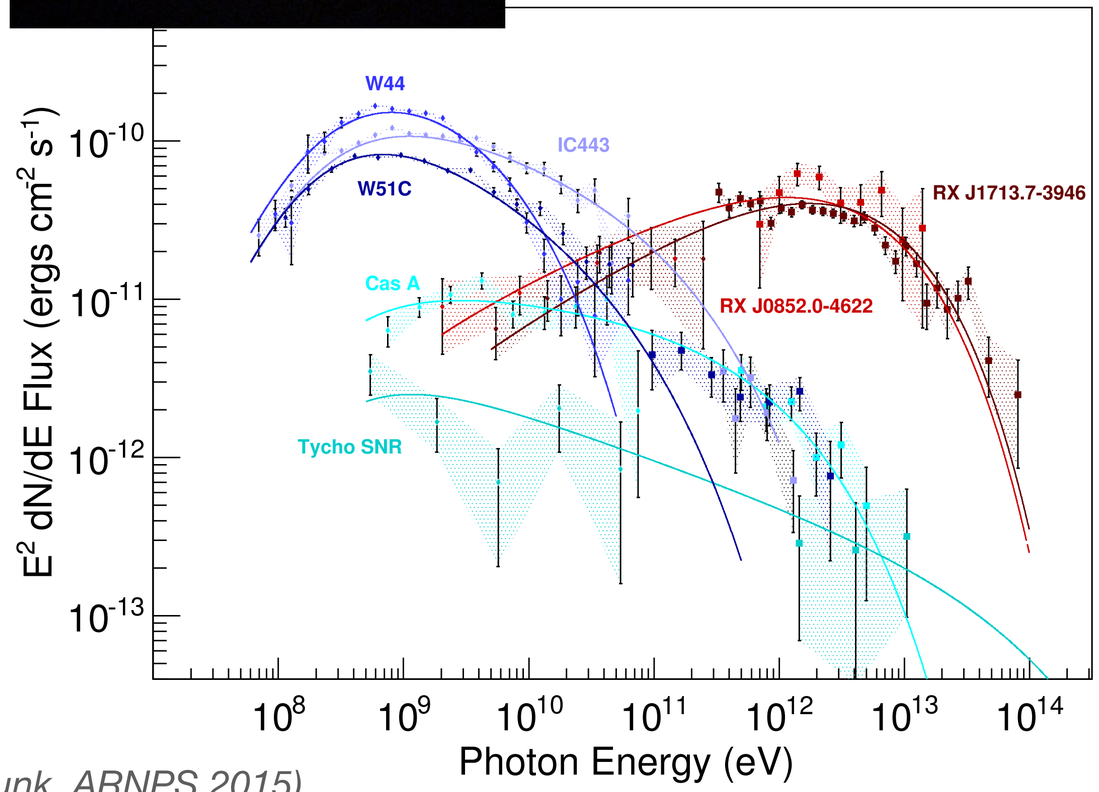

(Funk, ARNPS 2015)

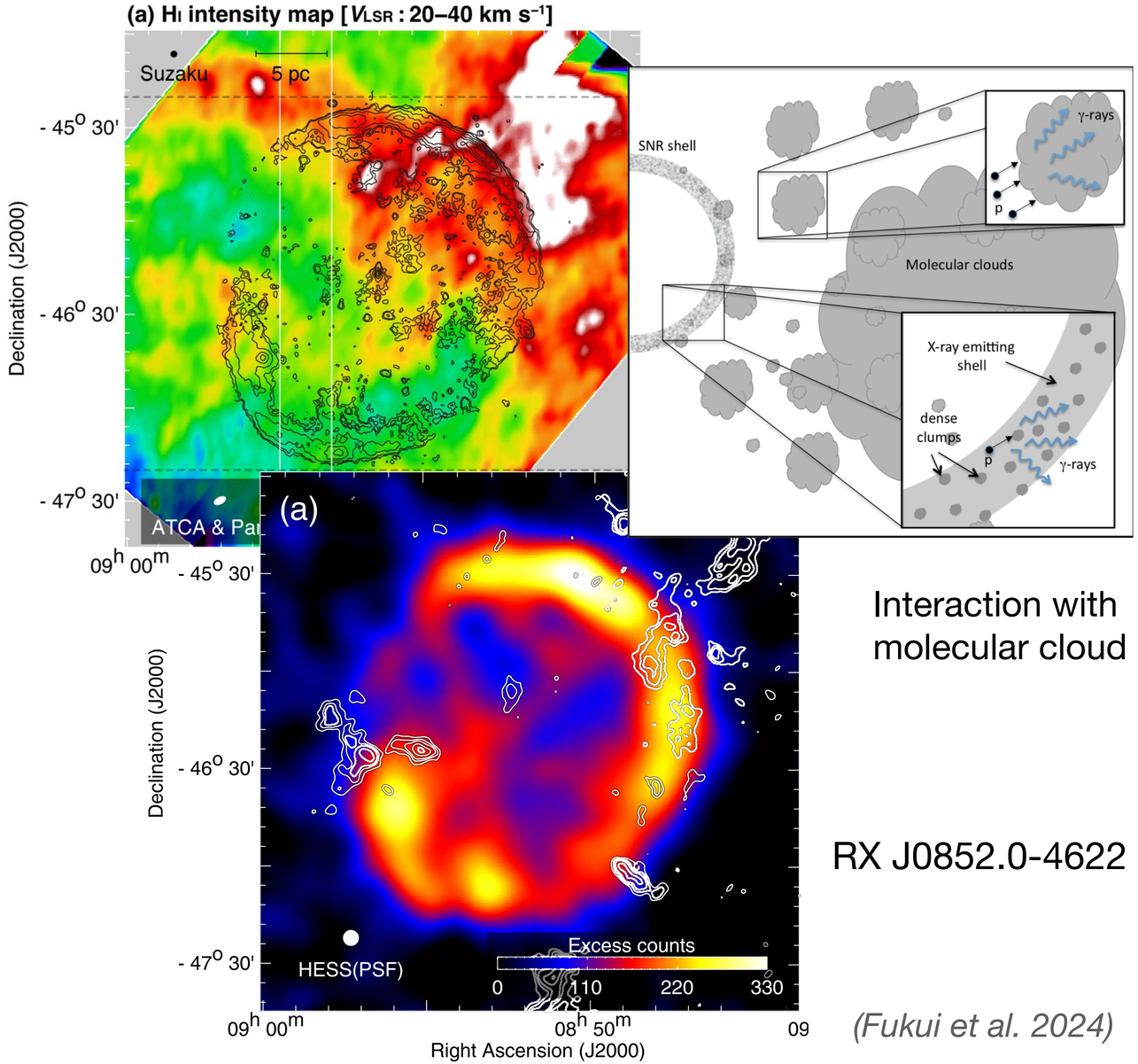

Interaction with molecular cloud

RX J0852.0-4622

(Fukui et al. 2024)

Gamma-ray observations – LHAASO

Gamma-ray observations (ii)

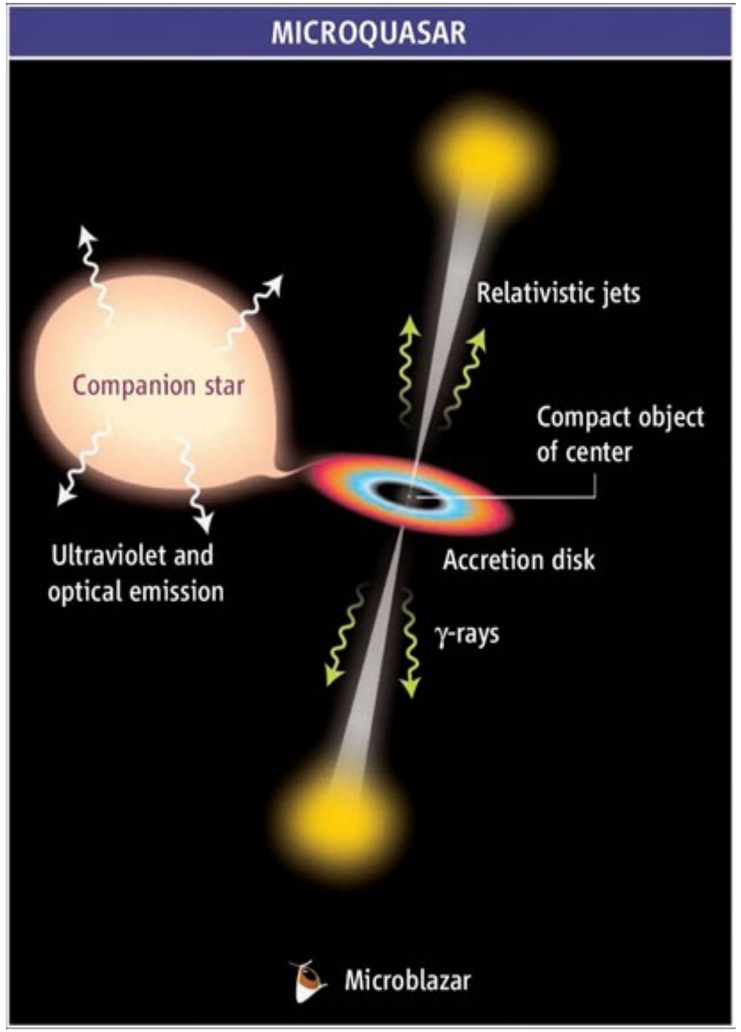

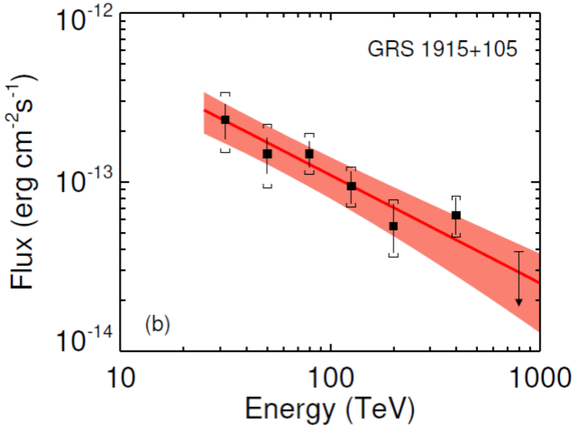

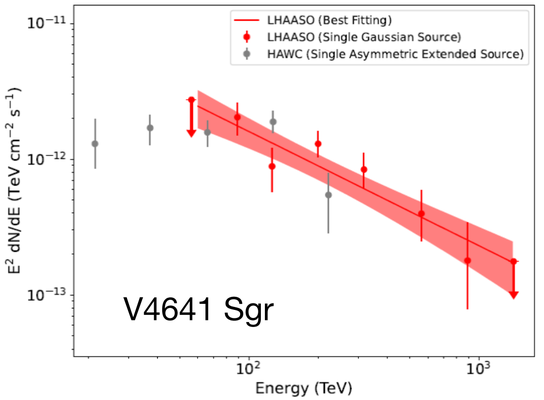

Microquasar	Distance (kpc)	LHAASO Source	Significance (σ)	Photon Index	Energy Range (TeV)	Extension[a]	Flux[b] (Crab Unit)
SS 433 E.		J1913+0455	9.9[c]	2.82 ± 0.16	$25 - 100$	$0.73° \pm 0.07°$	0.10
SS 433 W.	4.6 ± 1.3[31]	J1910+0509	6.3[c]	2.94 ± 0.38	$25 - 100$		0.082
SS 433 central		J1911+0510	8.0	3.96 ± 0.25	$100 - 630$	$0.32° \pm 0.04°$	0.32
V4641 Sgr	6.2 ± 0.7[32]	J1819-2541	10.5	2.84 ± 0.17	$40 - 1000$	$0.33° \pm 0.08°$	2.6
GRS 1915+105	9.4 ± 0.6[33]	J1915+1052	13.9	2.64 ± 0.14	$25 - 1000$	$0.25° \pm 0.05°$	0.11
MAXI J1820+070	2.96 ± 0.33[34]	J1821+0723	6.0	3.25 ± 0.26	$25 - 400$	$< 0.28°$	0.02
Cygnus X-1	2.2 ± 0.2[35]	J1958+3522	4.4	3.98 ± 0.40	$25 - 100$	$< 0.22°$	< 0.01
XTE J1859+226	4.2 ± 0.5[36]	–	2.7	–	–	–	< 0.02
GS 2000+251	2.7 ± 0.7[37]	–	2.3	–	–	–	< 0.04
CI Cam	$4.1^{+0.3}_{-0.2}$[38]	–	1.6	–	–	–	< 0.02
GRO J0422+32	2.49 ± 0.3[39]	–	0.7	–	–	–	< 0.01
V404 Cygni	2.39 ± 0.14[40]	–	1.5	–	–	–	< 0.03
XTE J1118+480	1.7 ± 0.1[41]	–	0.4	–	–	–	< 0.02
V616 Mon	1.06 ± 0.1[42]	–	0.4	–	–	–	< 0.01

Searched for UHE emission within the PSF around 12 microquasars. Signals were detected around 5 microquasars, suggesting possible associations.

Example: acceleration in microquasar cocoons

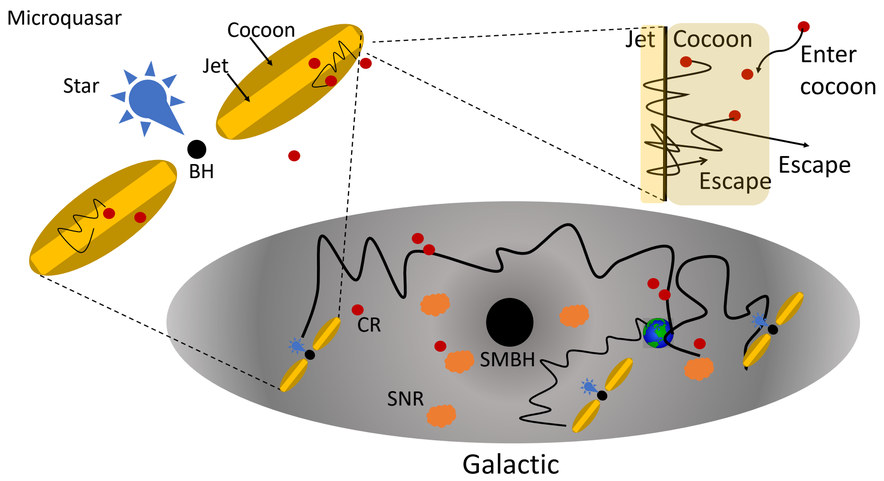

Re-acceleration of low-energy cosmic rays

(Zhang et al. 2025)

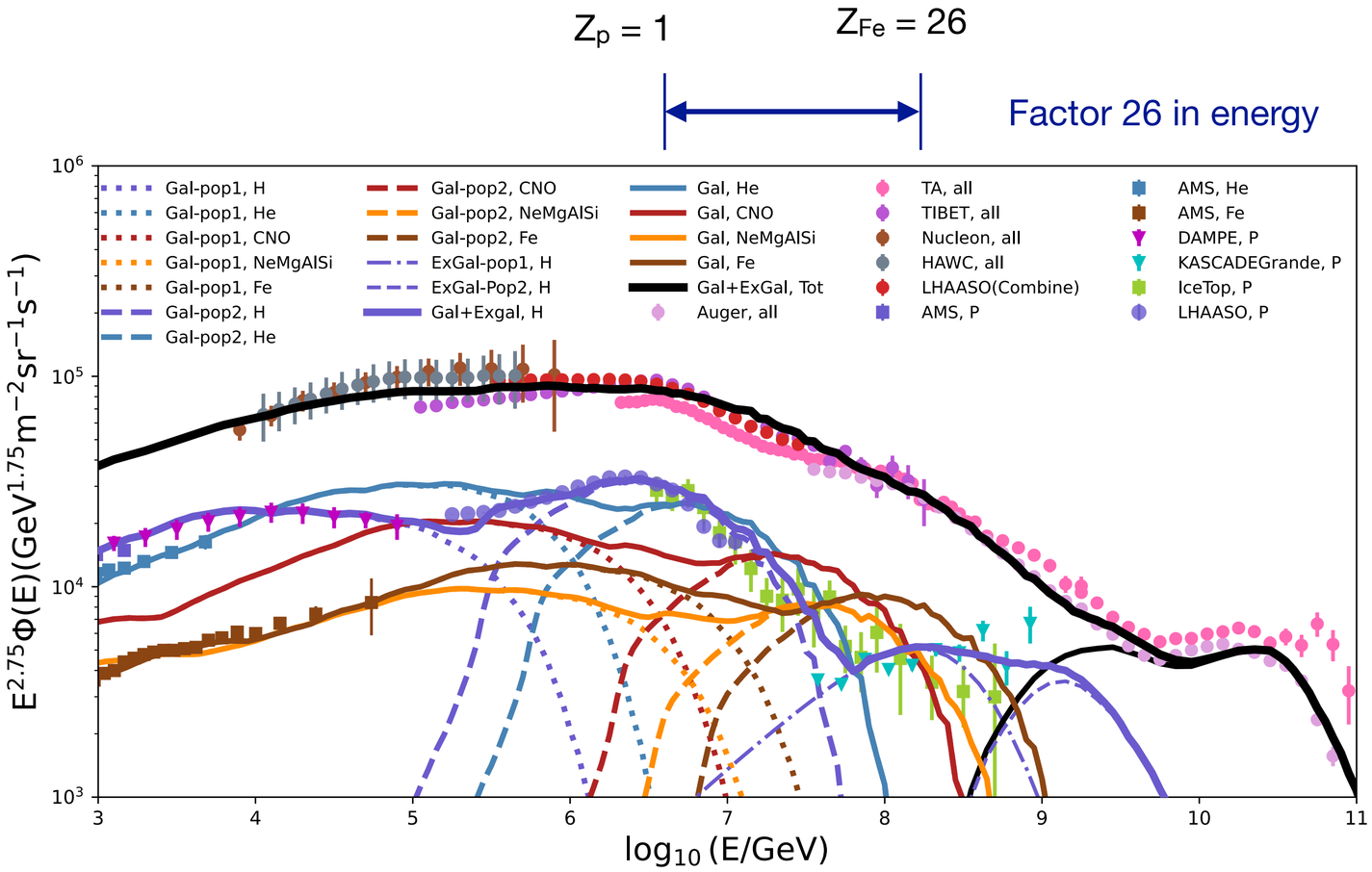

Note: SNRs still provide main energy source for CRs (low-energy cosmic rays)

SNRs

Microquasars

(probably 5 – 10 active sources in Galaxy)

Extragal. sources

Extragalactic cosmic ray sources

What an energy of 10^{20} eV really means

(MIAPP review, Front.Astron.Space Sci. 6 (2019) 23)

Particle on circular orbit

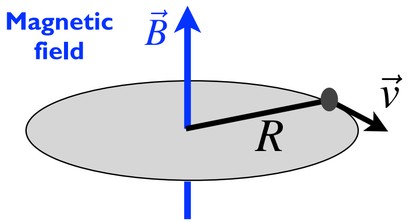

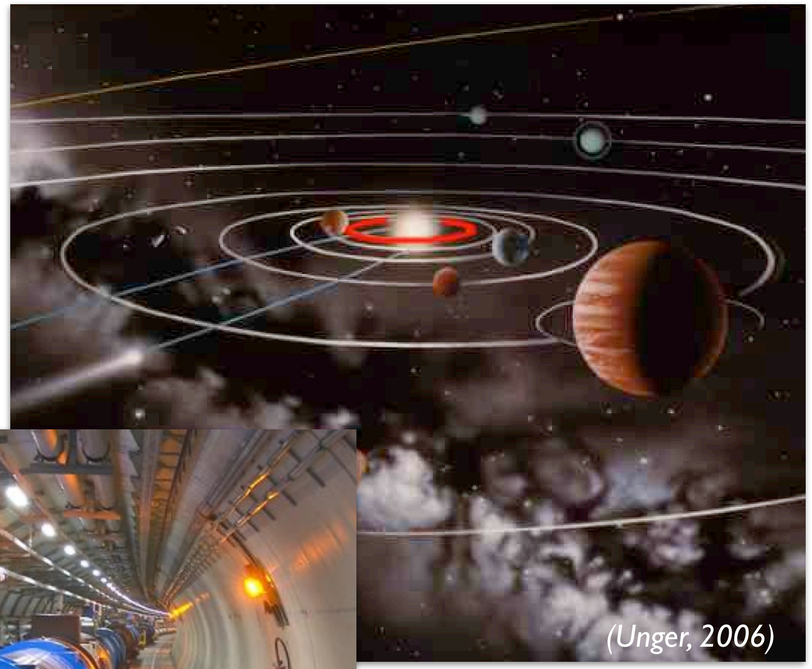

Need accelerator of size of the orbit of the planet Mercury to reach 10^{20} eV with LHC technology

Hillas plot (1984)

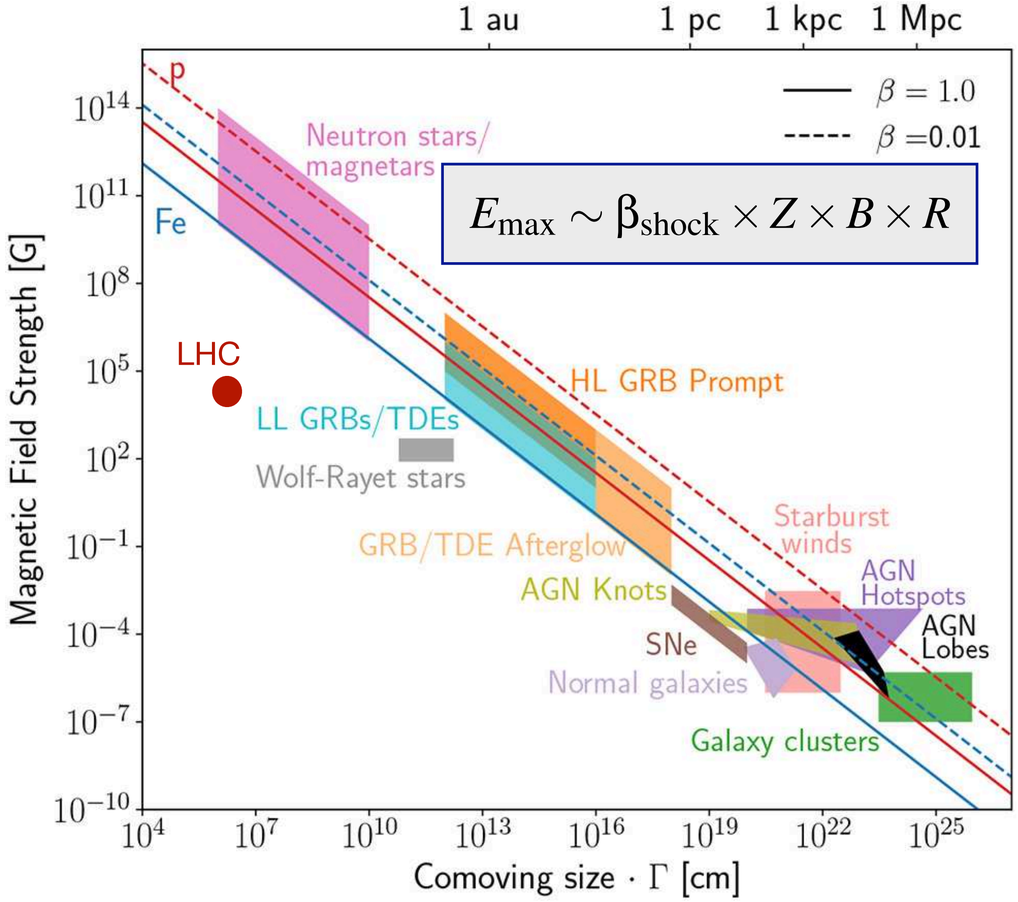

Hardly any source expected to accelerate protons to 10^{20} eV

Examples of astrophysical source candidates

Diffusive shock acceleration

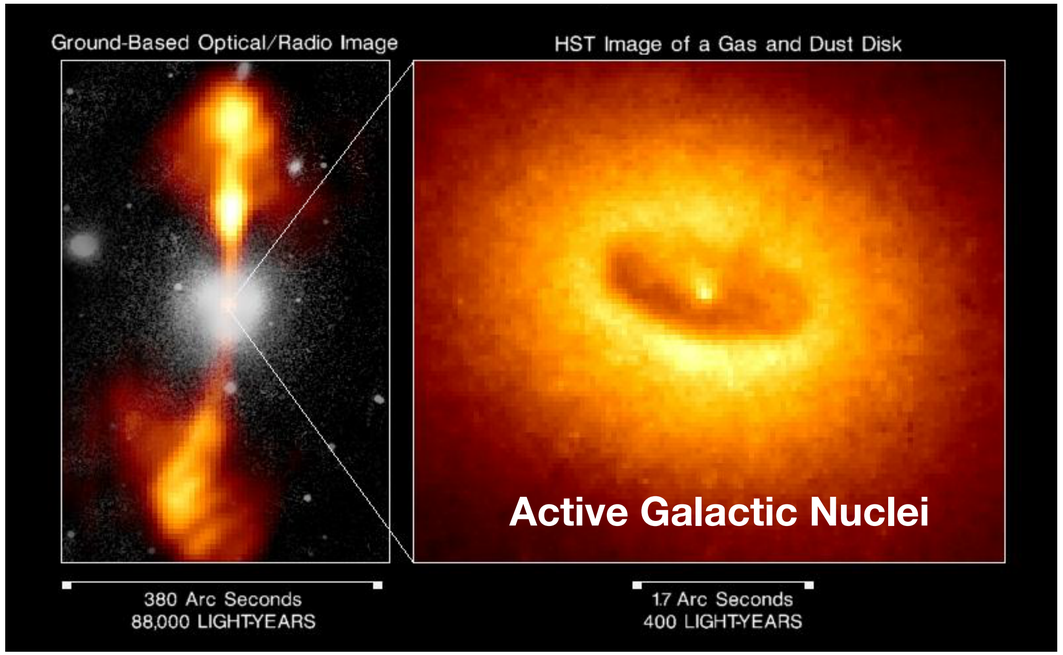

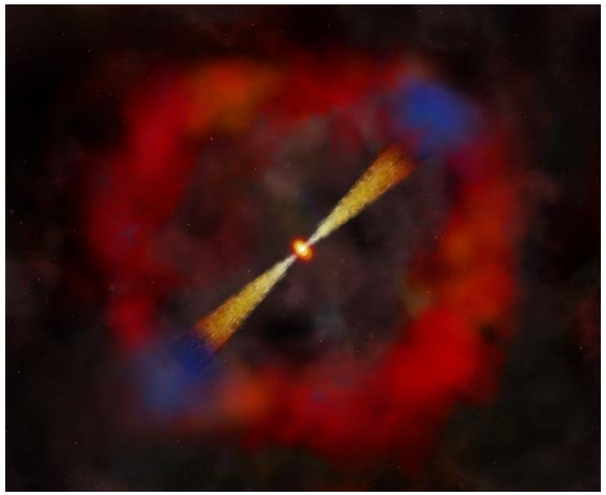

$$\frac{\mathrm{d}N_{\mathrm{inj}}}{\mathrm{d}E} \sim E^{-2}$$

Gamma ray bursts (GRBs)

Inductive acceleration

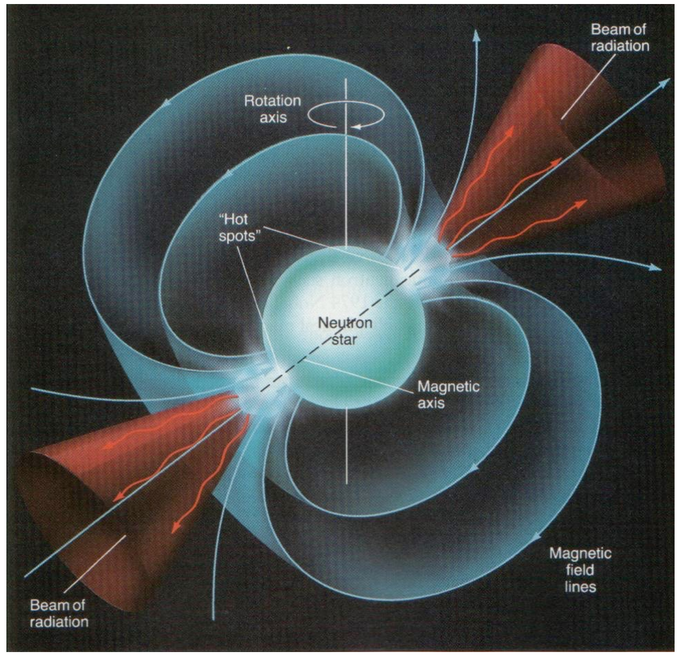

Rapidly spinning neutron stars

$$\frac{\mathrm{d}N_{\mathrm{inj}}}{\mathrm{d}E} \sim E^{-1}\left(1+\frac{E}{E_g}\right)^{-1}$$

Single (relativistic) reflection

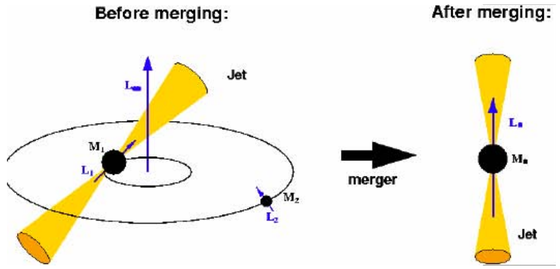

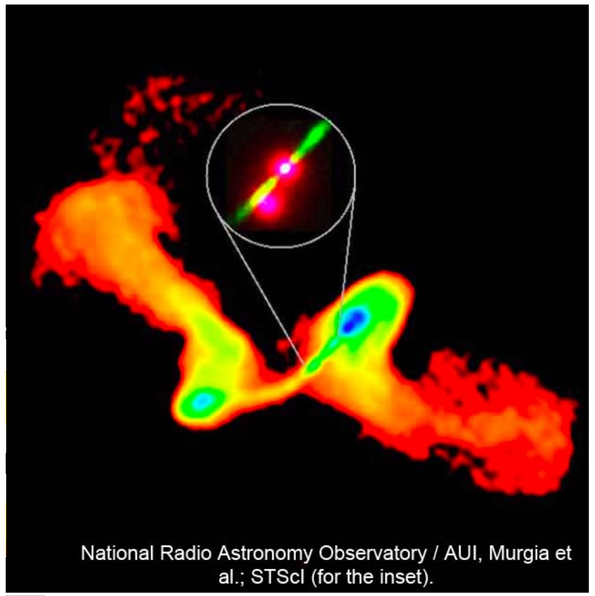

Tidal disruption events (TDEs)

Propagation of ultra-high energy particles

Greisen Zatsepin Kuzmin



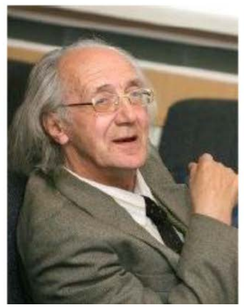

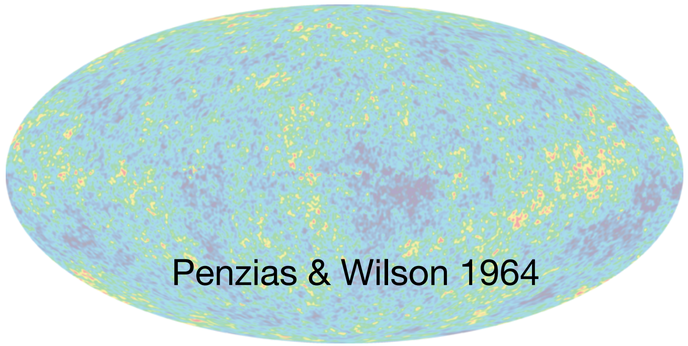

Greisen, Zatsepin & Kuzmin (GZK) effect, 1966

Protons → n p π^+ π^0

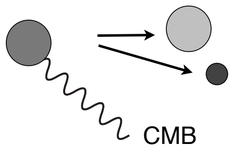

Photo-pion production
(mainly Δ resonance)

Nuclei →

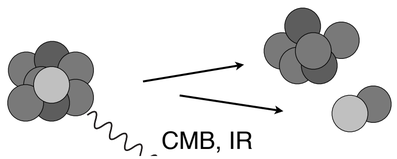

Photo-dissociation
(giant dipole resonance)

$\gamma A \rightarrow X$

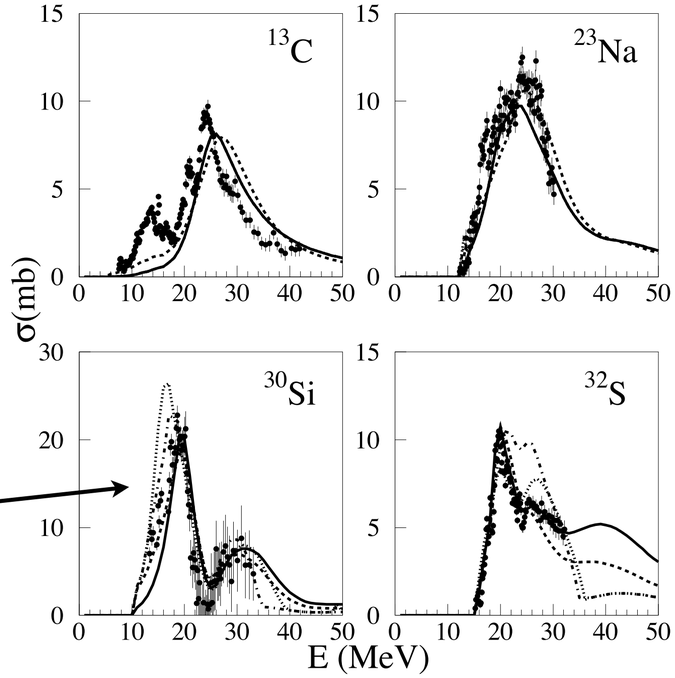

Giant dipole resonance

$\gamma p \rightarrow X$

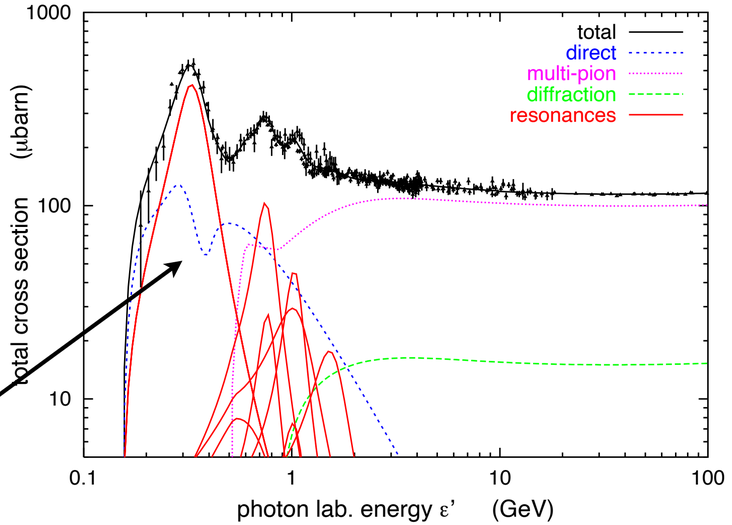

Delta resonance
(m=1.232 GeV)

Standard models for extragalactic cosmic rays (2005)

Dip model: Berezinsky et al.

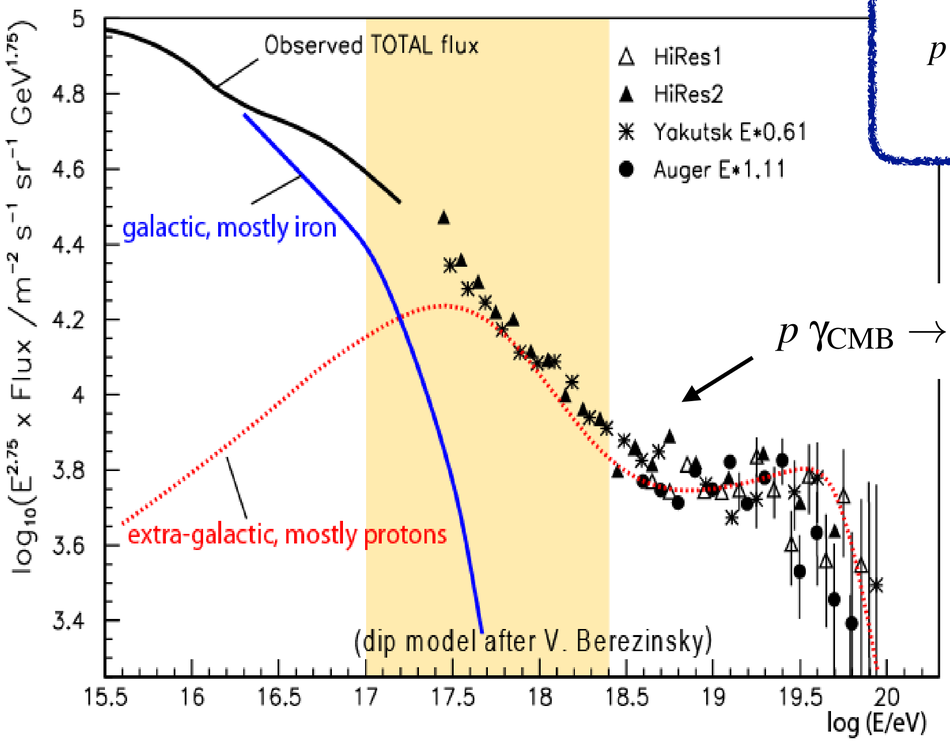

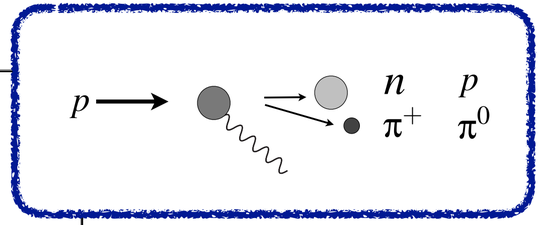

Neutrons leave sources

$$p\,\gamma_{\mathrm{CMB}} \rightarrow p\,e^{+}e^{-}$$

$$\frac{\mathrm{d}N_p}{\mathrm{d}E} \sim E^{-2.7}$$

(PRD 74 (2006) 043005)

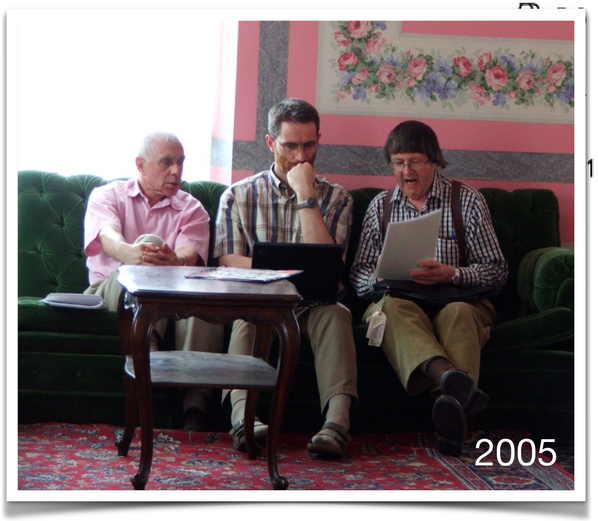

Ankle model: Hillas, Wolfendale et al.

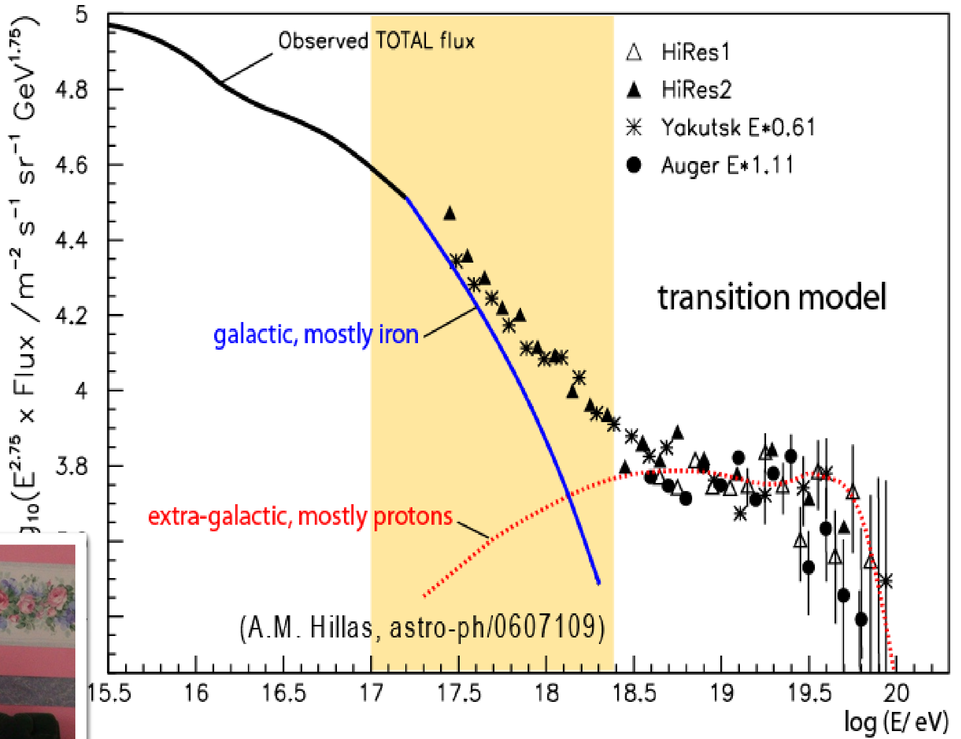

$$\frac{\mathrm{d}N_p}{\mathrm{d}E} \sim E^{-2.3}$$

(J. Phys. G31 (2005) R95)


The Pierre Auger Observatory

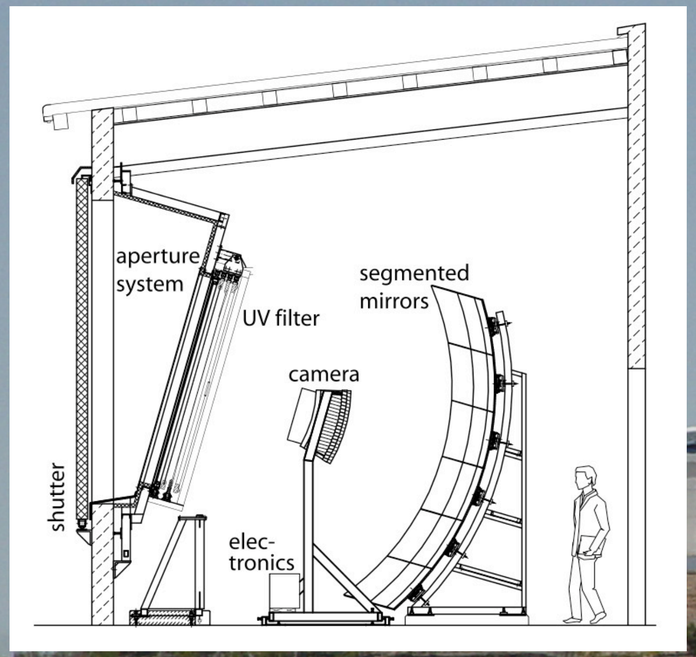

Fluorescence telescopes

PMT camera with 440 pixels, 1.5° FoV per pixel, 10 MHz, 3.4 m segmented mirror

Particle detectors

10 m^2 area, 1.20 m high, 12 tons of water, 3 PMTs (9 inch), 40 MHz

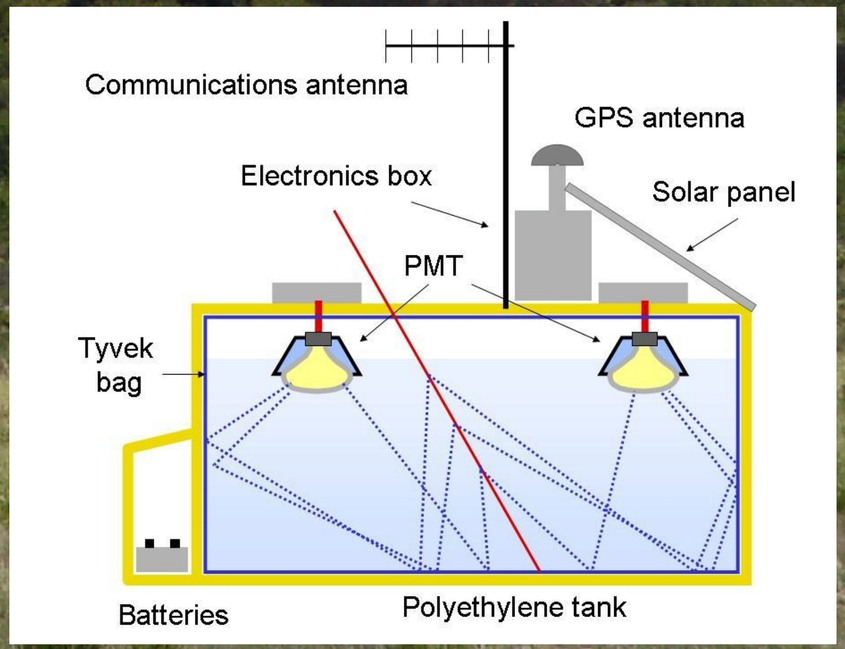

Measurement principles (hybrid observation)

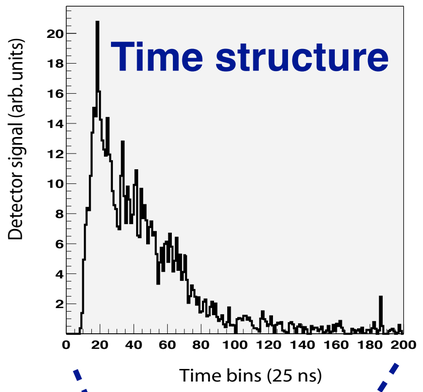

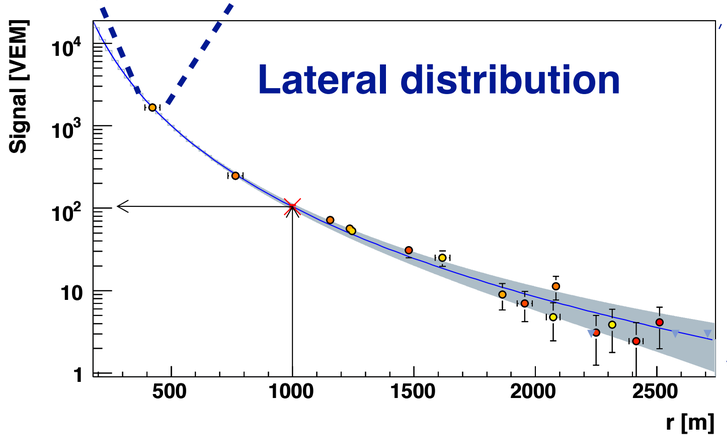

Surface Detector (SD)
100% duty cycle

Fluorescence Detector (FD):
15% duty cycle

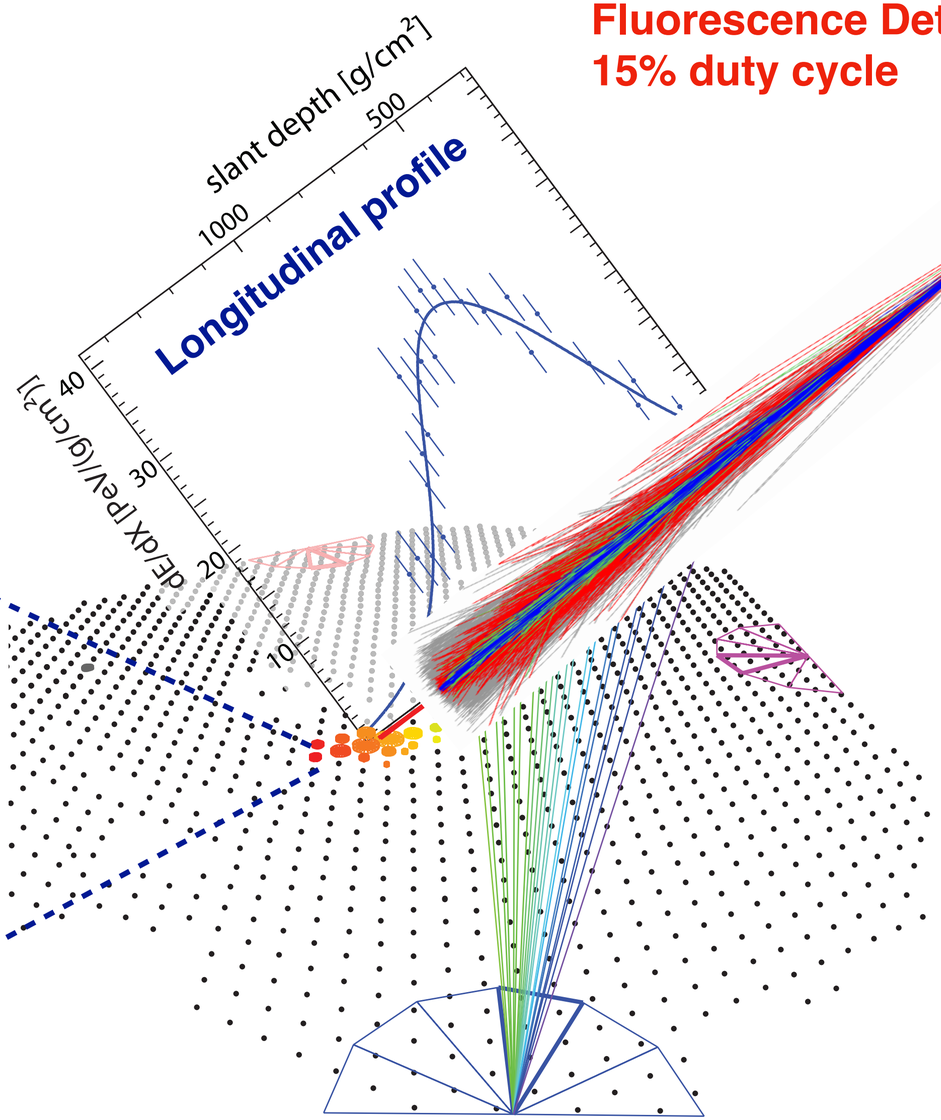

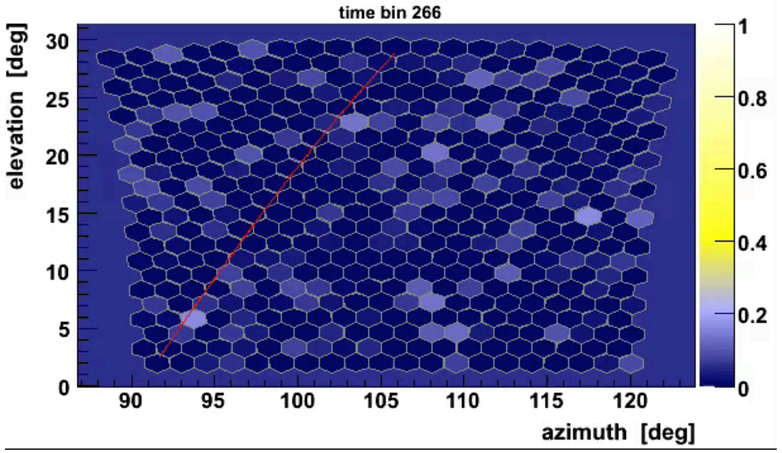

Fluorescence signal:

- calorimetric in shower energy
- calibration of surface detector array

Energy spectrum and GZK expectation (early data)

Proton dominated flux

Suppression: delta resonance

Ankle: e^+e^- pair production

$$\frac{dN_{inj}}{dE} \sim E^{-\gamma} \exp\left(-\frac{E}{E_{cut}}\right)$$

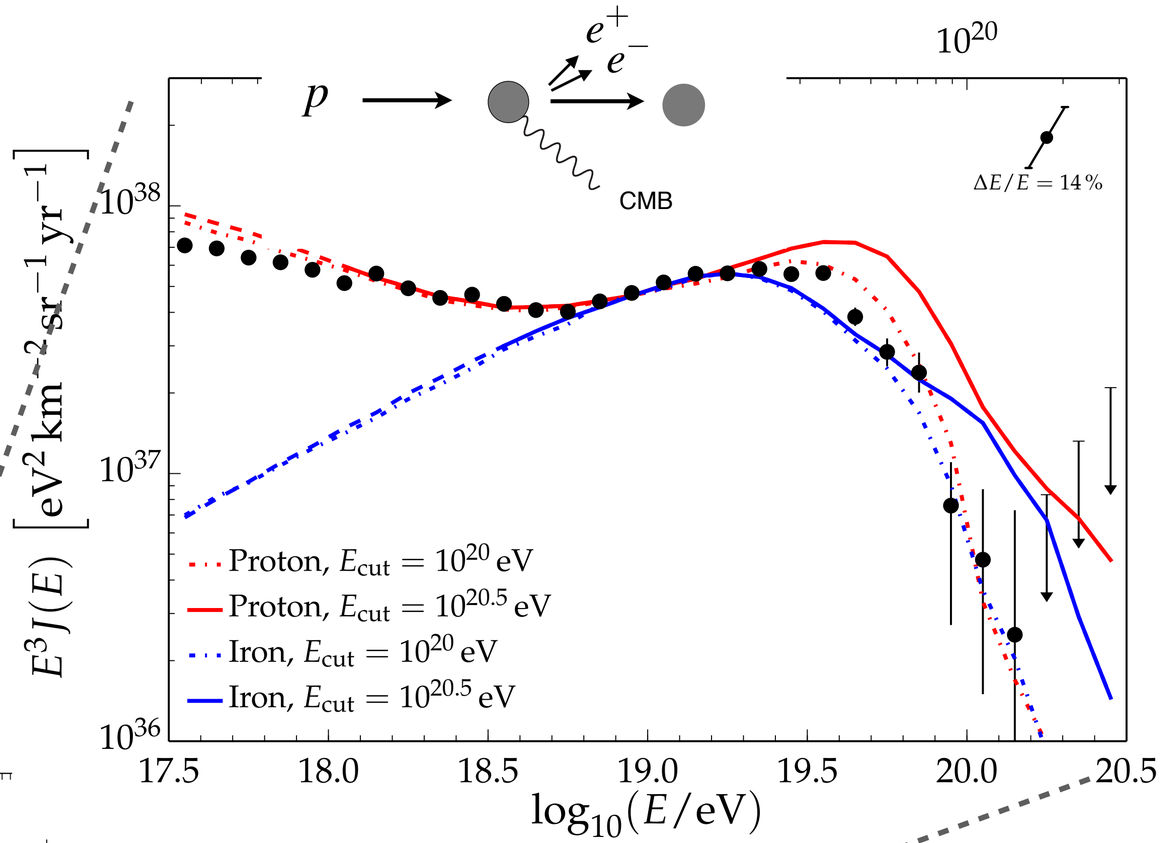

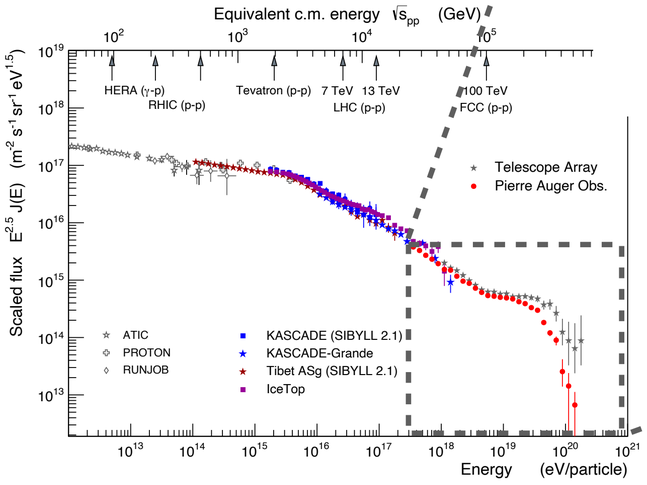

Iron dominated flux

Suppression: giant dipole resonance

Ankle: transition to galactic sources

Greisen-Zatsepin-Kuzmin (GZK) effect

Photo-pion production
(mainly Δ resonance)

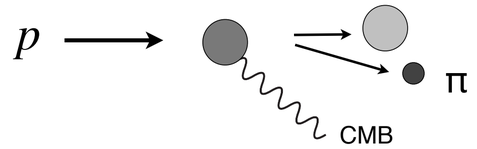

GZK secondaries
- Photons
- Neutrinos

Photo-dissociation
(giant dipole resonance)

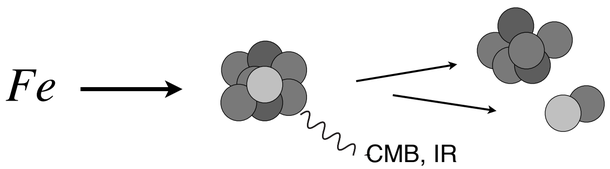

Neutral (secondary) particles as messengers

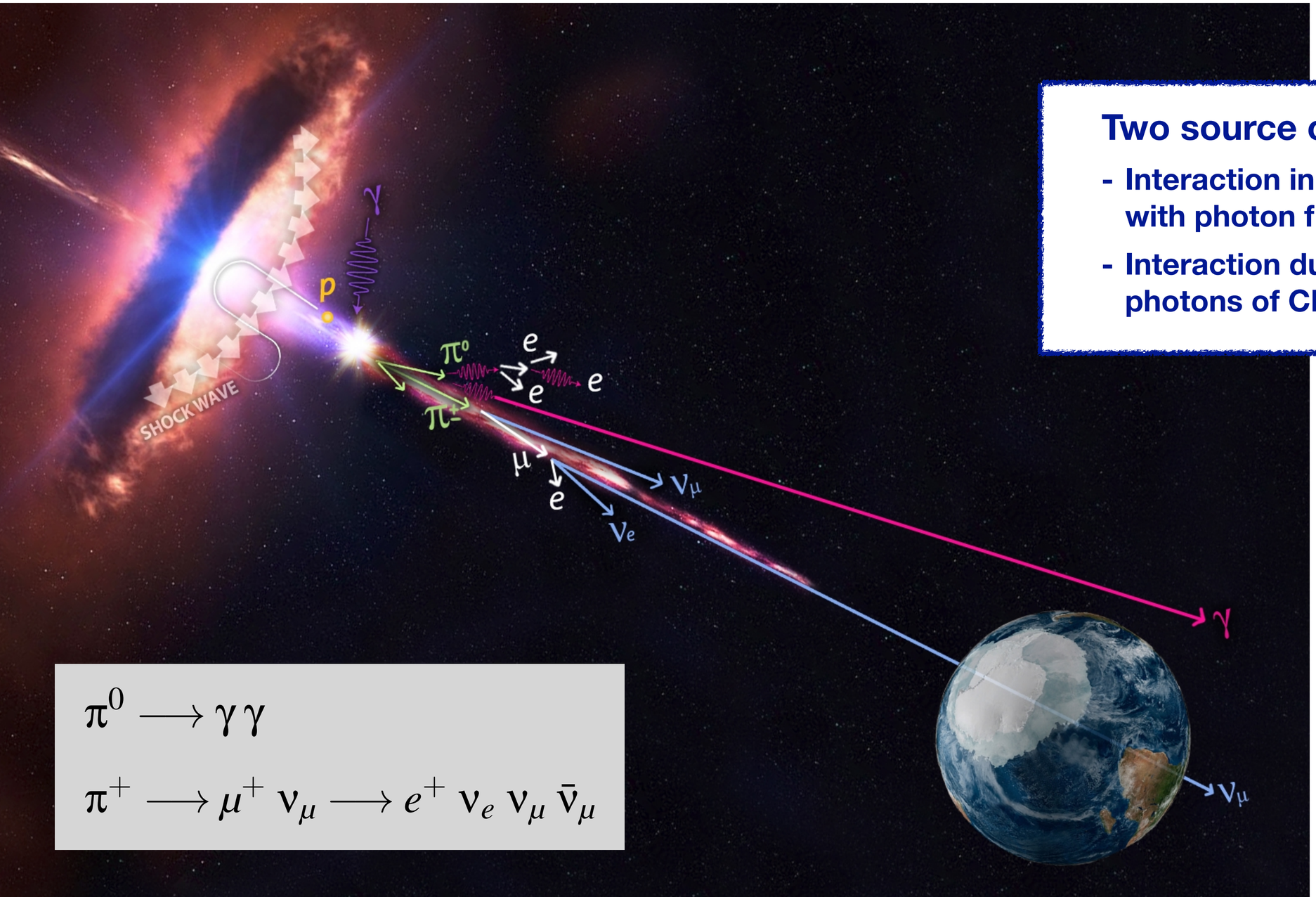

Two source classes

- **Interaction in dense source regions with photon field or gas**
- **Interaction during propagation with photons of CMB and other backgrounds**

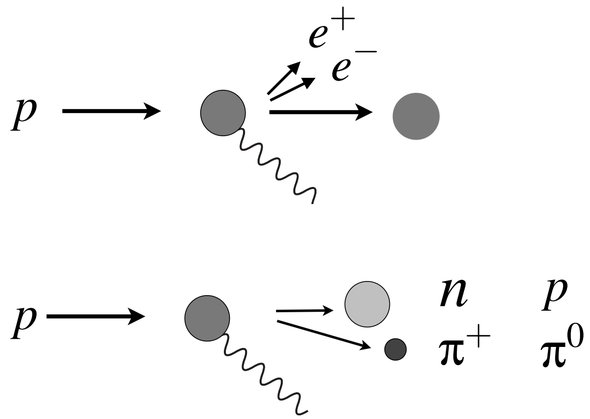

and similar interactions of nuclei, as well as dissociation of nuclei

$$\pi^0 \longrightarrow \gamma\,\gamma$$

$$\pi^+ \longrightarrow \mu^+\,\nu_\mu \longrightarrow e^+\,\nu_e\,\nu_\mu\,\bar{\nu}_\mu$$

Waxman-Bahcall upper bound (2000)

(Waxman & Bahcall, Phys. Rev. D59 (1999) 023002)

(Bahcall & Waxman, Phys. Rev. D64 (2001) 023002)

Waxman

Bahcall

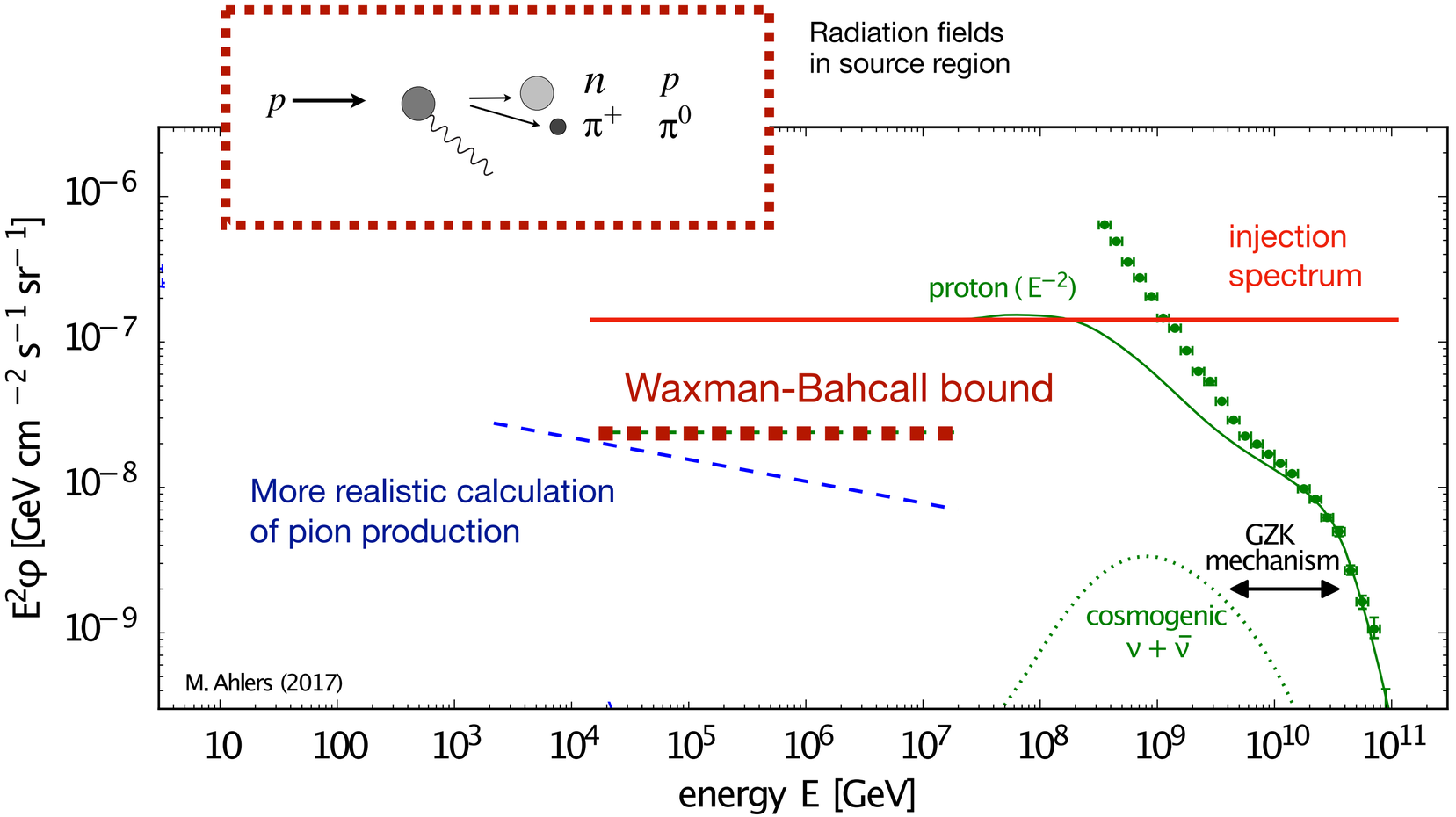

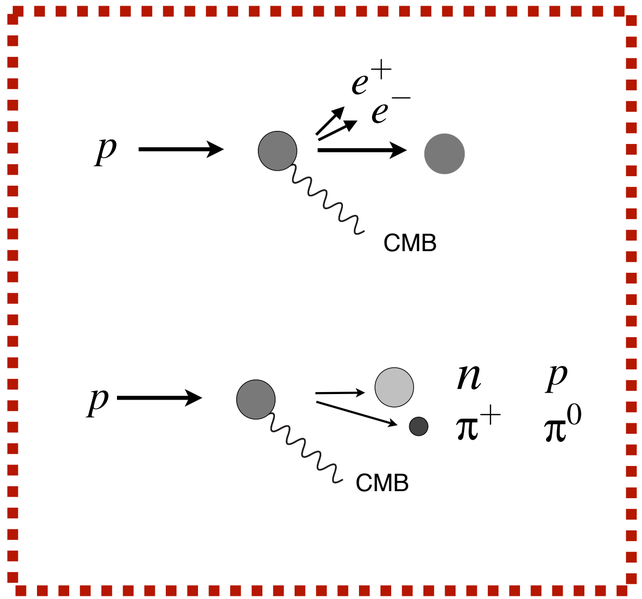

Radiation fields in extragalactic. propagation

Summary of assumption of WB upper bound

(Waxman & Bahcall, Phys. Rev. D59 (1999) 023002)

- Extragalactic cosmic-ray protons extending to the highest energies

- One interaction with photon field per proton in source or source region

- Source production spectrum similar to Fermi acceleration

$$\frac{\mathrm{d}N}{\mathrm{d}E} \sim E^{-\gamma} \qquad \gamma = 1.8 \ldots 2.3$$

- Energy production rate (normalization) of 4 x 10^{44} erg Mpc^{-1} yr^{-1}

(Waxman, ApJ 452 (1995) L1)

Size of neutrino detector (water, ice) for observing this flux has to be V ~ 1 km^3

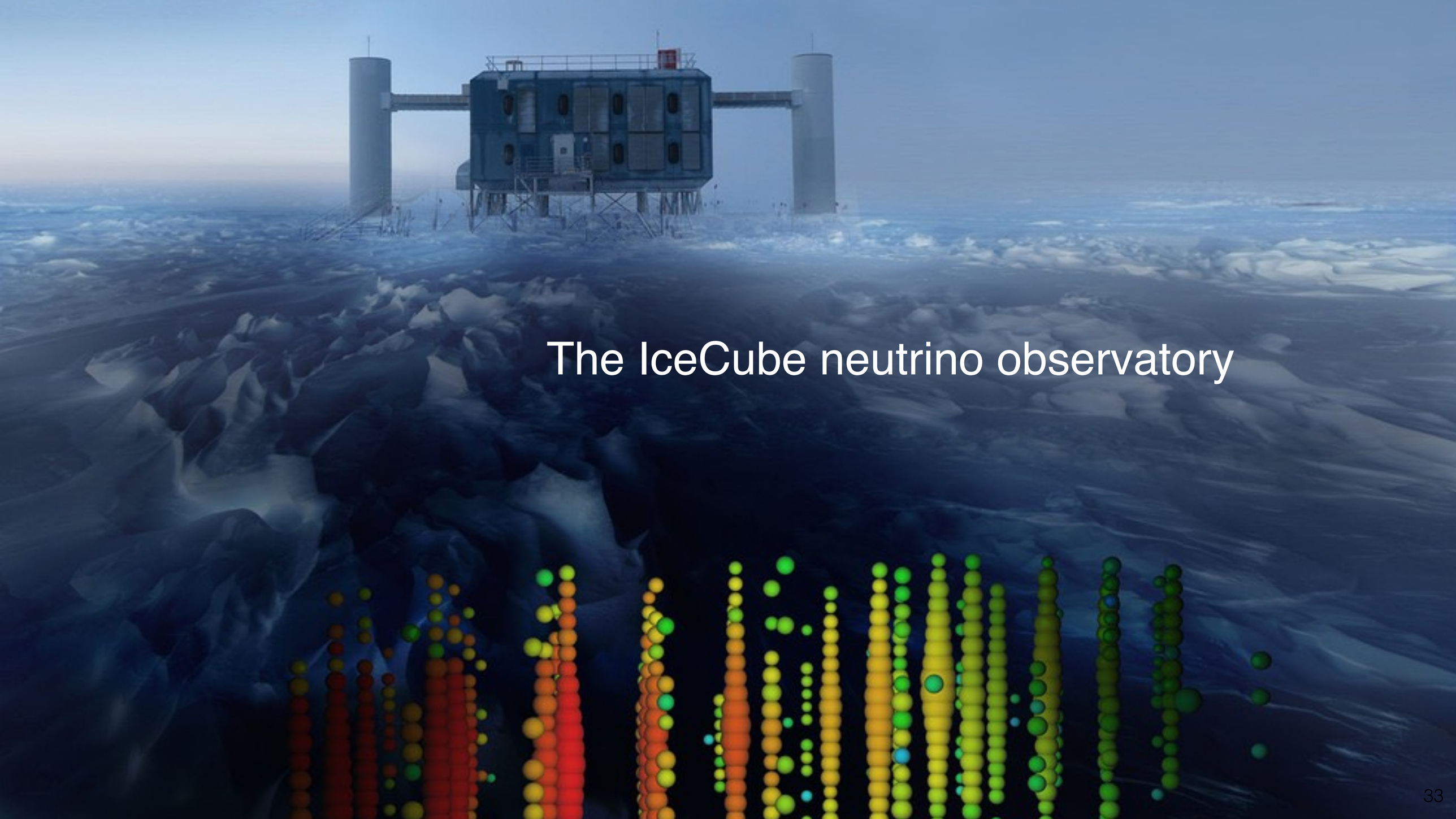
The IceCube neutrino observatory

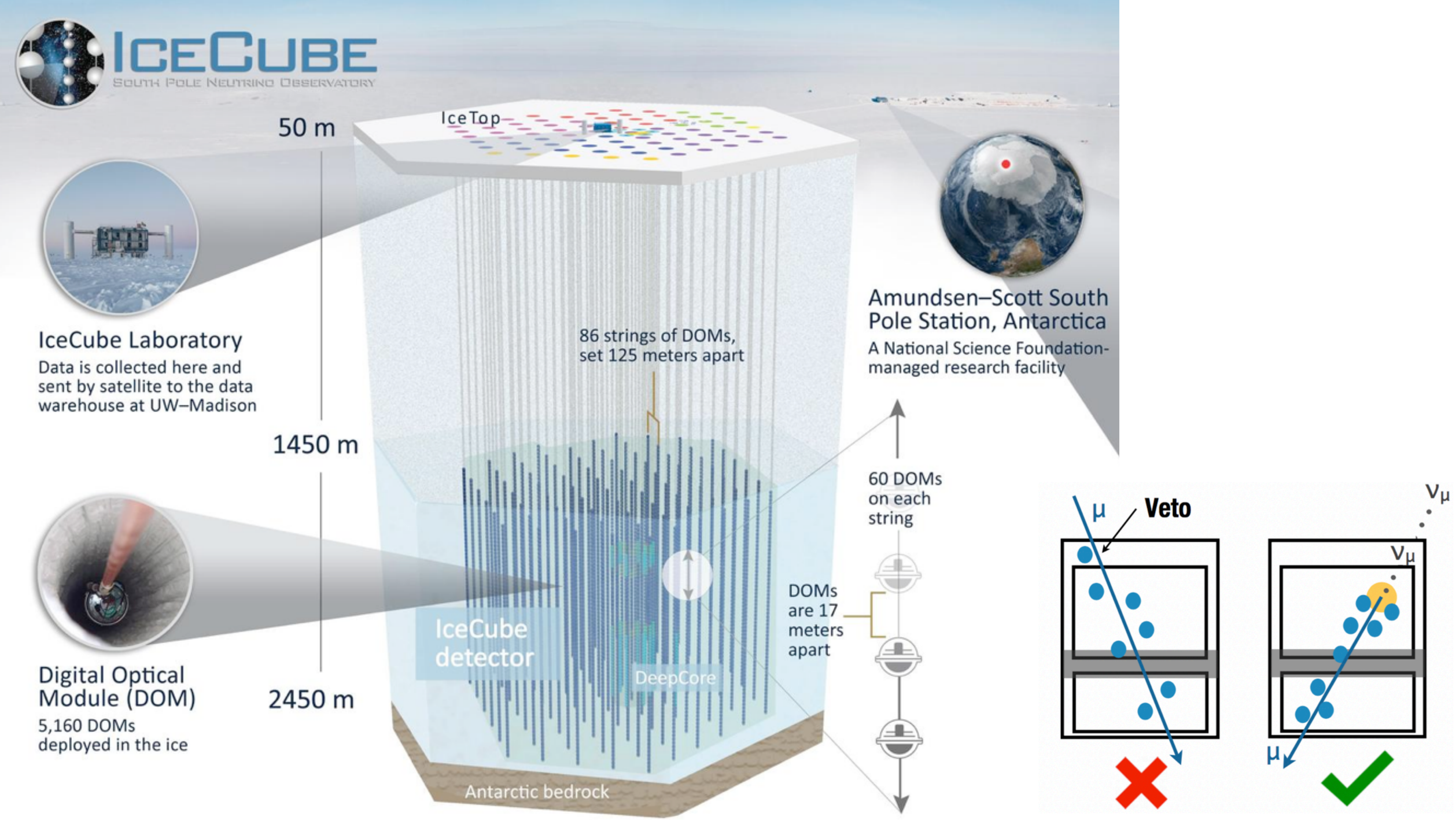
IceCube
South Pole Neutrino Observatory
50 m
IceTop
IceCube Laboratory
Data is collected here and sent by satellite to the data warehouse at UW–Madison
1450 m
86 strings of DOMs, set 125 meters apart
Amundsen–Scott South Pole Station, Antarctica
A National Science Foundation-managed research facility
60 DOMs on each string
DOMs are 17 meters apart
IceCube detector
DeepCore
Digital Optical Module (DOM)
5,160 DOMs deployed in the ice
2450 m
Antarctic bedrock
μ
Veto
νμ
νμ
μ

Discovery of high-energy astrophysical neutrinos (2013)

"Bert"

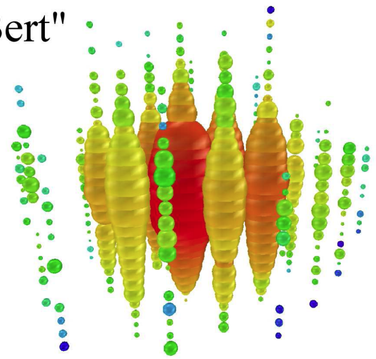

1.04±0.16 PeV

"Ernie"

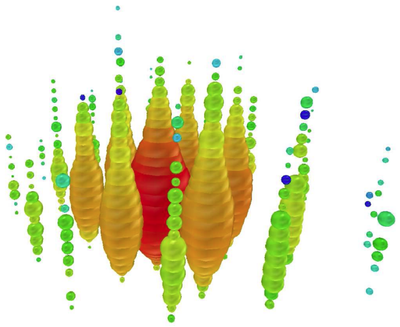

1.14±0.17 PeV

First events found in search for high energy cascades (GZK neutrinos)

(Cowen, Blois 2013)

Veto technique

High energy starting events (HESE)

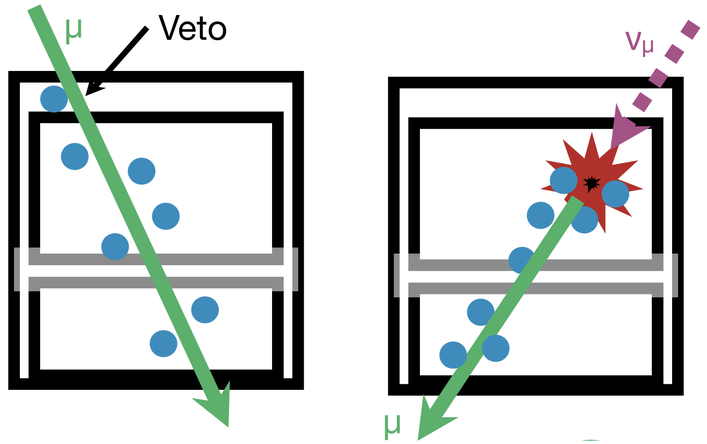

Science publication of 28 events

Neutrino flux found at level of Waxman-Bahcall bound

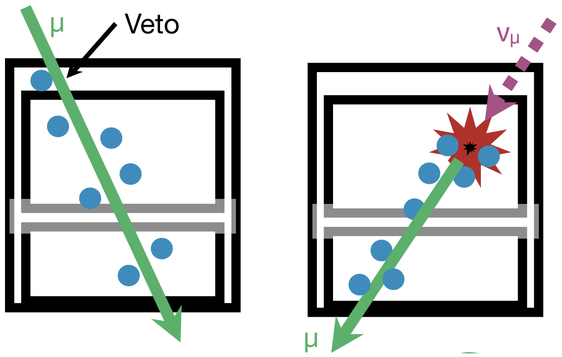

Veto technique

High energy starting events (HESE)

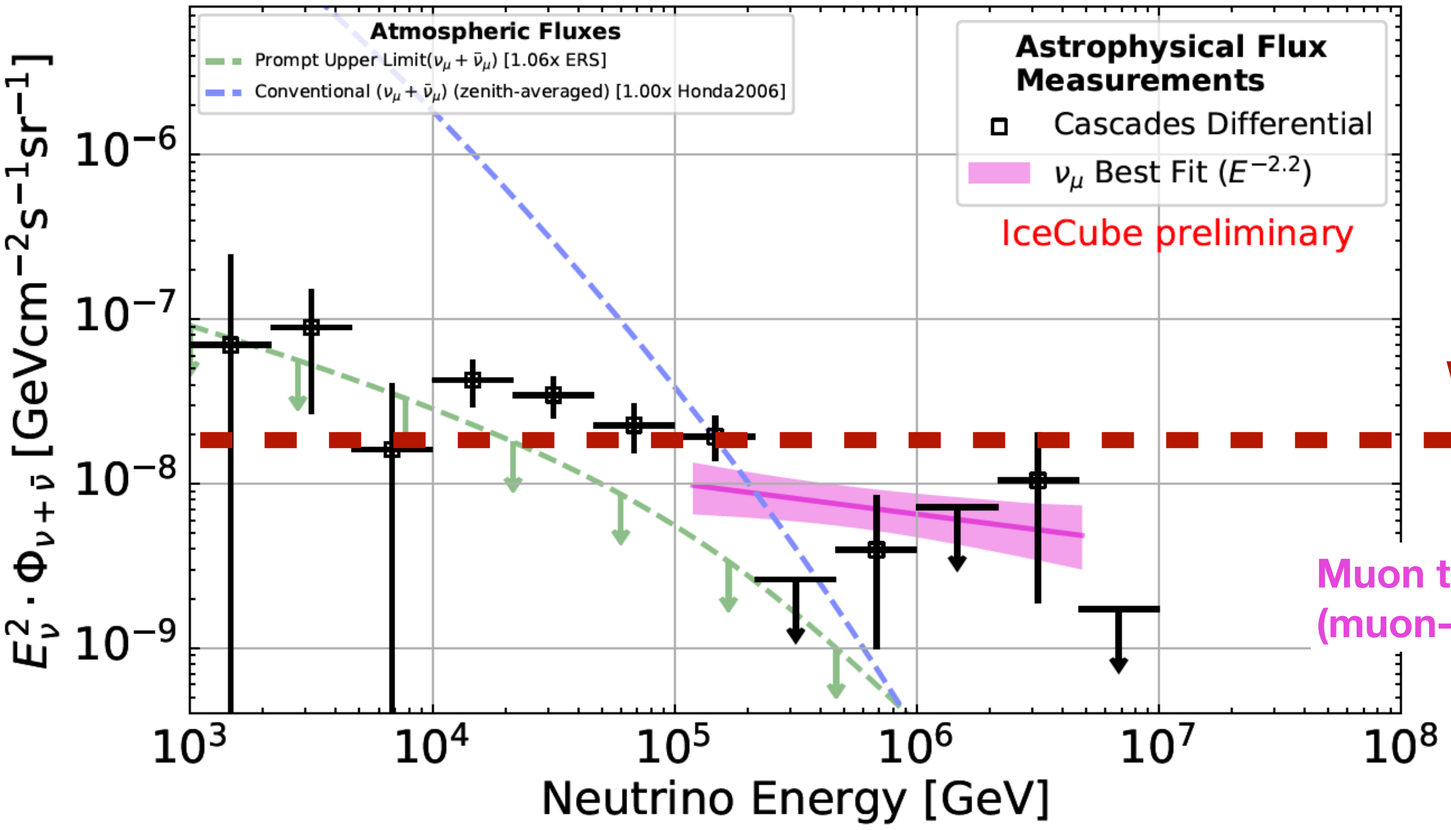

Auger data show that WB assumptions do not apply

Waxman-Bahcall bound

Muon track events (muon-neutrino through Earth)

Energy spectrum of Auger Observatory (2021)

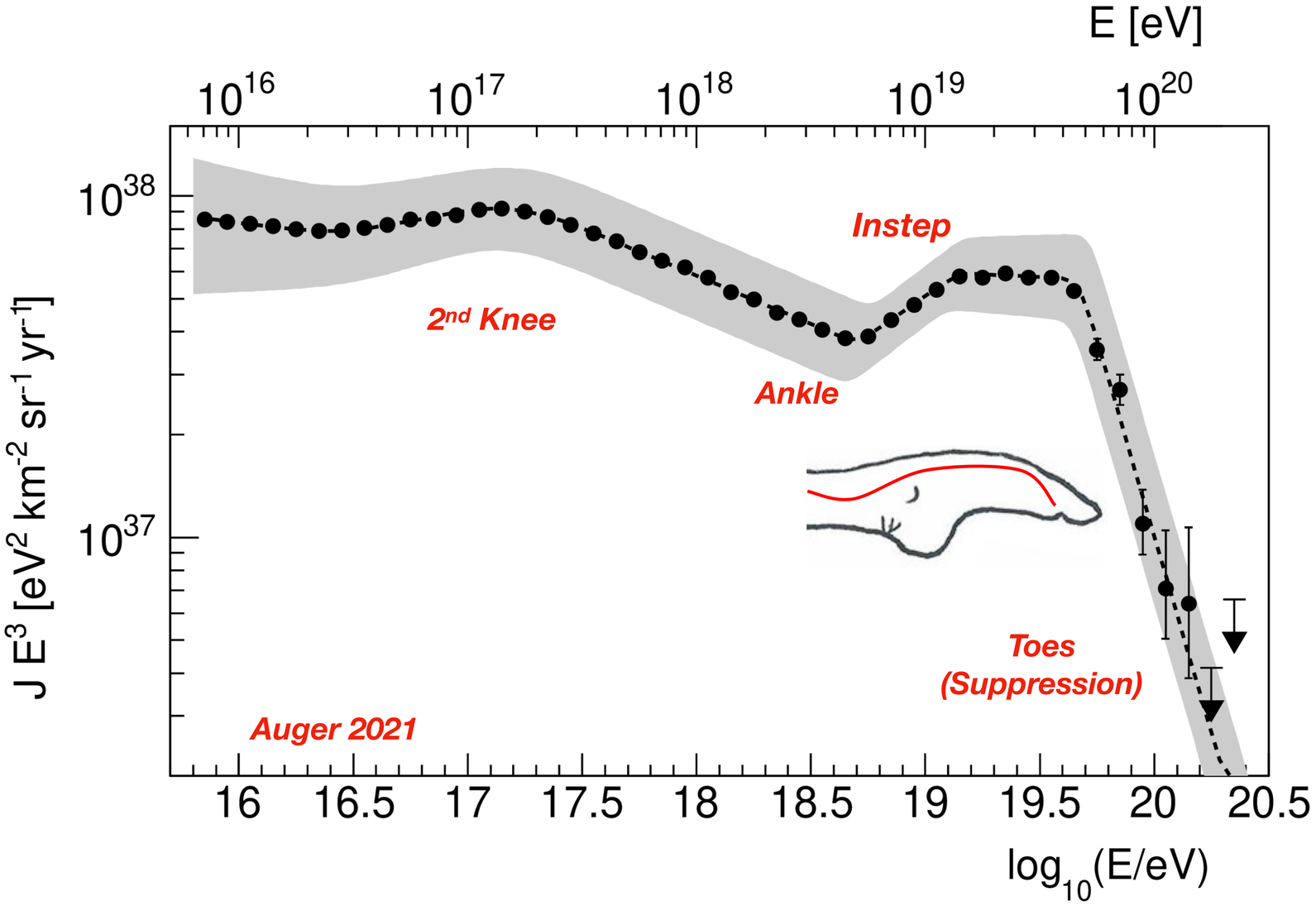

Phys. Rev. Lett. 125 (2020) 121106
Phys. Rev. D102 (2020) 062005
Eur. Phys. J. C81 (2021) 966

PIERRE AUGER OBSERVATORY

Band: uncertainty, mainly 14% sys. energy scale

Spectrum shape and Instep not compatible with source models of single mass group (p, …, Fe)

Auger data on mass composition (2023)

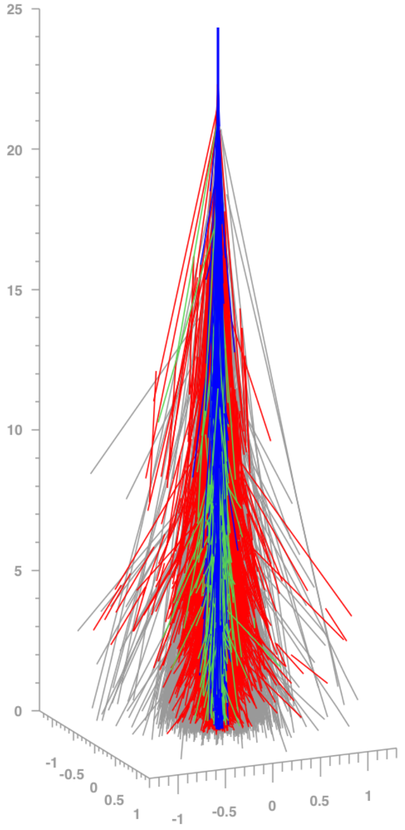

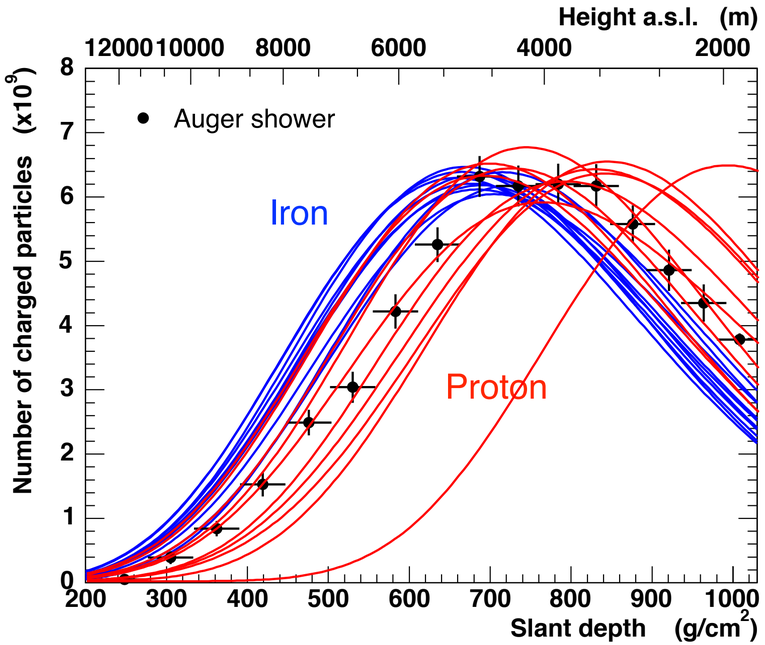

Example: event measured by Auger

Average X_{max}

Shower-by-shower fluctuations

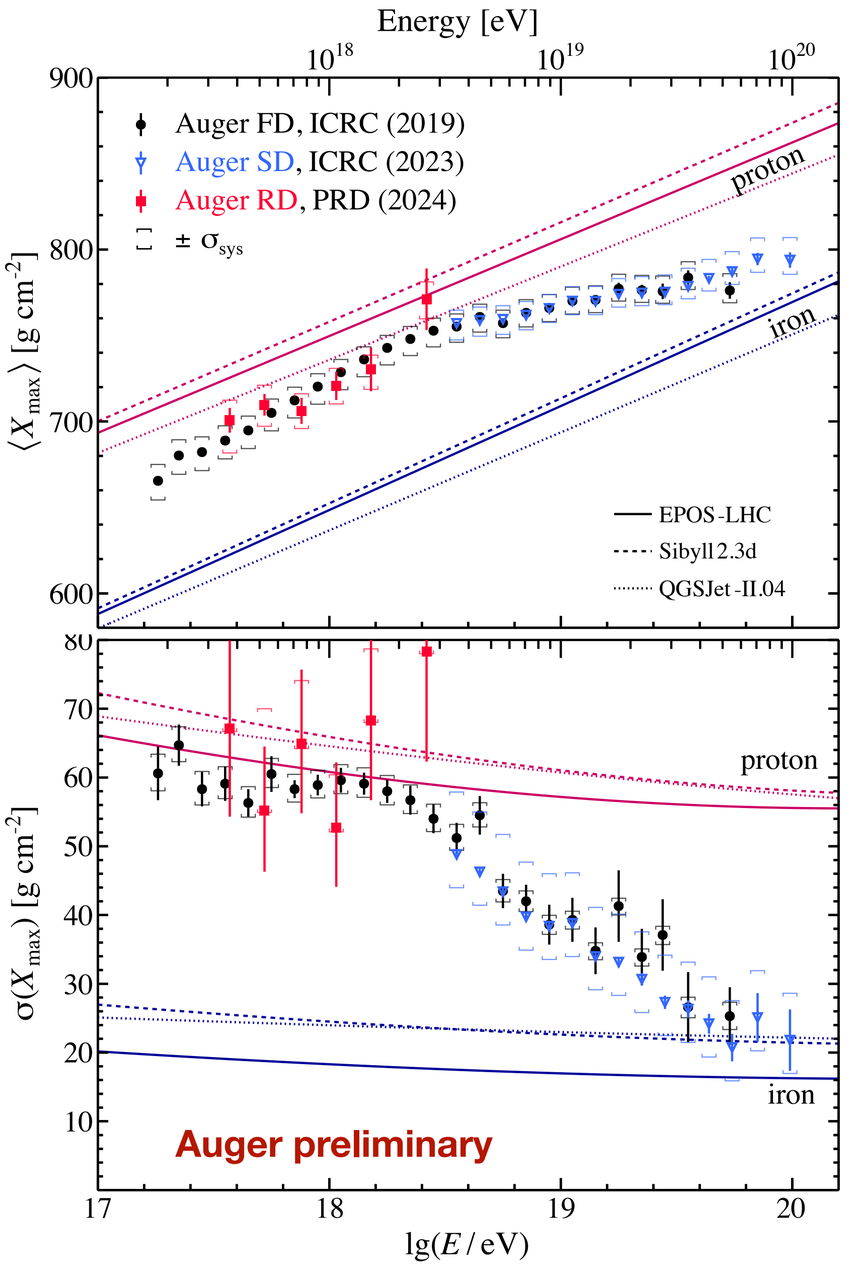

(FD telescopes: PRD 90 (2014), 122005 & 122005, updated ICRC 2023)

(SD risetime: Phys. Rev. D96 (2017), 122003)

(AERA/radio: Phys. Rev. Lett. 132 (2024) 021001 & PRD 2024)

(SD DNN: ICRC 2023, to be published)

Model calculations for mass composition and flux

(Auger, JCAP 05 (2023) 024 & JCAP 01 (2024) 022 & JCAP 07 (2024) 094)

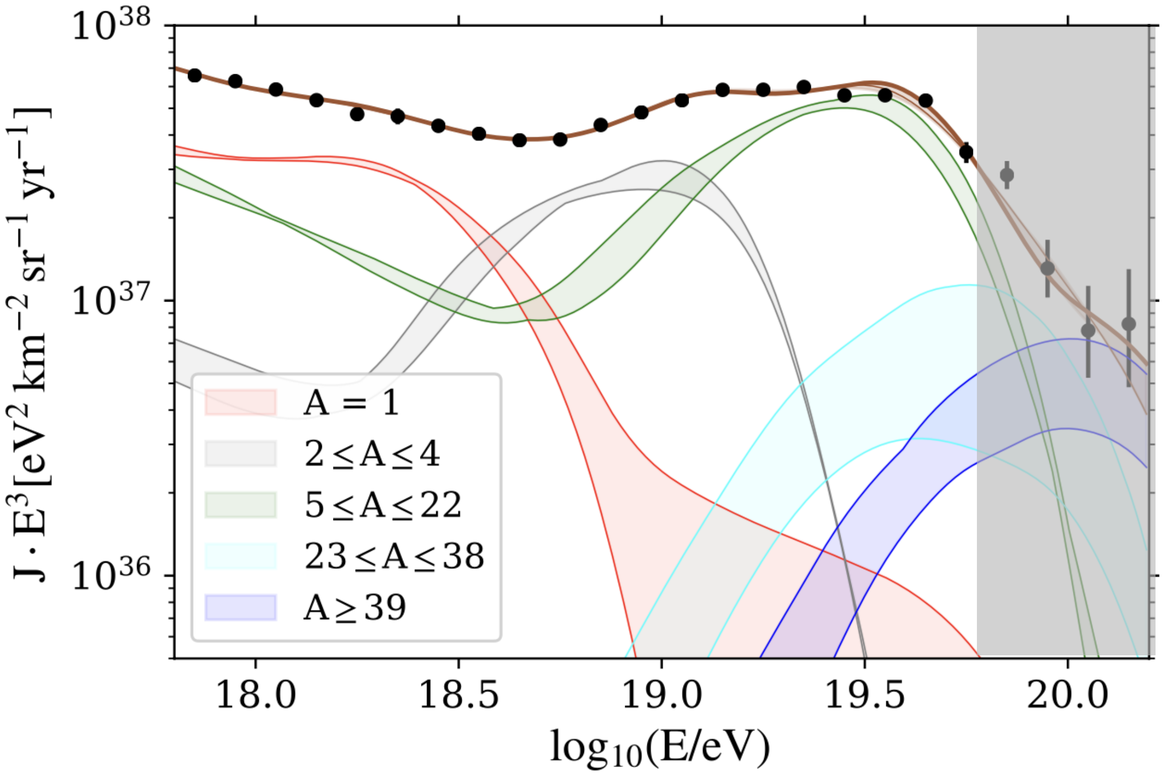

Flux suppression due mainly to limit of injection energy of sources

New problem of limited source variance *(Ehlert et al. PRD 2023)*

Assumption: source injection spectra universal in rigidity $R = E/Z$ (acceleration, scaling with charge Z)

$$E_{\mathrm{p,cut}} = 1.4 \ldots 1.6 \times 10^{18}\,\mathrm{eV}$$

Exceptionally hard injection spectrum (except for very strong mag. horizon)

$$\frac{\mathrm{d}N}{\mathrm{d}E} \sim E^{1.5\ldots2}$$

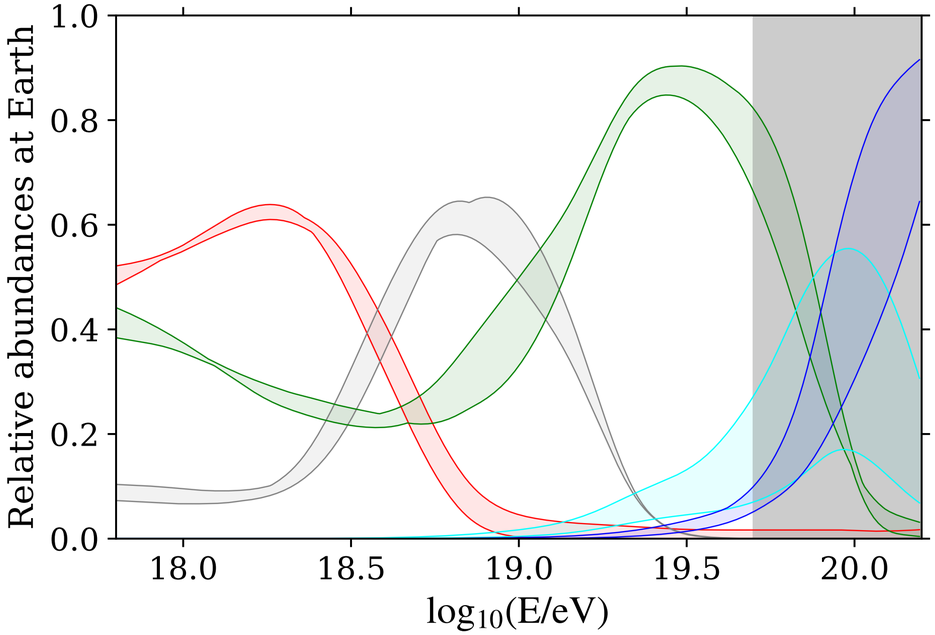

No direct composition data

Index depends on suppression function

(Comisso et al. ApJL 977 (2025) 18)

Cross-check of assumption of WB upper bound

(Waxman & Bahcall, Phys. Rev. D59 (1999) 023002)

- Extragalactic cosmic-ray protons extending to the highest energies ✗

- One interaction with photon field per proton in source or source region

- Source production spectrum similar to Fermi acceleration ✗

$$\frac{\mathrm{d}N}{\mathrm{d}E} \sim E^{-\gamma} \qquad \gamma = 1.8 \ldots 2.3$$

- Energy production rate (normalization) of 4 x 10^{44} erg Mpc^{-1} yr^{-1} ✓

(Waxman, ApJ 452 (1995) L1)

PIERRE AUGER OBSERVATORY

Size of neutrino detector (water, ice) for observing this flux has to be V ~ 1 km^3

Transition from galactic to extragalactic cosmic rays

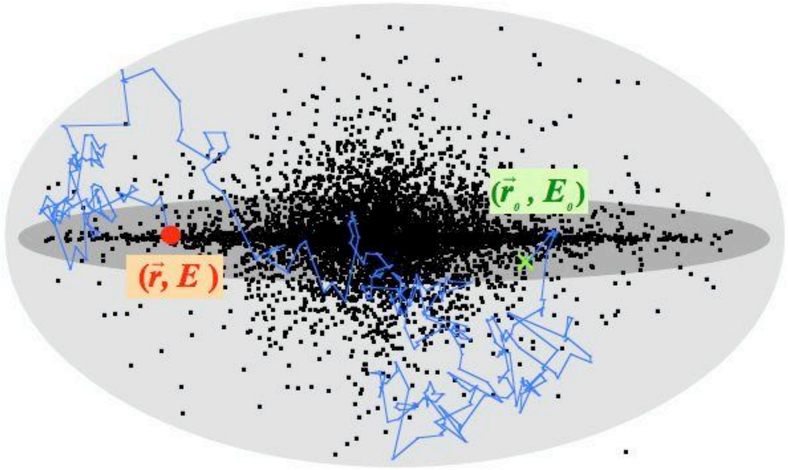

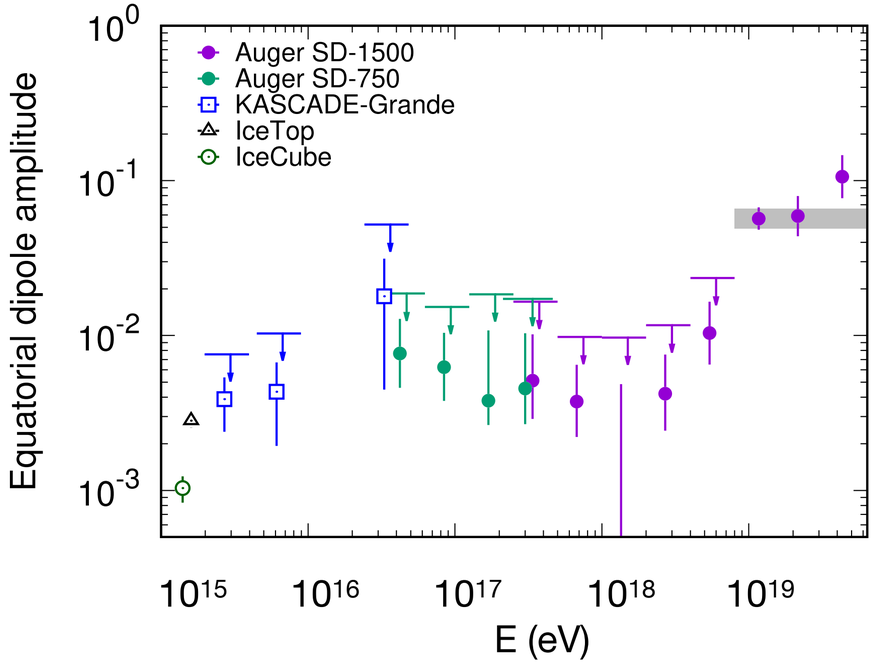

Expected anisotropy from escape from Galaxy

(Auger, ApJ 203, 2012, Giacinti et al. JCAP 2012, 2015)

Simulation: Sources in galactic plane

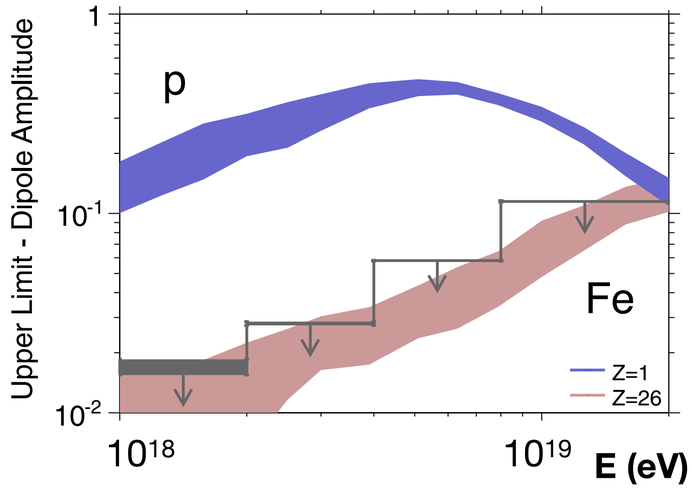

Large proton fraction just below $10^{18.5}$ eV and lack of anisotropy:

Transition from galactic to extragalactic sources below 10^{18} eV

None of these scenarios realized in nature

Dip model: Berezinsky et al.

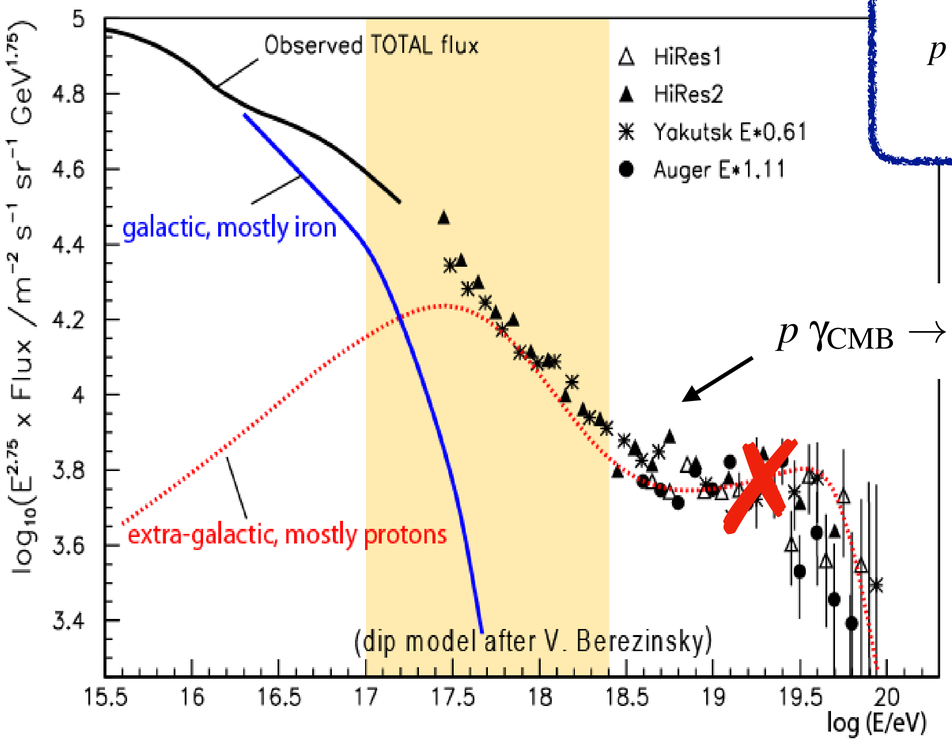

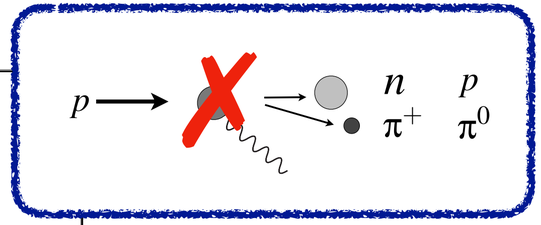

Neutrons leave sources

$$p\,\gamma_{\mathrm{CMB}} \rightarrow p\,e^{+}e^{-}$$

$$\frac{\mathrm{d}N_p}{\mathrm{d}E} \sim E^{-2.7}$$

(PRD 74 (2006) 043005)

Ankle model: Hillas, Wolfendale et al.

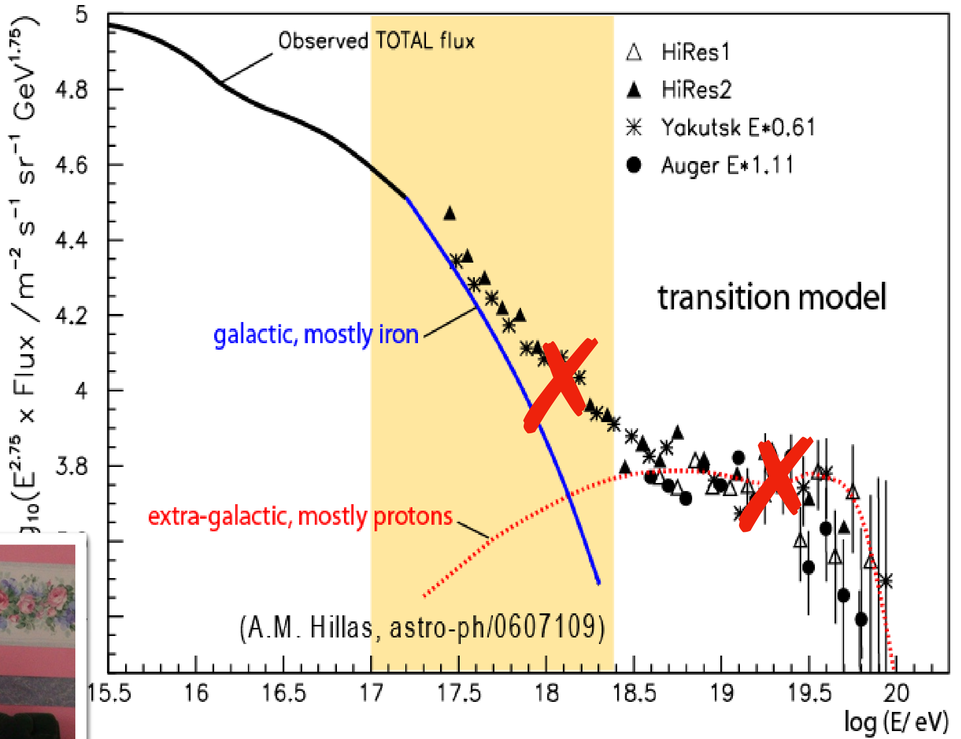

$$\frac{\mathrm{d}N_p}{\mathrm{d}E} \sim E^{-2.3}$$

(J. Phys. G31 (2005) R95)

It’s all about the mass composition

Mass composition results of Auger Observatory

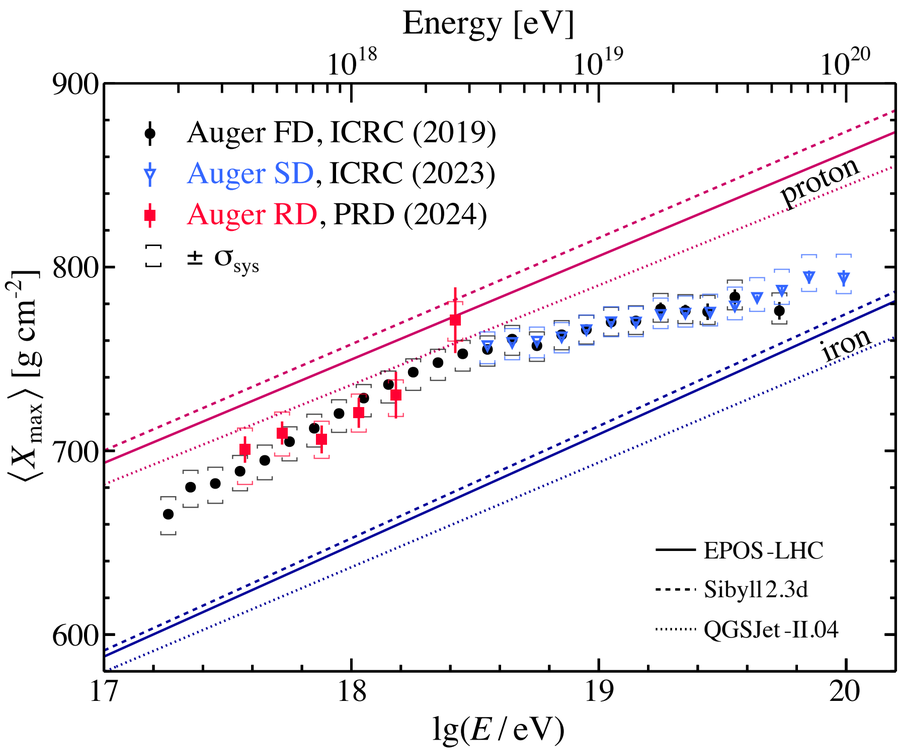

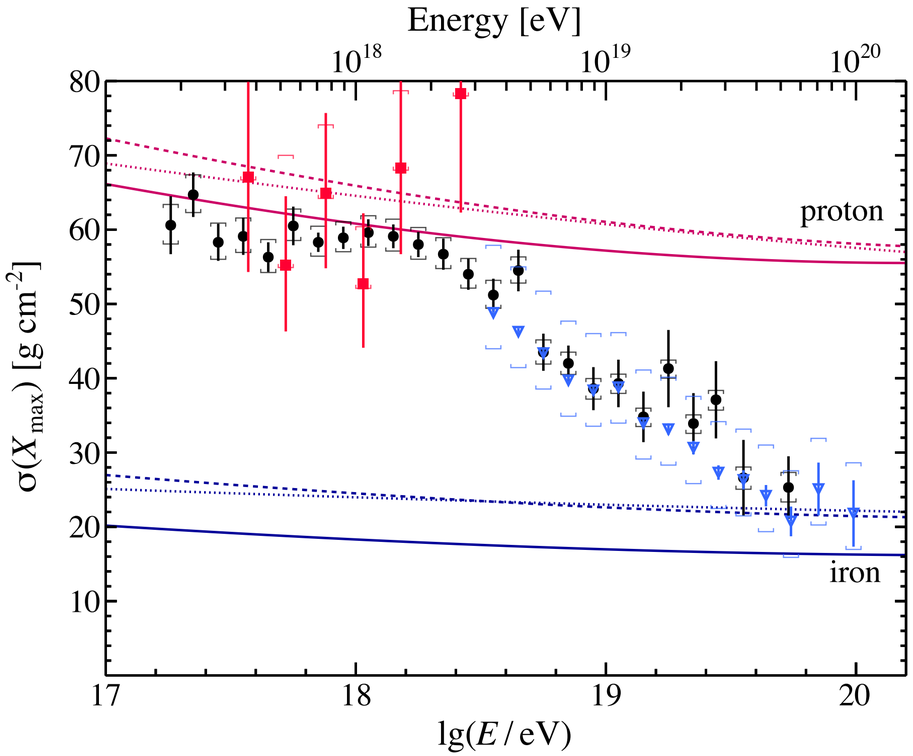

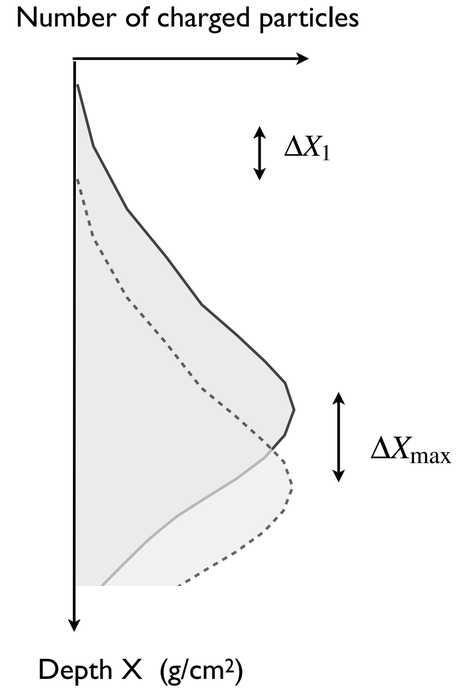

$$\frac{dP}{dX_1} = \frac{1}{\lambda_{int}} e^{-X_1/\lambda_{int}}$$

Important: LHC-tuned interaction models used for interpretation

$$\sigma_{X_1,p} \sim 45 - 55\,\mathrm{g/cm^2}$$
$$\sigma_{X_1,Fe} \sim 10\,\mathrm{g/cm^2}$$
$$(E \sim 10^{18}\,\mathrm{eV})$$

(FD telescopes: PRD 90 (2014), 122005 & 122005, updated ICRC 2023)

(SD risetime: Phys. Rev. D96 (2017), 122003)

(AERA/radio: PRL & PRD 2023)

(SD DNN: ICRC 2023, to be published)

Energy dependence – Elongation rate theorem

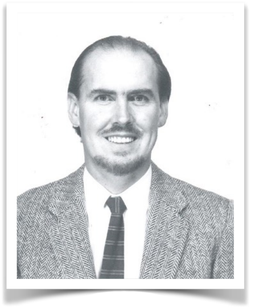

John Linsley

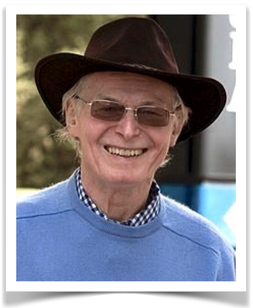

Alan Watson

(Linsley, Watson PRL46, 1981)

$$D_{10}^{\mathrm{had}} = D_{10}^{\mathrm{em}}(1 - B_n - B_\lambda)$$

$$B_n = \frac{d\ln n_{\mathrm{tot}}}{d\ln E}$$

p-air multiplicity

$$B_\lambda = -\frac{1}{X_0}\frac{d\lambda_{\mathrm{int}}}{d\ln E}$$

p-air cross section

$$D_{10} = \frac{\Delta\langle X_{\max}\rangle}{\Delta\log_{10}E}$$

$$D_{10} = \frac{\Delta\langle X_{\max}\rangle}{\Delta\log_{10}E} \approx 87\,\mathrm{g/cm^2}$$

$$D_{10} \approx 50 - 60\,\mathrm{g/cm^2}$$

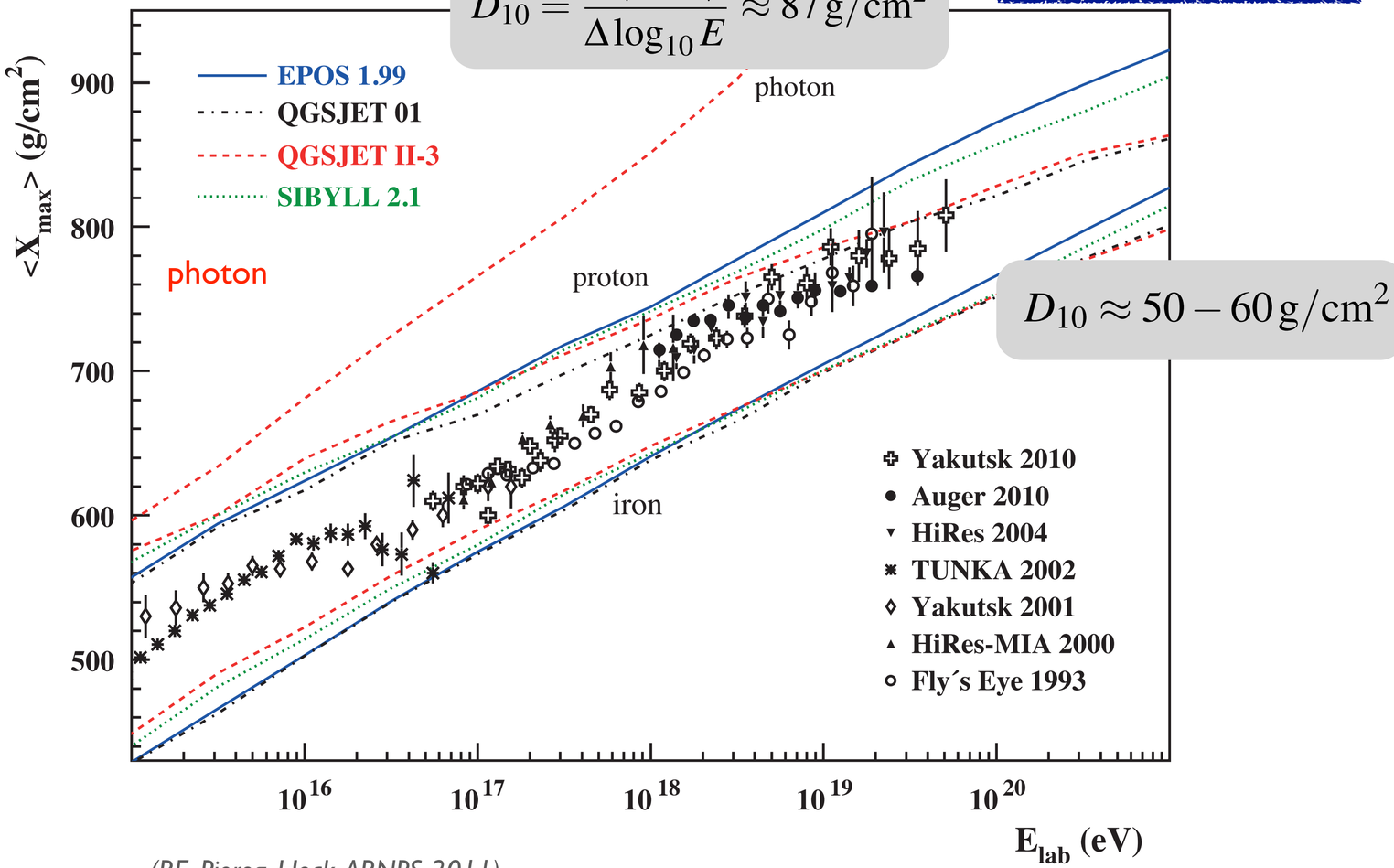

(RE, Pierog, Heck, ARNPS 2011)

LHC and charged particle distribution in pseudorapidity

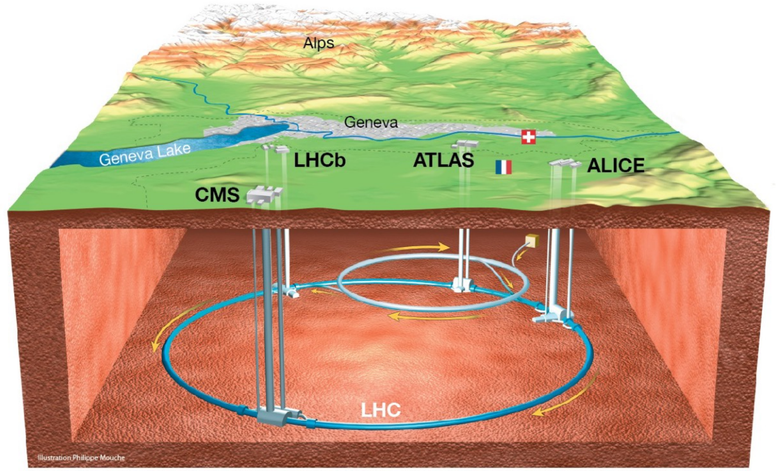

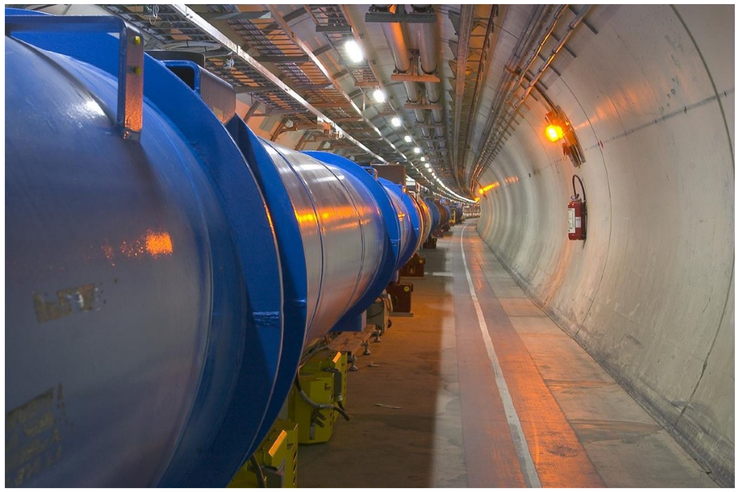

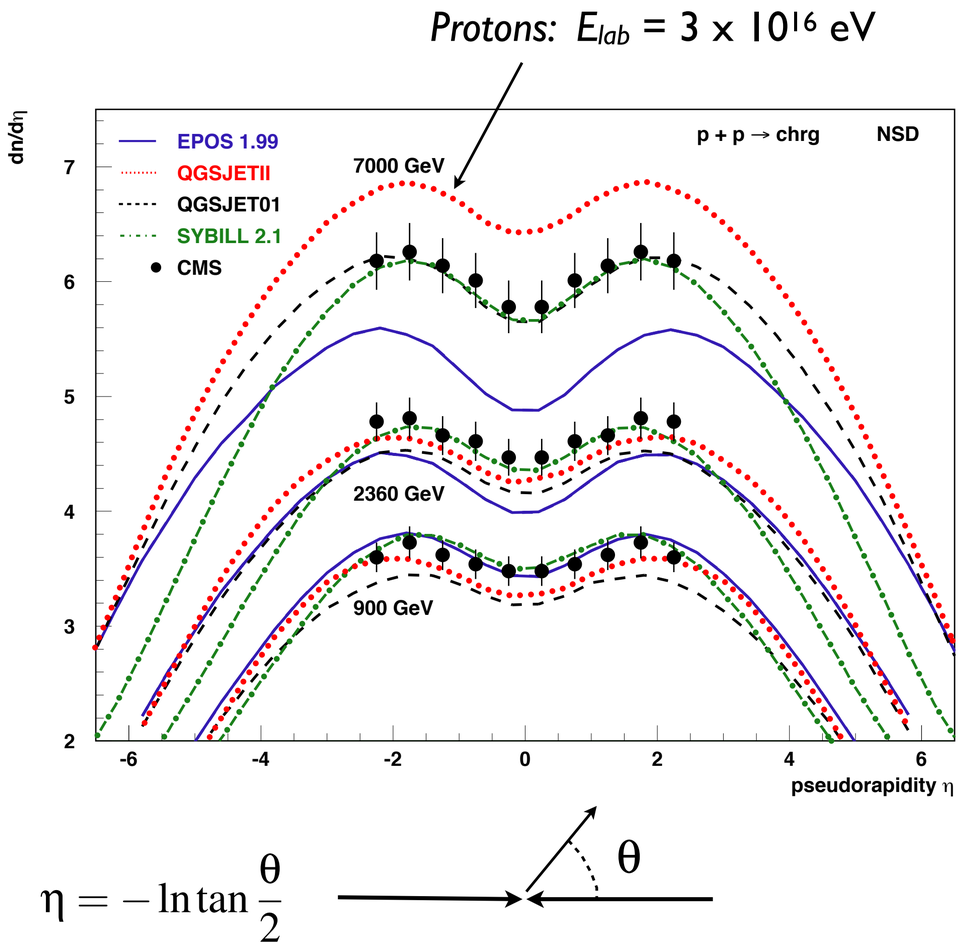

$$\eta = -\ln\tan\frac{\theta}{2}$$

Detailed LHC comparison

(D'Enterria et al., APP 35, 2011)

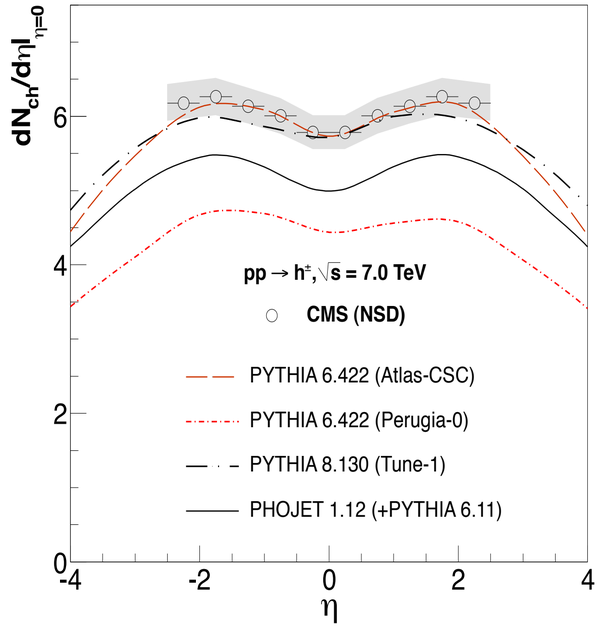

Models for air showers typically better in agreement with LHC data

Cross section measurements at LHC

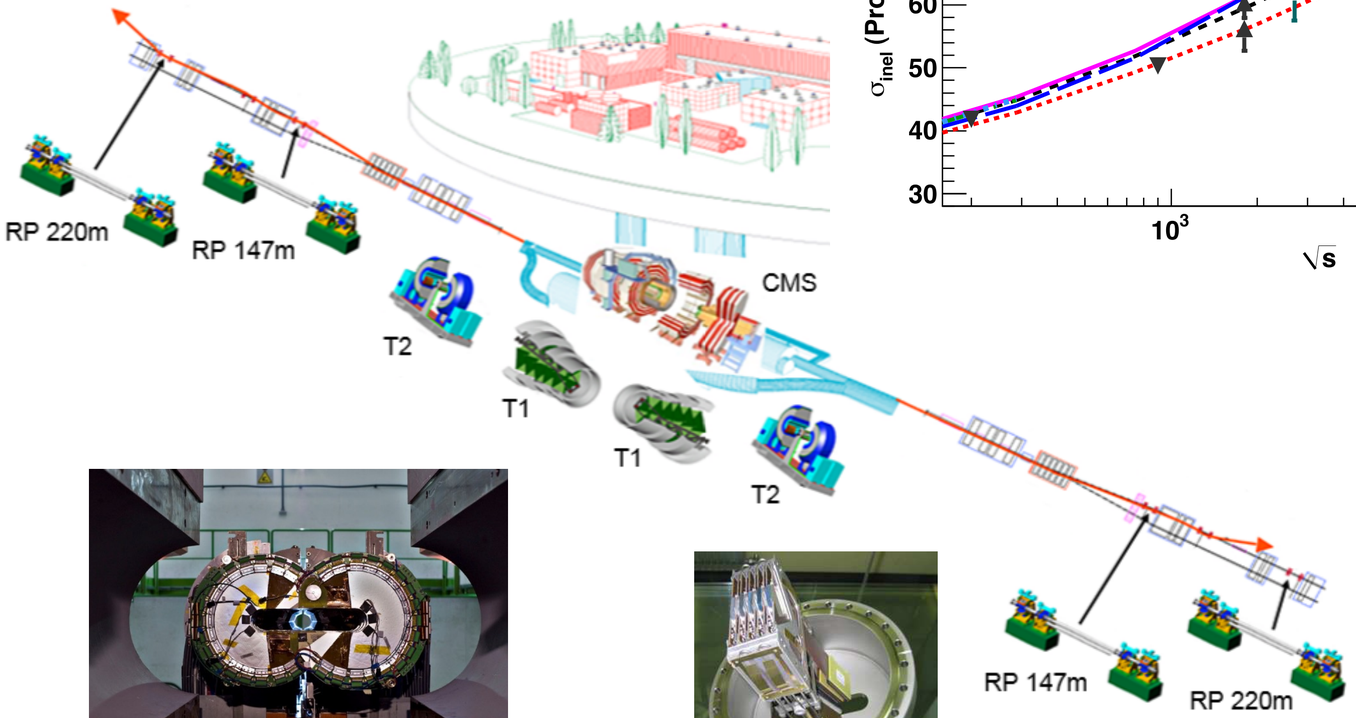

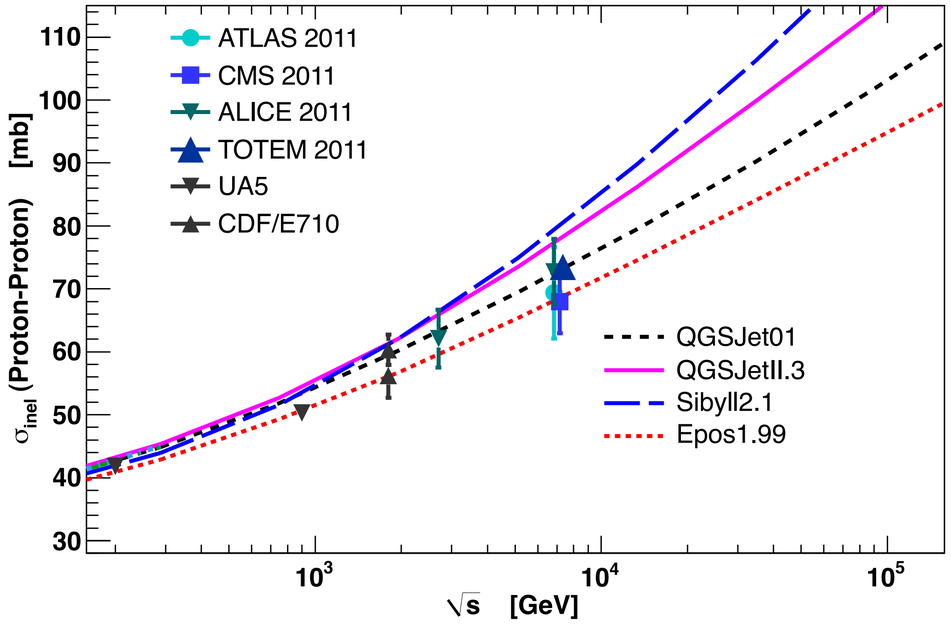

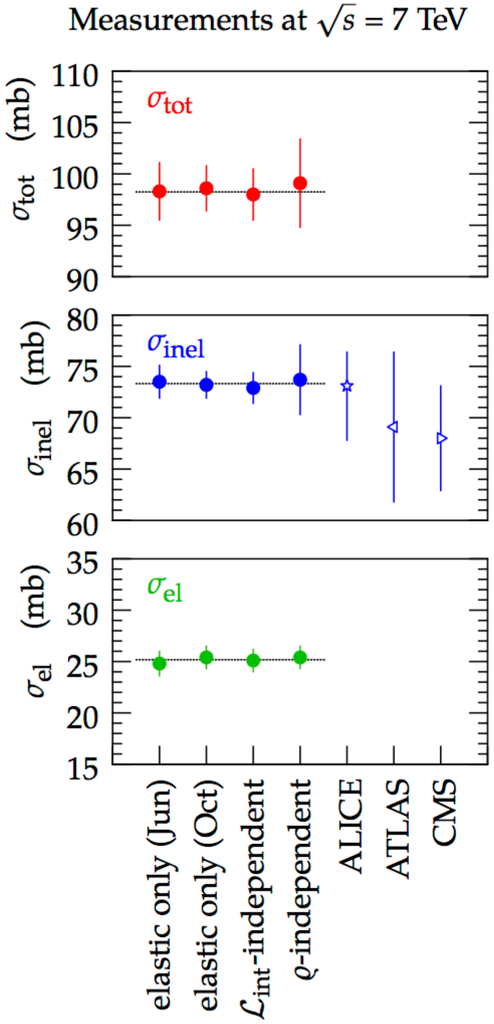

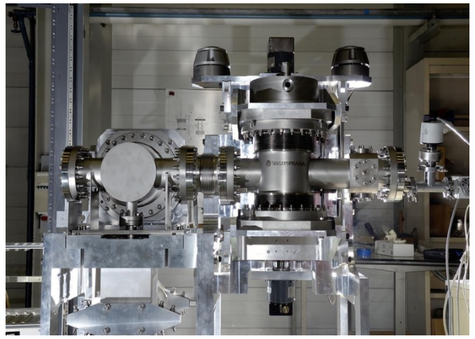

LHCf: very forward photon production at 7 TeV

Arm 2

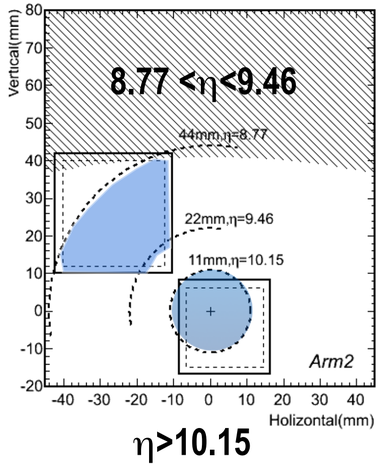

η>10.15

The LHCf experimental setup

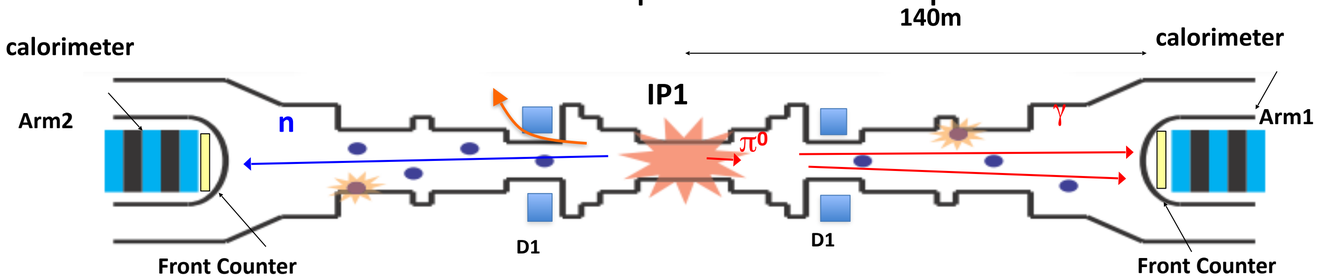

Arm 1

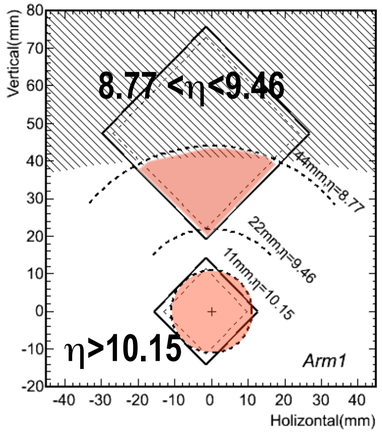

$$pp \rightarrow \gamma X$$

(LHCf Collab., Phys. Lett. B 703, 2011)

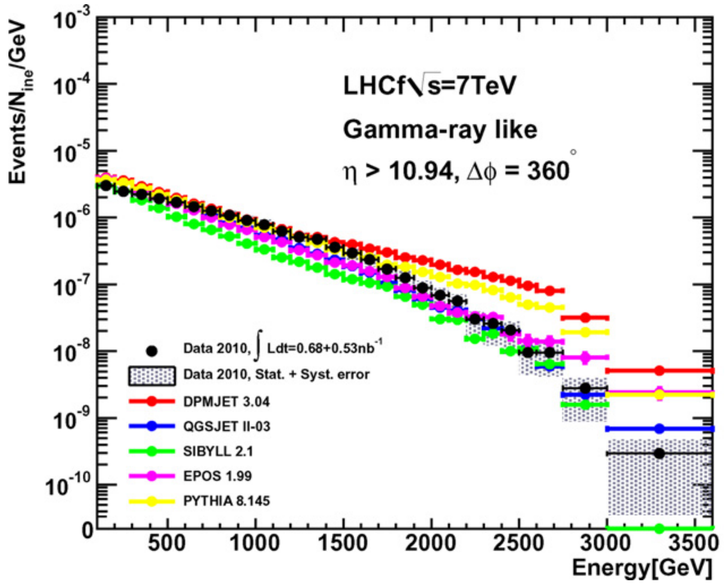

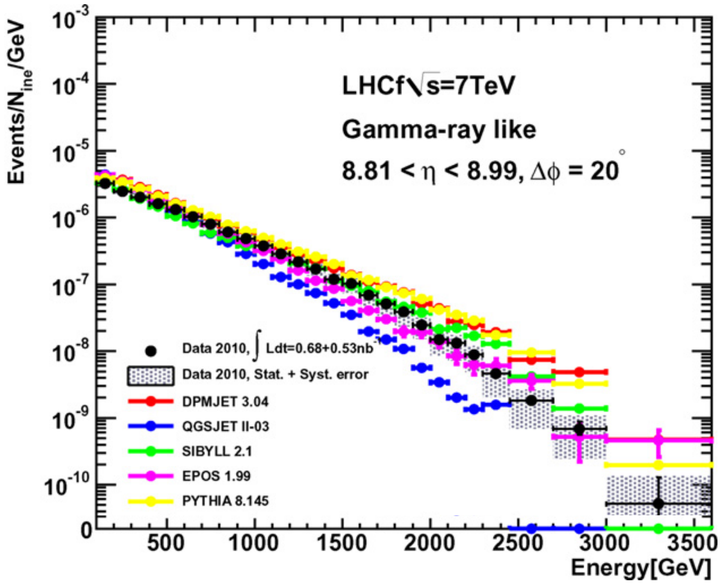

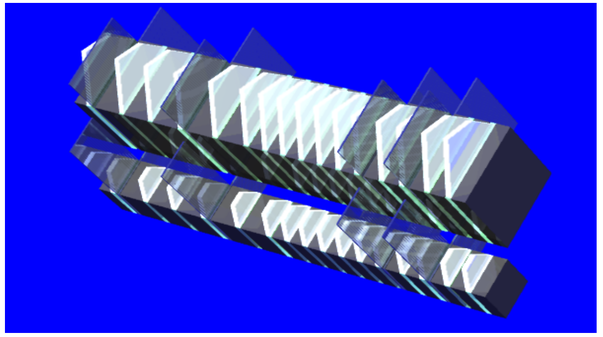

Combined CMS and TOTEM measurements

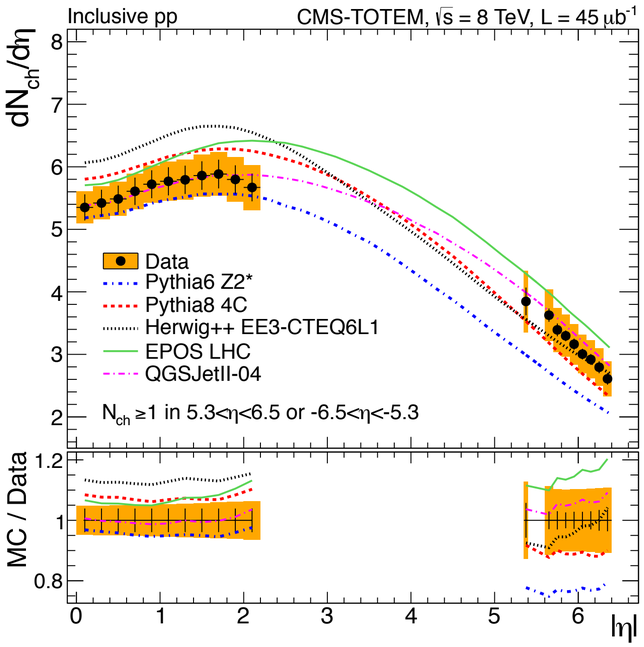

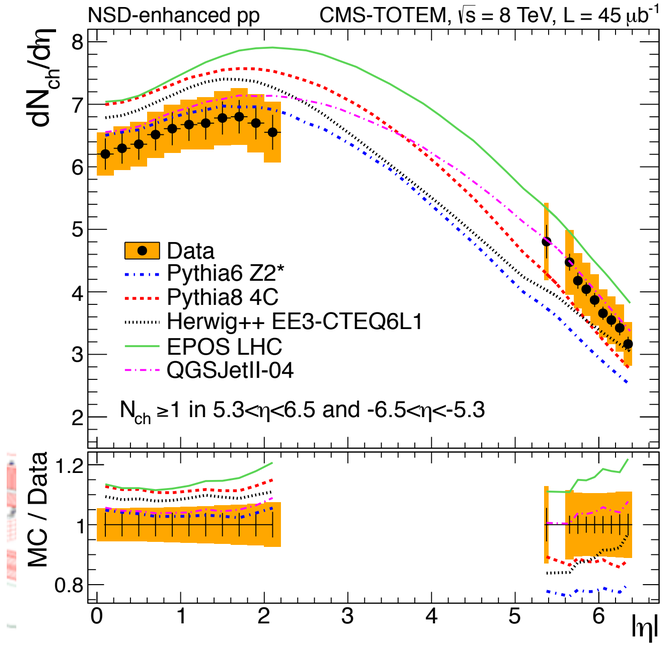

Nominal vertex

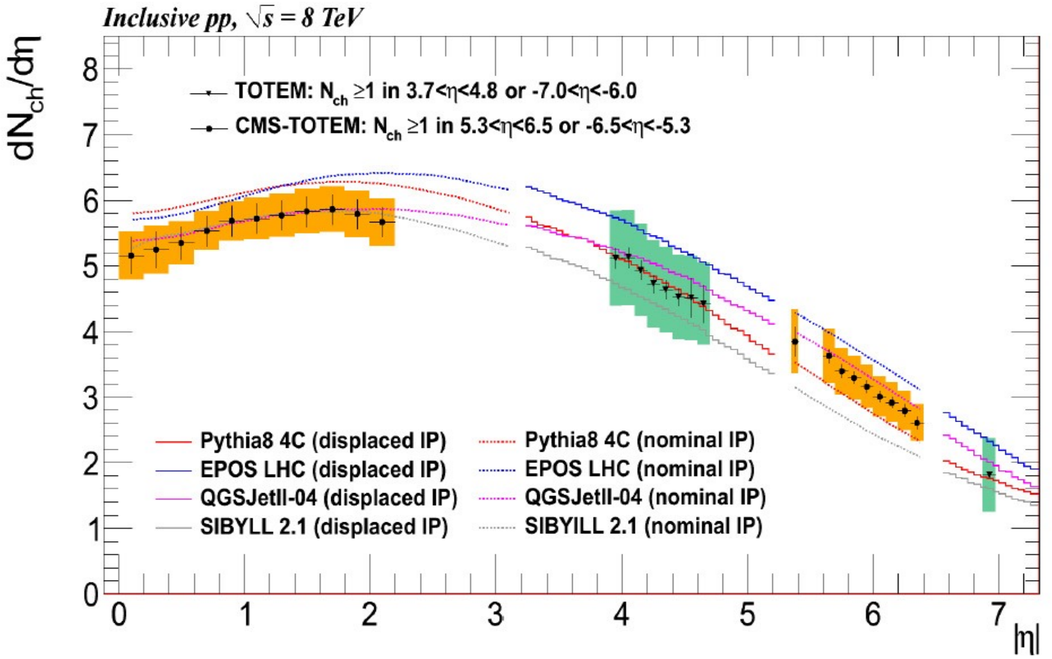

Shifted vertex

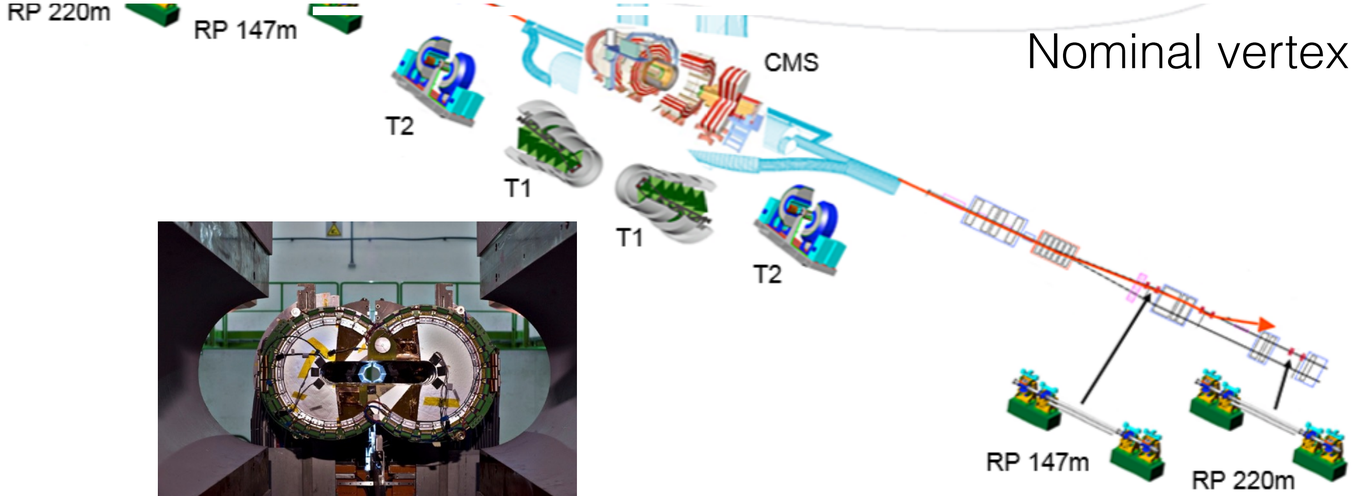

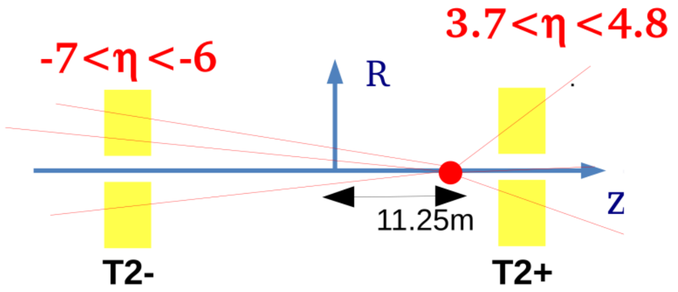

Importance of LHC data for composition interpretation

pre-LHC models

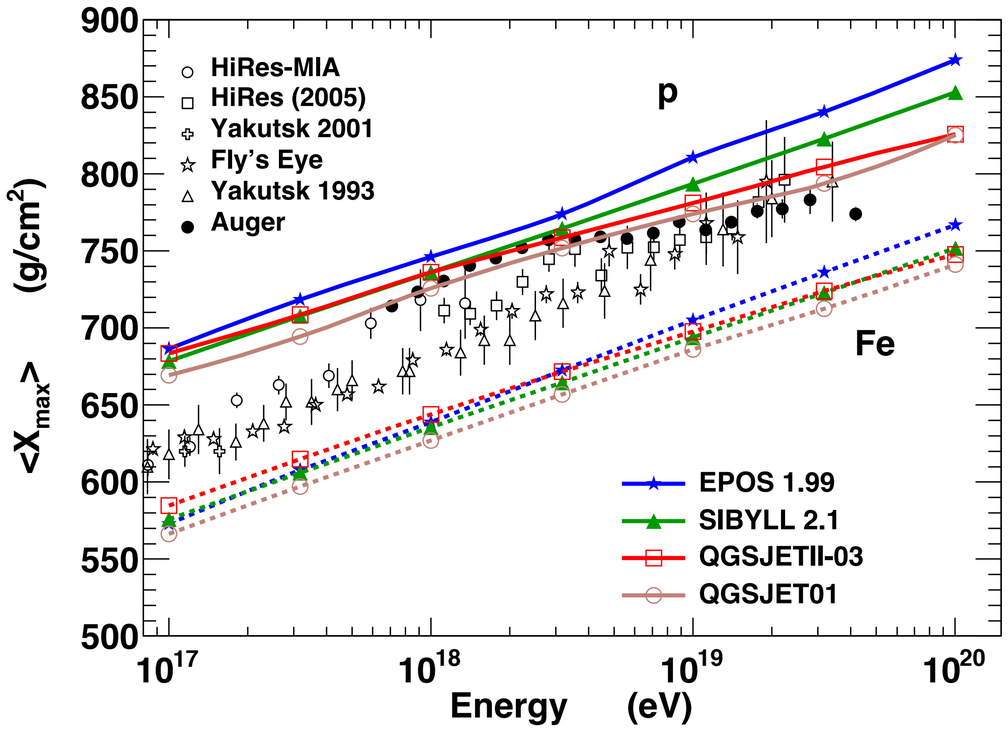

post-LHC models

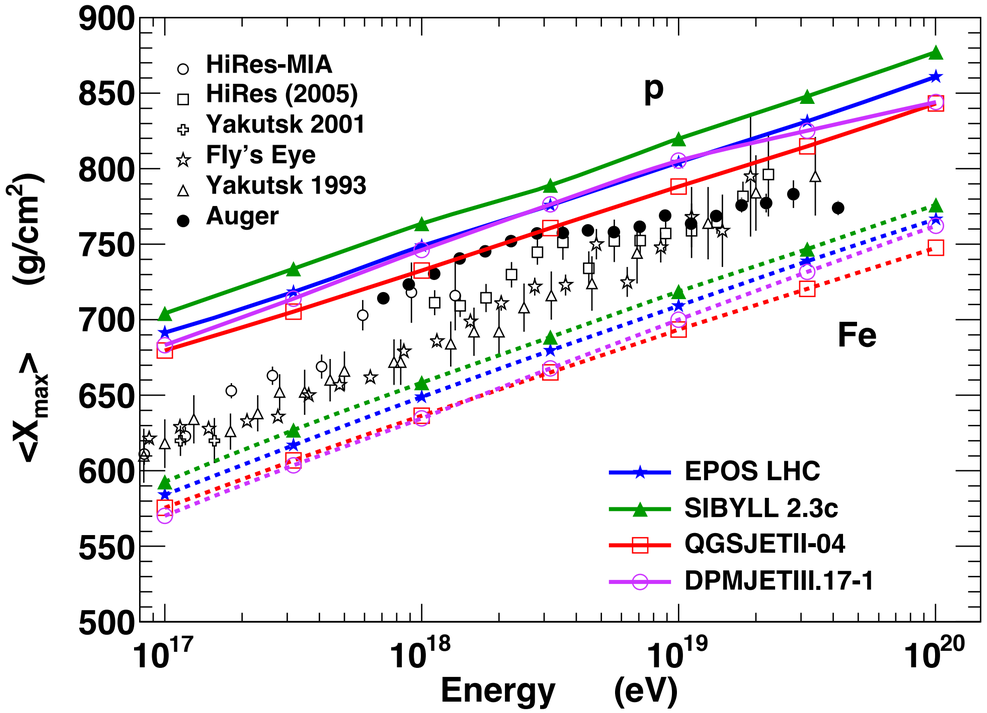

(Pierog, ICRC 2017)

Sys. X_{max} uncertainty

Auger: $\Delta X_{\max} = -10\,\mathrm{g/cm^2} \; +8\,\mathrm{g/cm^2}$

TA: $\Delta X_{\max} = \pm 20\,\mathrm{g/cm^2}$

LHC-tuned models should be used for data interpretation

(see also discussion Lipari, Phys.Rev.D 103 (2021) 103009)

Discovery of first continuously emitting source NGC 1068

Significance ~4.2 σ

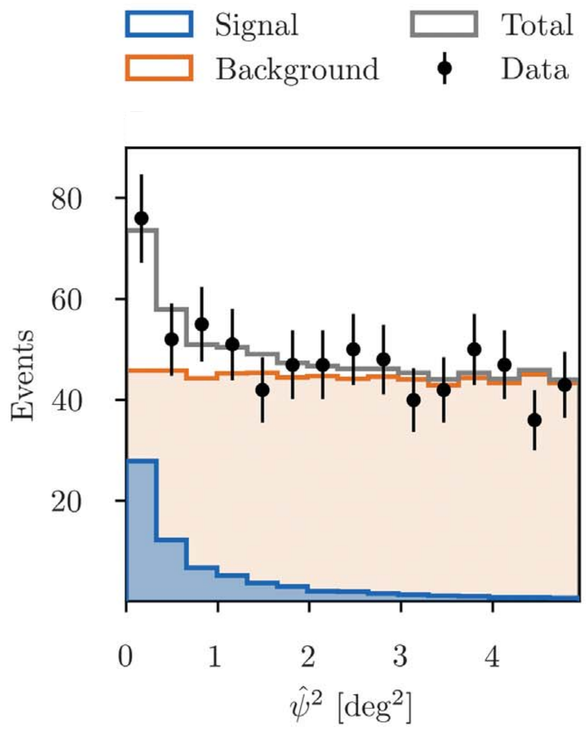

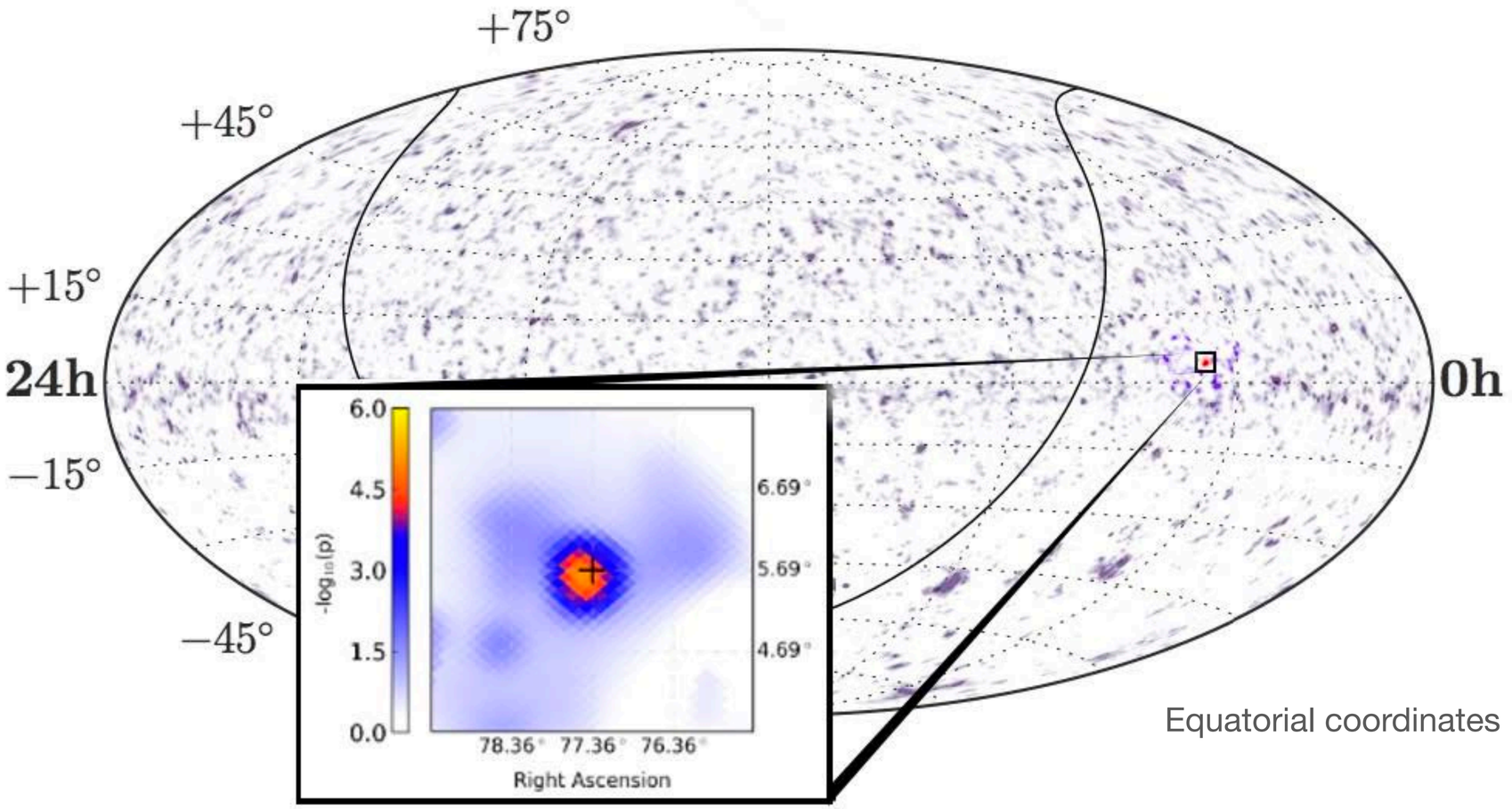

Equatorial coordinates

79^{+22}_{-20} Neutrinos

IceCube Collaboration, *Science* **378**, 538–543 (2022)

NGC 1068 (M77)

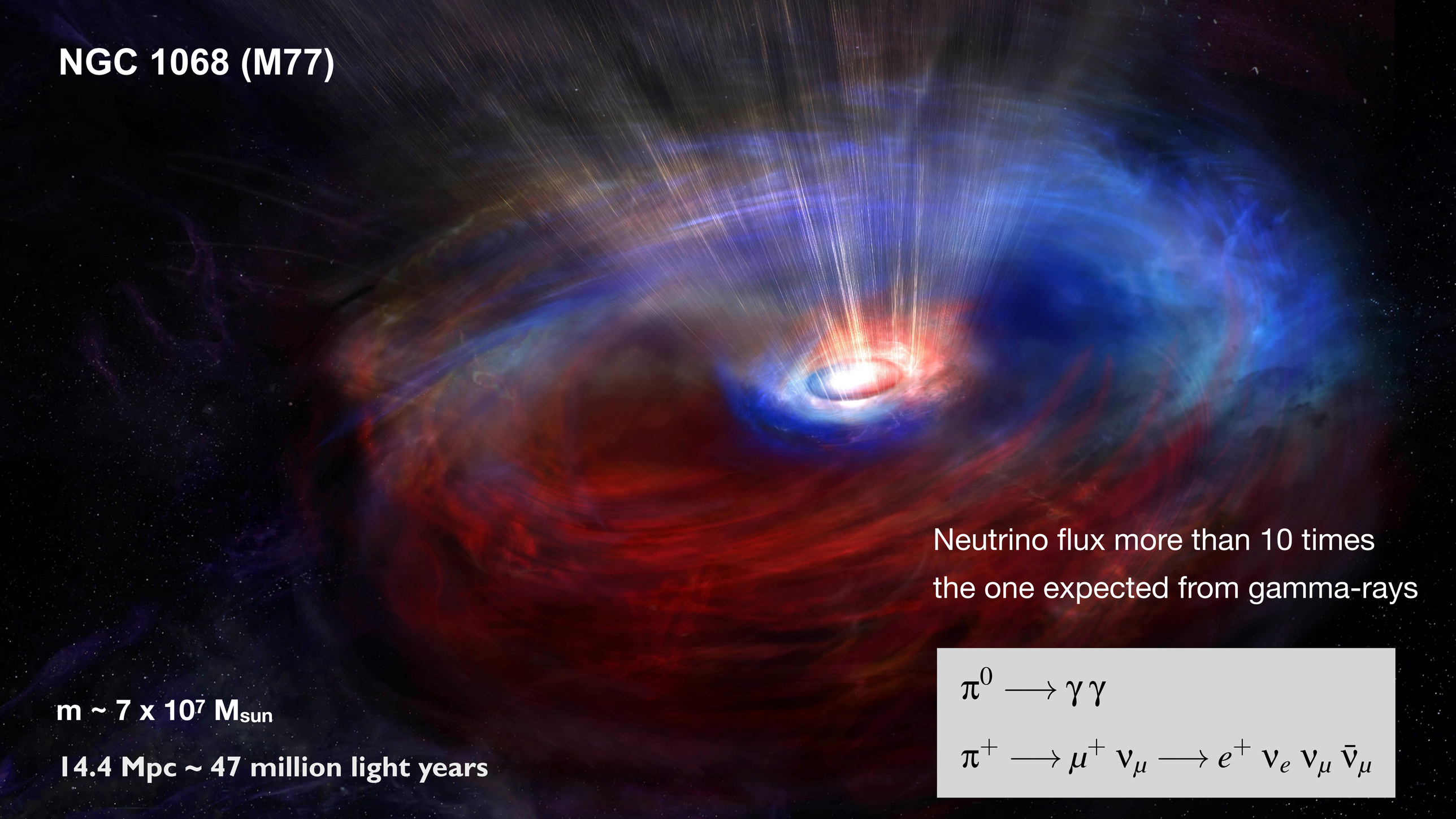

Neutrino flux more than 10 times
the one expected from gamma-rays

$$\pi^0 \longrightarrow \gamma\,\gamma$$

$$\pi^+ \longrightarrow \mu^+\,\nu_\mu \longrightarrow e^+\,\nu_e\,\nu_\mu\,\bar{\nu}_\mu$$

m ~ 7 x 10^7 M_{sun}

14.4 Mpc ~ 47 million light years

Cores of active galaxies (AGN) as cosmic accelerators

Radiatively inefficient accretion flows:
acceleration of electrons and protons
in the high field regions associated
with the accretion disk and the optically
thick corona (0.1 pc) emitting most of the X-rays

Core is the target for neutrino production
and gamma-ray obscured (gamma-rays absorbed)

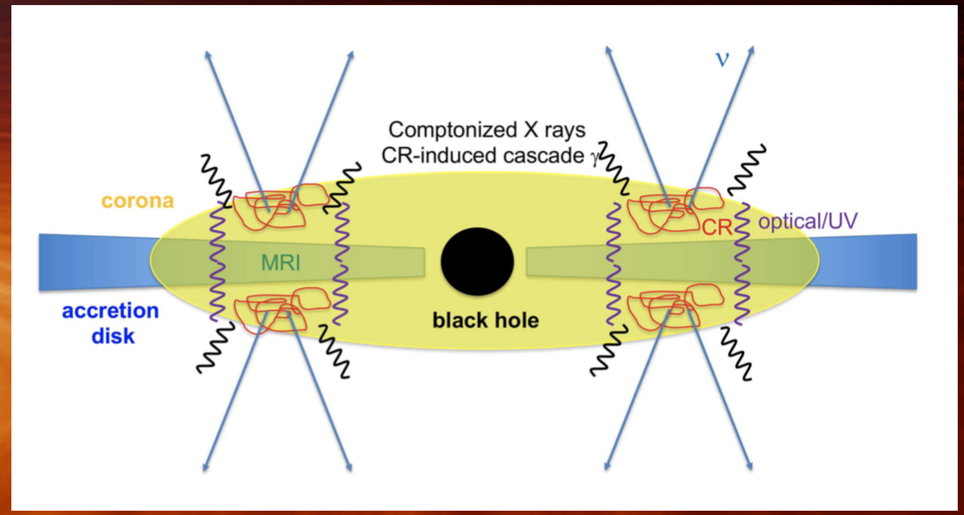

(Halzen, 2022)

A new generation of source models

Constraints following from mass composition

(Auger, JCAP 05 (2023) 024 & JCAP 01 (2024) 022 & JCAP 07 (2024) 094)

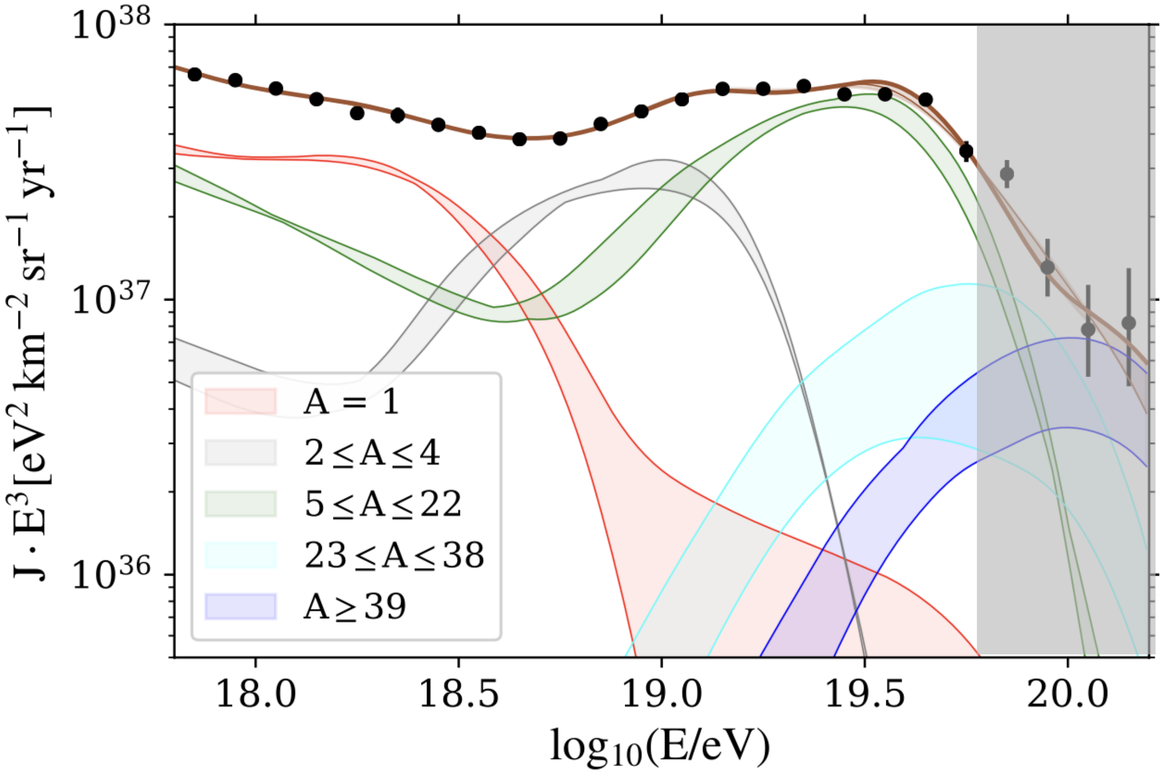

Flux suppression due mainly to limit of injection energy of sources

New problem of limited source variance *(Ehlert et al. PRD 2023)*

Assumption: source injection spectra universal in rigidity $R = E/Z$ (acceleration, scaling with charge Z)

$$E_{\mathrm{p,cut}} = 1.4 \ldots 1.6 \times 10^{18}\,\mathrm{eV}$$

Exceptionally hard injection spectrum (except for very strong mag. horizon)

$$\frac{\mathrm{d}N}{\mathrm{d}E} \sim E^{1.5\ldots2}$$

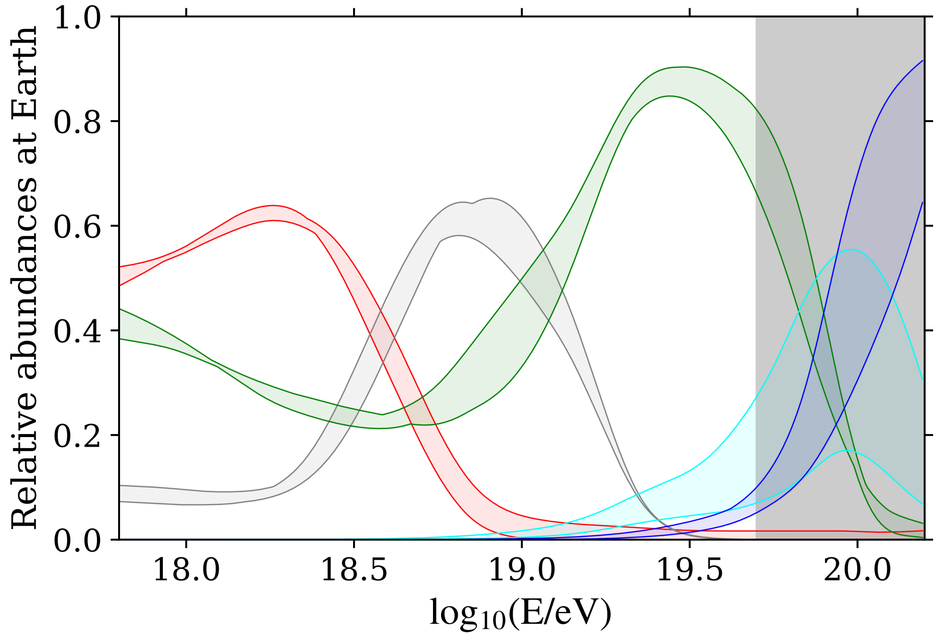

No direct composition data

Index depends on suppression function

(Comisso et al. ApJL 977 (2025) 18)

Importance of source regions

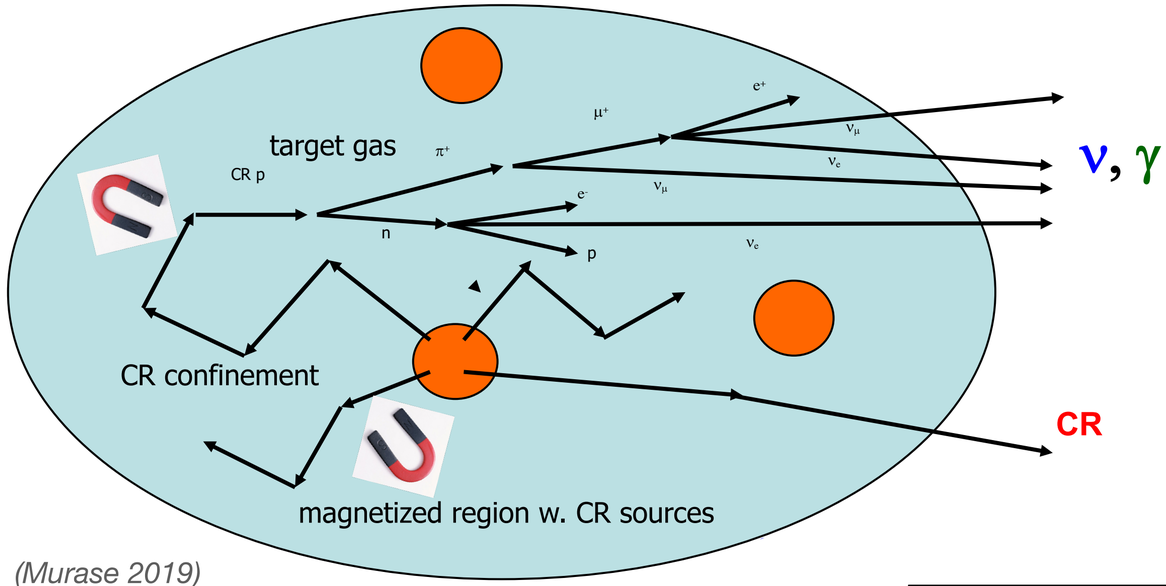

(Murase 2019)

Interplay between
- **Energy-dependent escape from source region**
- **Interaction with high photon densities**
- **Energy loss and secondary particle production**

$$\frac{\mathrm{d}N_{\mathrm{ini}}}{\mathrm{d}E} \sim E^{-1}$$

Nuclear disintegration in source region (scaling with mass *A*)

(Globus et al. 2015, Unger et al. 2015, Fang & Murase 2017)

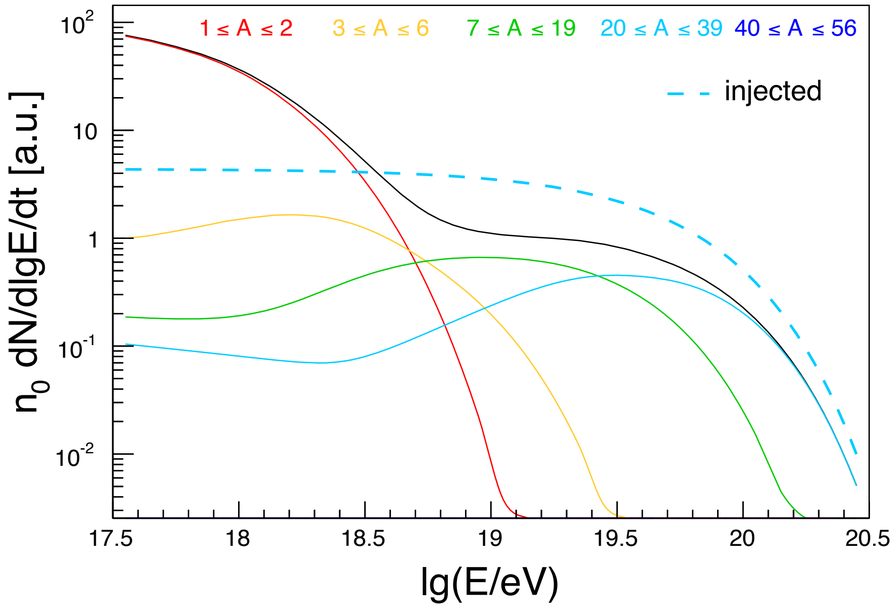

(Unger, Farrar, Anchordoqui, PRD 92, 2015)

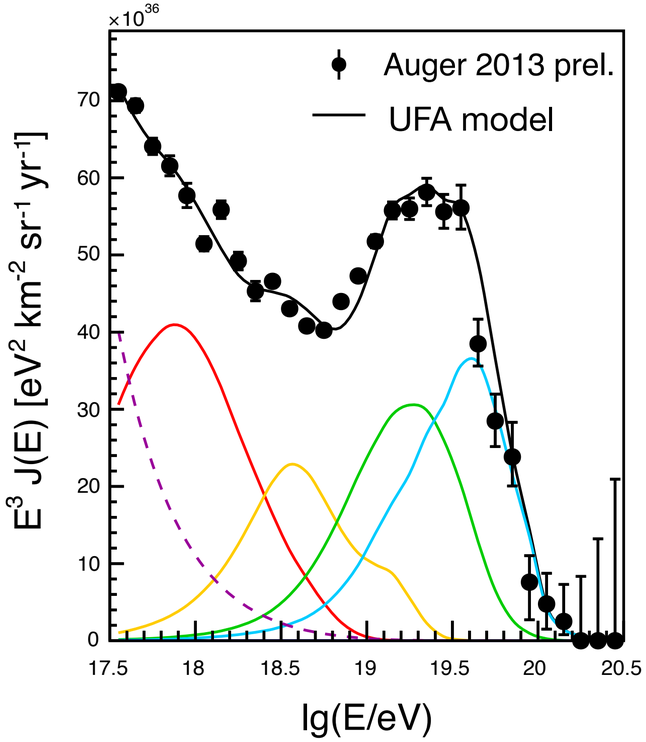

New generation of complex model scenarios

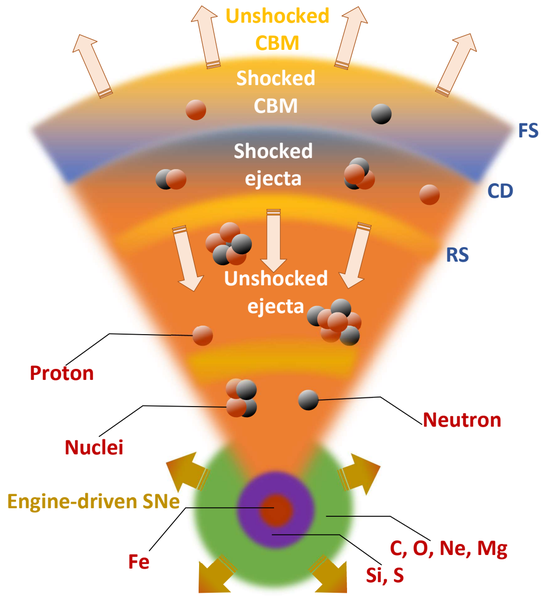

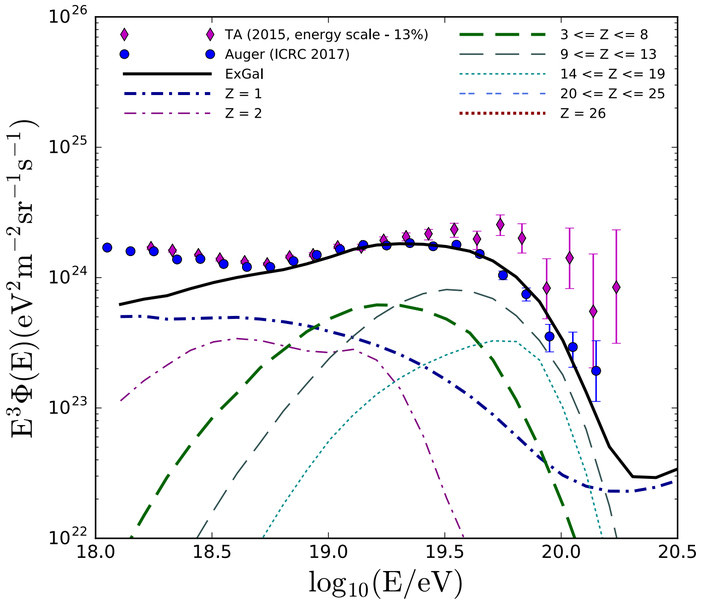

Interplay between **confinement in source** and disintegration of nuclei: hard energy spectra

(Aloisio et al. 2014, Taylor et al. 2015, Globus et al. 2015, Unger et al. 2015, Fang & Murase 2017)

Reverse shock scenario in **low-luminosity long GRBs**

(Zhang, Murase et al 2019+)

Tidal disruption events (TDEs) of WD or carbon-rich stars

(Farrar, Piran 2009, Pfeffer et al. 2017, Zhang et al 2017)

One-shot acceleration in rapidly spinning **neutron stars**

(Arons 2003, Olinto, Kotera, Feng, Kirk …)

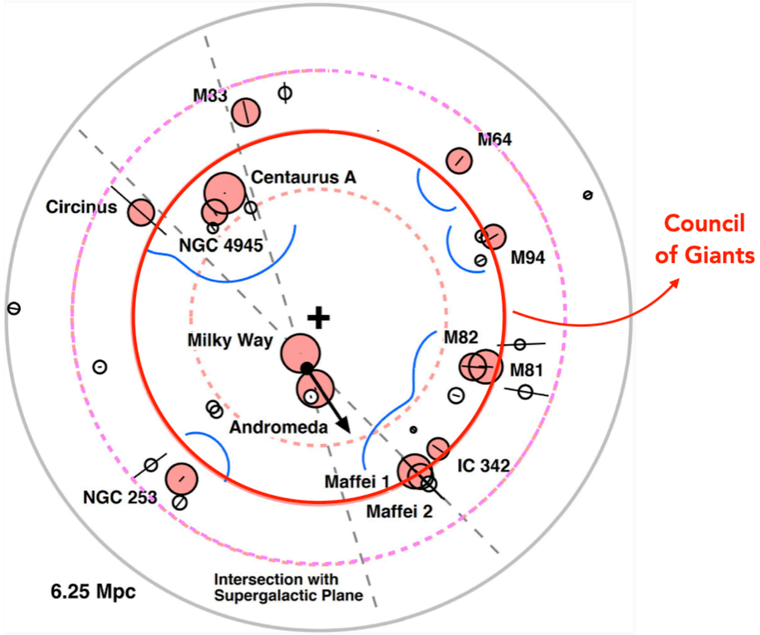

Cen-A bust & **deflection on Council of Giants**, solving isotropy and source diversity problem

(Taylor et al. 2023)

Relativistic reflection of existing CR population

(Biermann, Caprioli, Wykes, 2012+, Blandford 2023)

Latest addition – binary neutron star mergers

- Universal Maximum Rigidity is natural
  - $M_{BNS} = (2.64 \pm 0.14) M_\odot$
  - Gravitationally-driven dynamo
  - strong magnetic fields

Kiuchi+ NatureAstron23

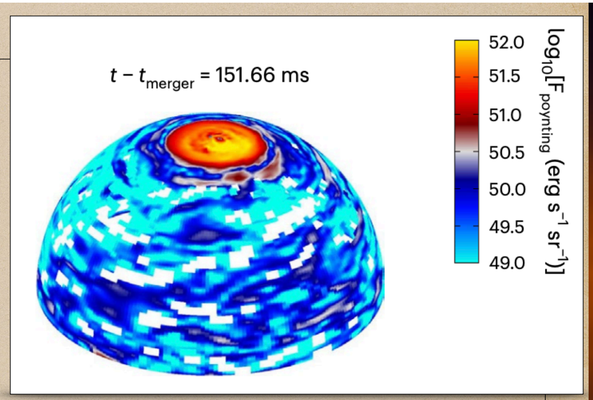

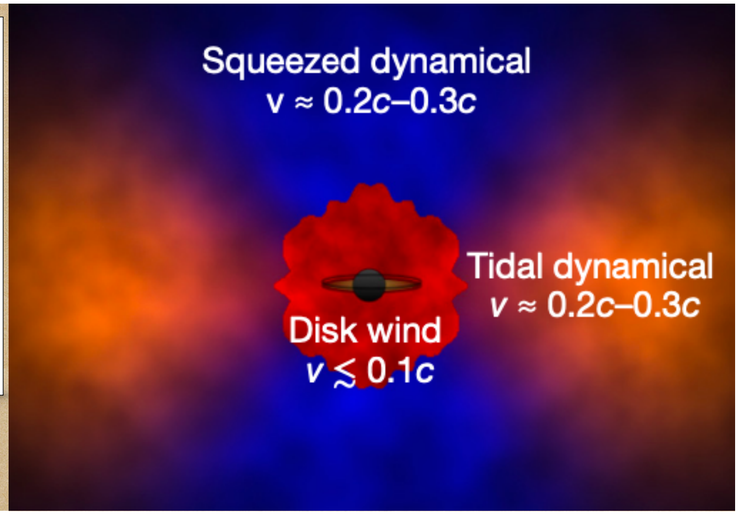

- Energy injection rate: (obs ≈ 6×10^{44} erg Mpc^{-3} yr^{-1})
  - BNS rate $\Gamma_{NSmerg} \approx 10$–$1700$ Gpc^{-3} yr^{-1} ✔ if $\Gamma_{NSmerg} \gtrsim 100$ Gpc^{-3} yr^{-1}
  - Energy in jet alone $E_j \approx 10^{51.5}$ erg (Kiuchi+23)
- Effective source density: ✔ as long as magnetic smearing

	Powerful AGN	long GRBs	TDEs	Accretion Shocks	BNS mergers
$n_S \gtrsim 10^{-3.5}$ Mpc^{-3}	[✘]	[✘]	?	?	✔
UHECR energy injection	✔	✘	?	?	[✔]
Ordinary galaxy	✘	✘	✔	[✘]	✔
Universal R_{max}	✘	✘	✘	✘	✔
Highest energy events?	✘	✘	✘	✘	✔

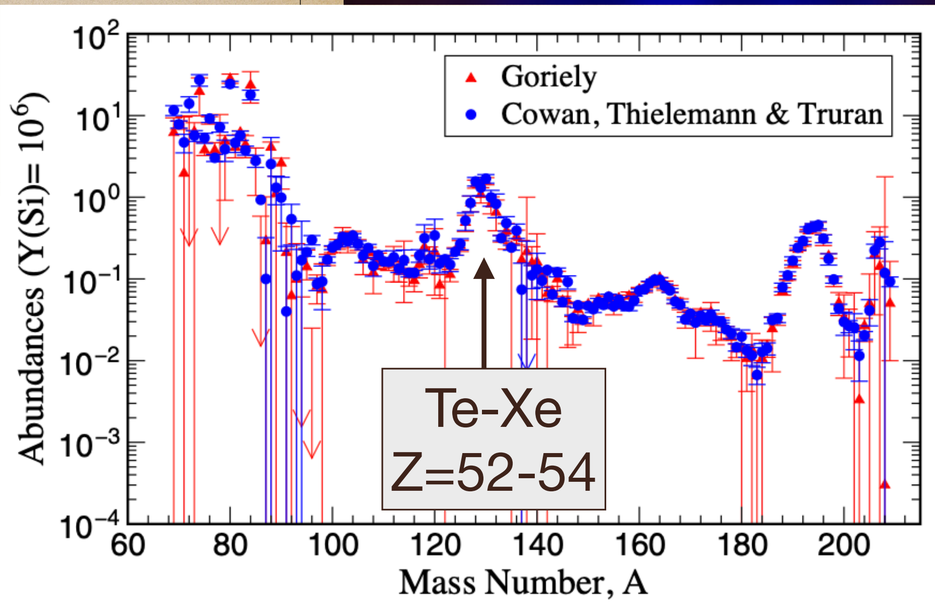

(Farrar Phys. Rev. Lett. 134 (2025) 081003)

Surprises in astroparticle physics – Summary

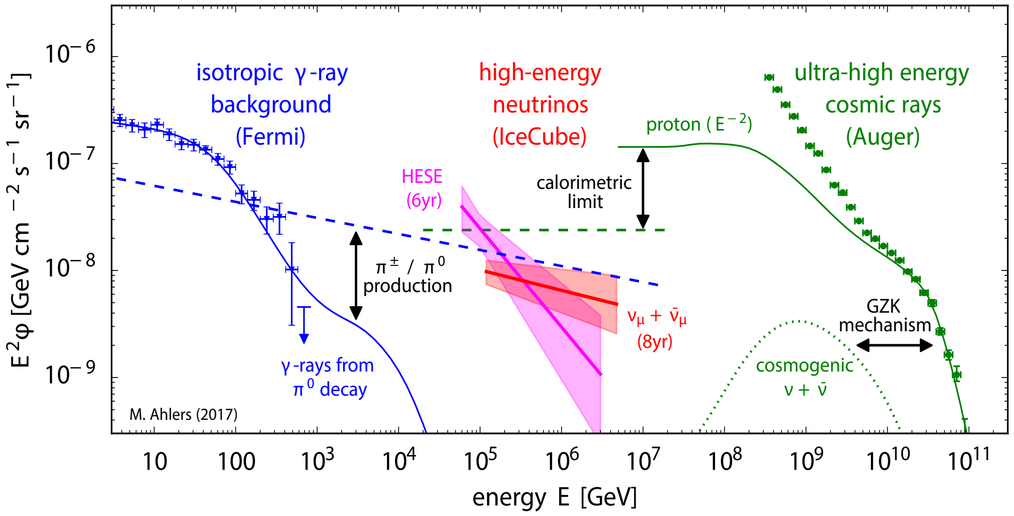

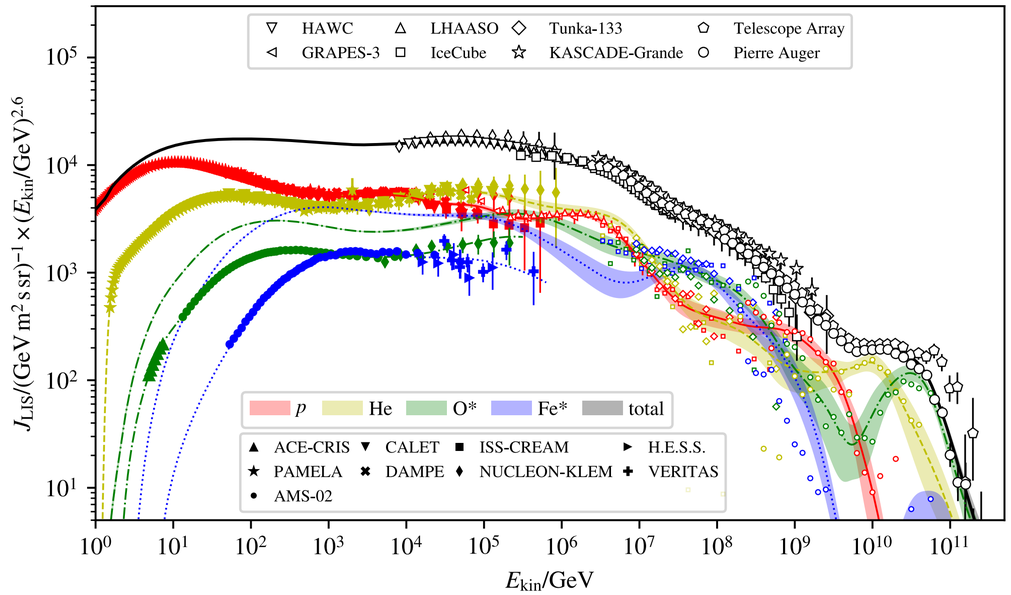

(Ahlers 2017, Halzen & Kheirandish 2022)

Assumptions have been wrong very often
but helped to make progress – new challenges

- Change of SNR paradigm imminent
- Transition to extragalactic cosmic rays at lower energy
- Waxman-Bahcall bound not applicable,
  simple multi-messenger scenario not realized
- Ultra-high energy cosmic rays and
  IceCube neutrinos come from different sources
- LHC of fundamental importance for data interpretation

(GSF, Dembinski et al. 2025)

Searching for sources at the highest energies

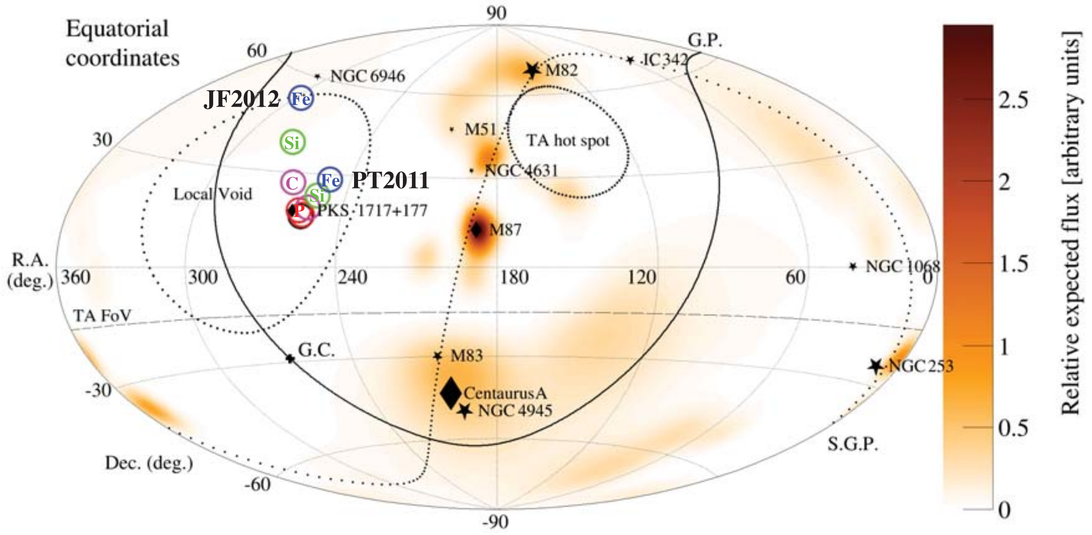

Amaterasu event (~2.4x10^{20} eV) *(TA, Science 382 (2023) 903)*

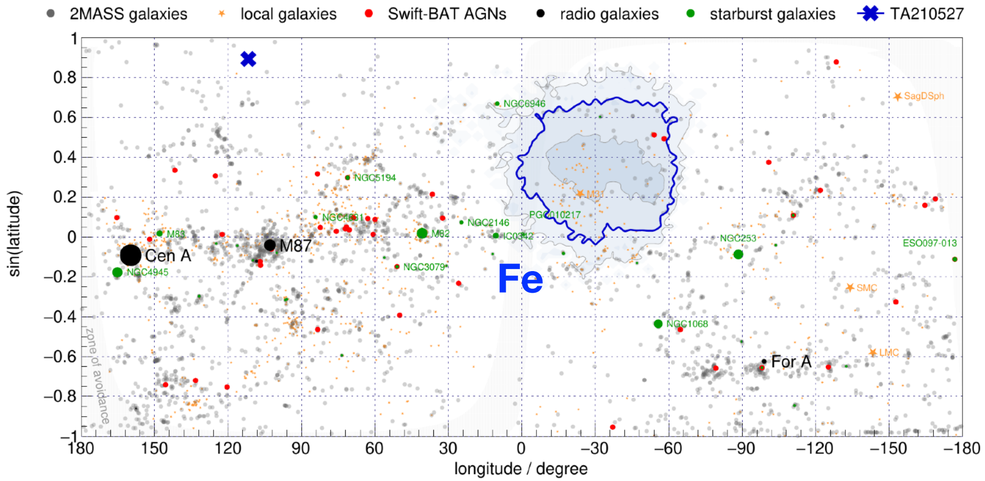

Amaterasu event (~1.7x10^{20} eV) *(Unger & Farrar, ApJ 962 (2024) L5)*

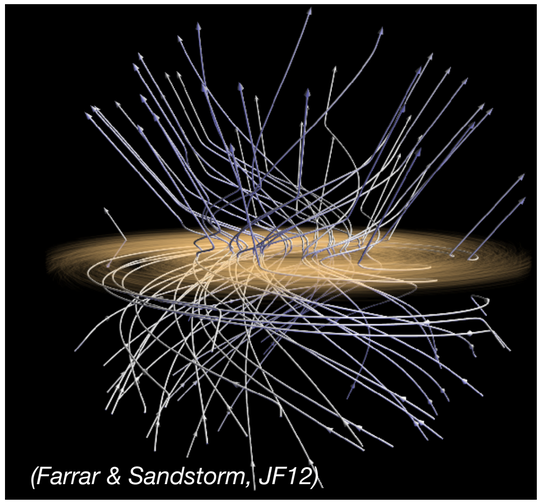

Transient sources?

Backtracking of particles through Galactic mag. field

New mag. field model UF24

(Unger & Farrar, ApJ 970 (2024) 95)

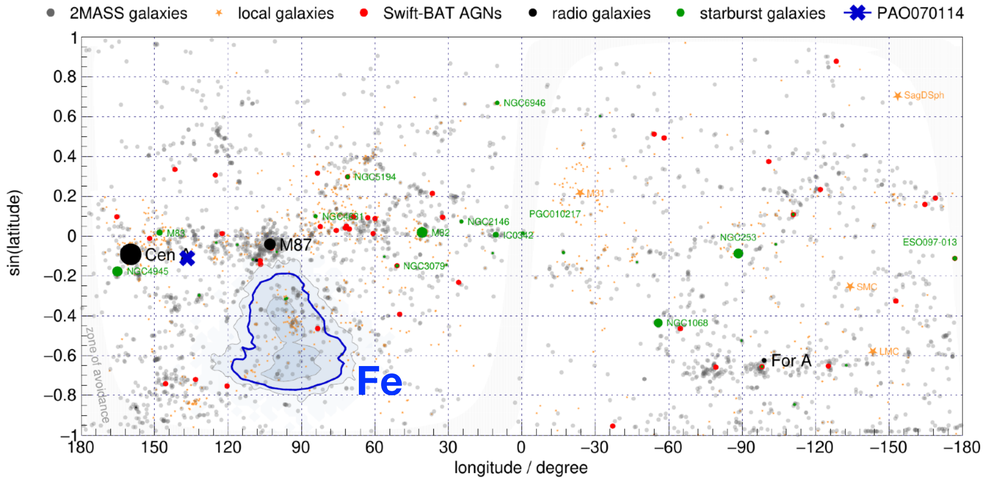

Auger highest energy event (~1.6x10^{20} eV) *(Unger UHECR 2024)*

KM3NeT – The first ultra-high energy neutrino

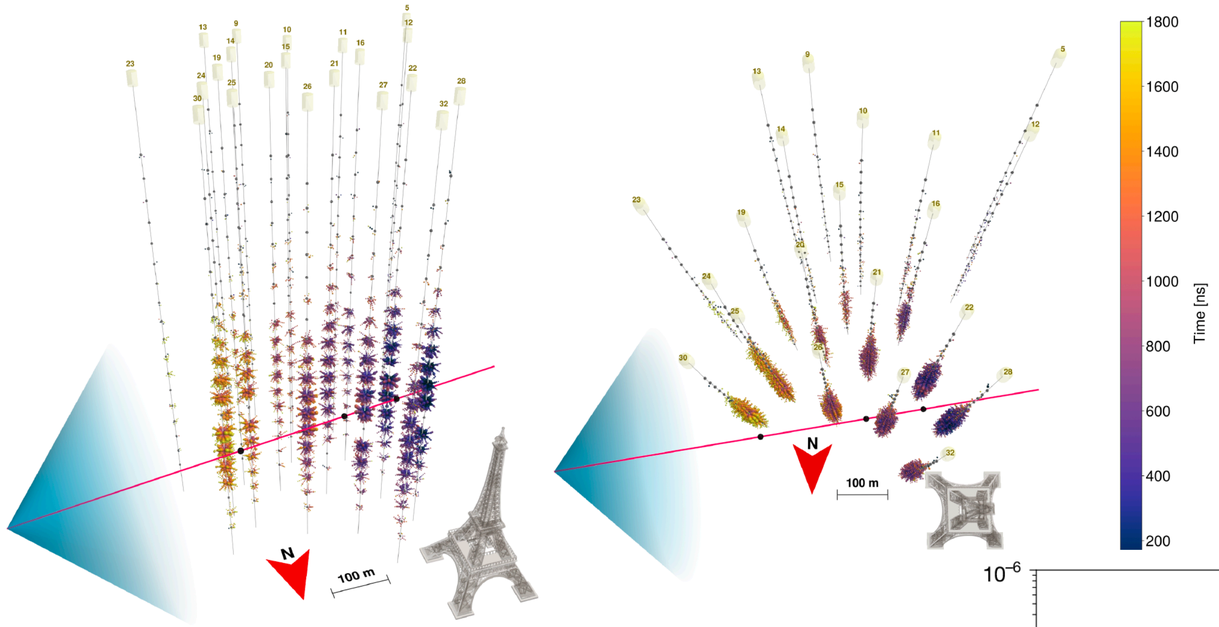

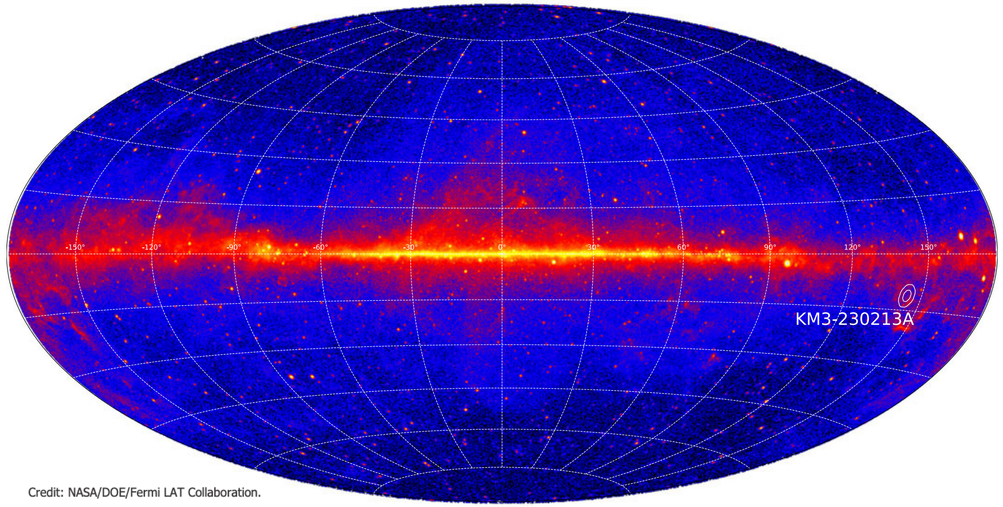

KM3-20230213A

$$E_\nu = 220^{+570}_{-110}\ \text{PeV}$$

Nature 638, (2025) 376

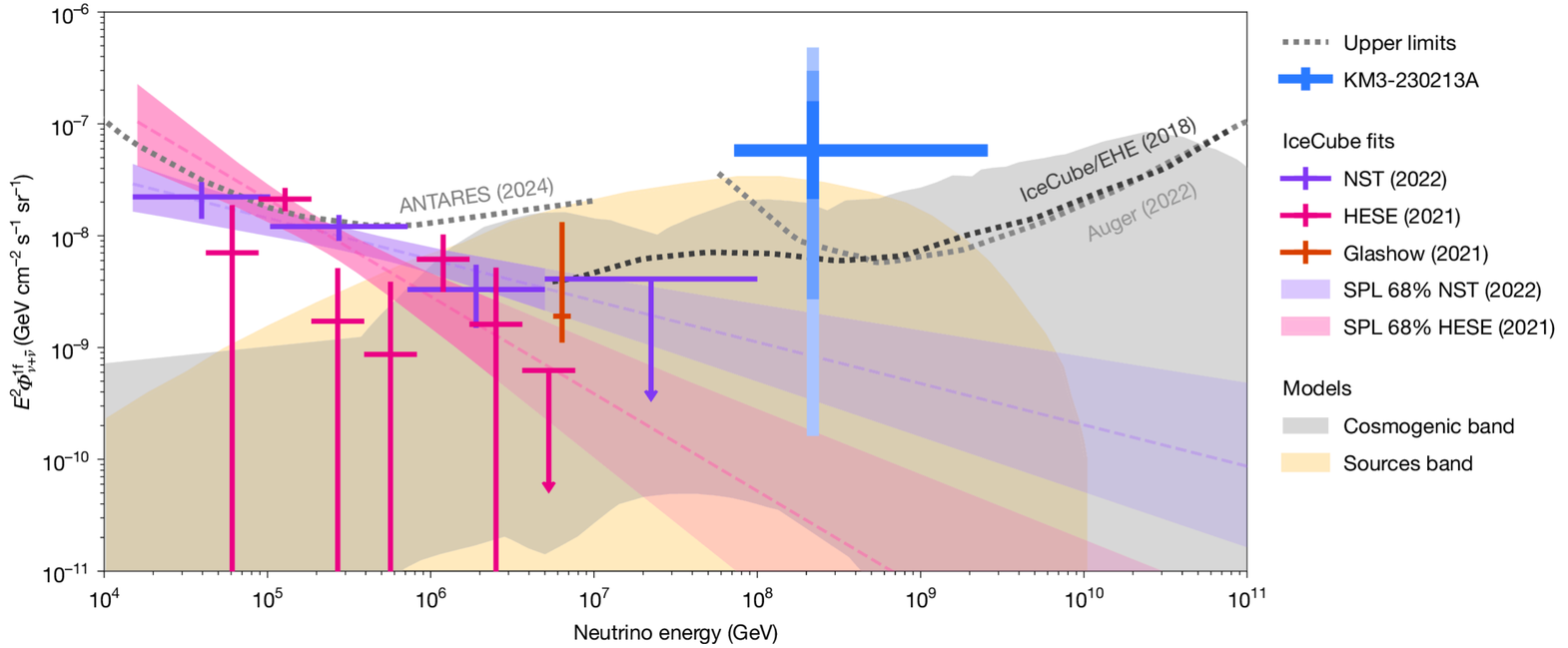

Backup slides

Galactic plane seen in neutrinos

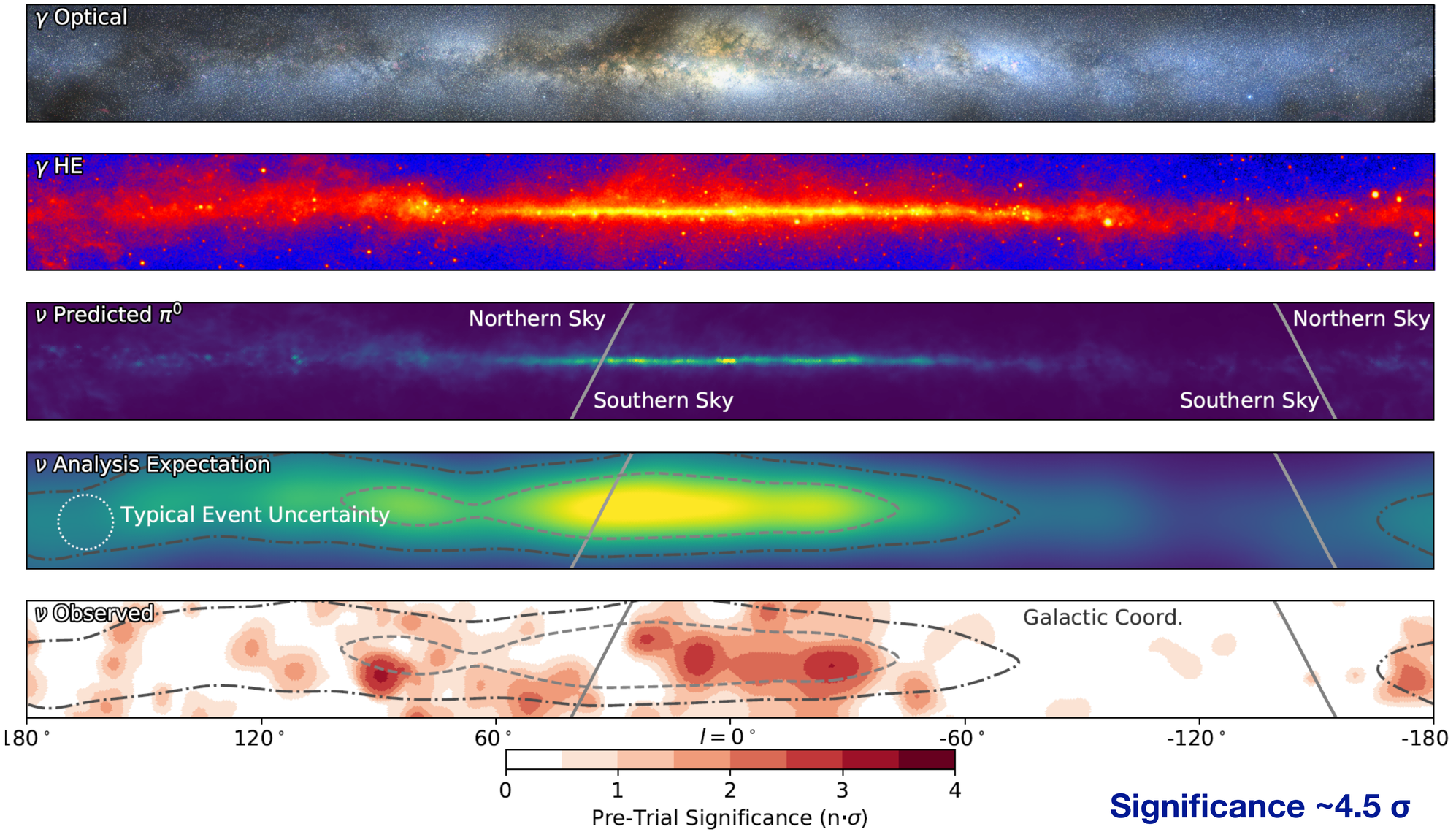

Cosmic rays interact with gas of interstellar medium

$$\pi^0 \rightarrow \gamma\,\gamma$$

$$\pi^+ \rightarrow \mu^+\,\nu_\mu$$
$$\rightarrow e^+\,\bar{\nu}_\mu\,\nu_\mu\nu_e$$

Significance ~4.5 σ

Science AAAS

IceCube, Science 380 (2023) 1338

Summary – GSF-2025 soon to be released

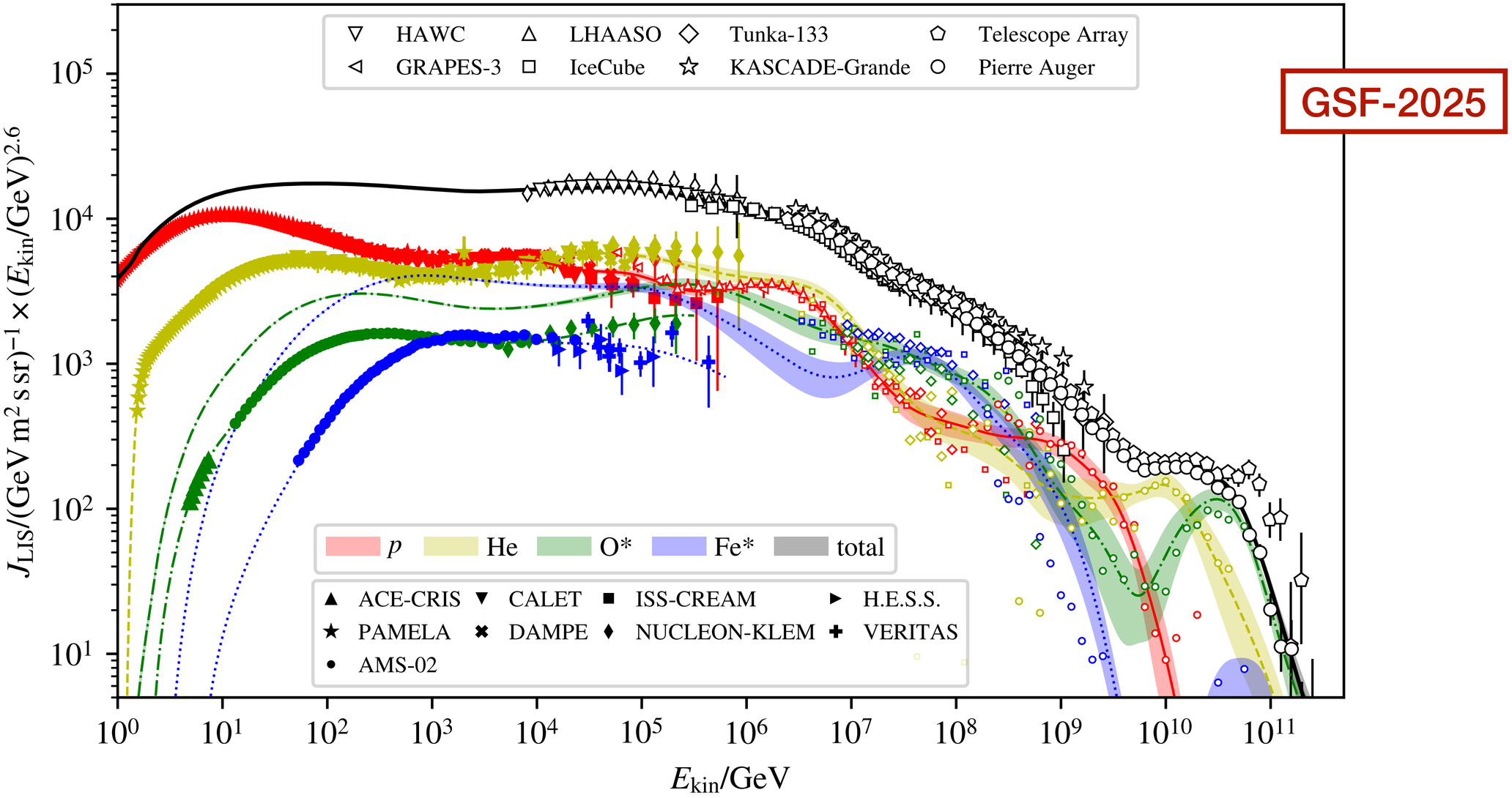

Examples of tuning interaction models to LHC data

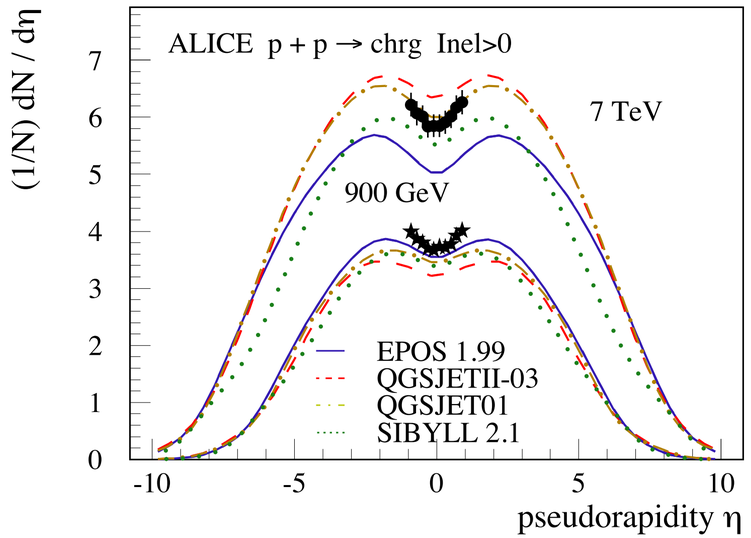

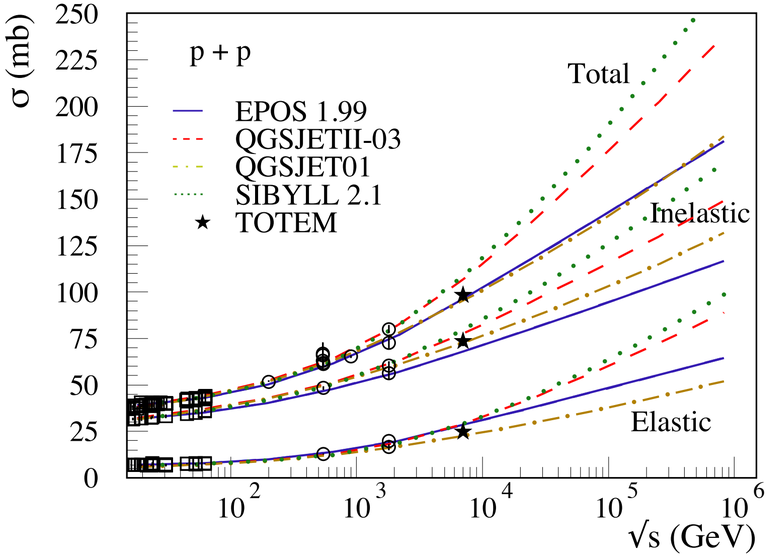

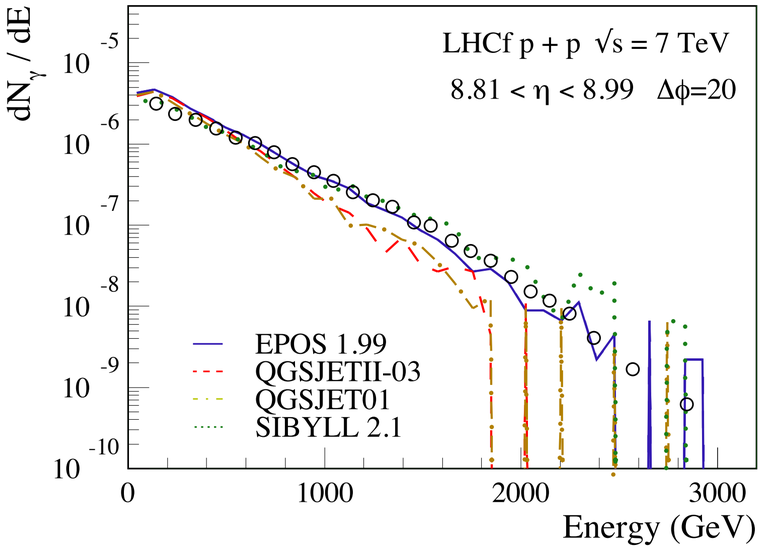

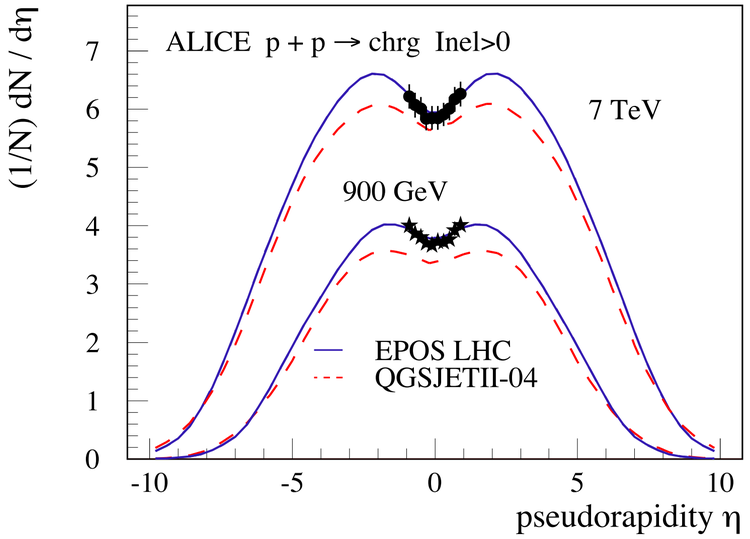

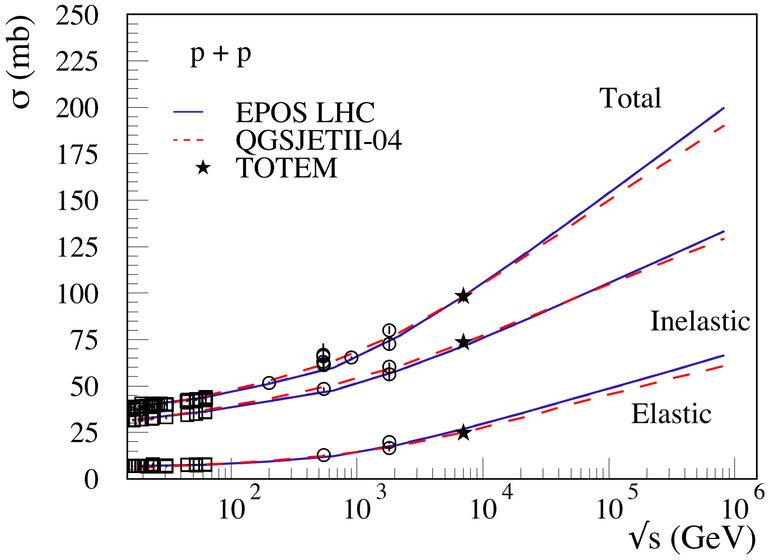

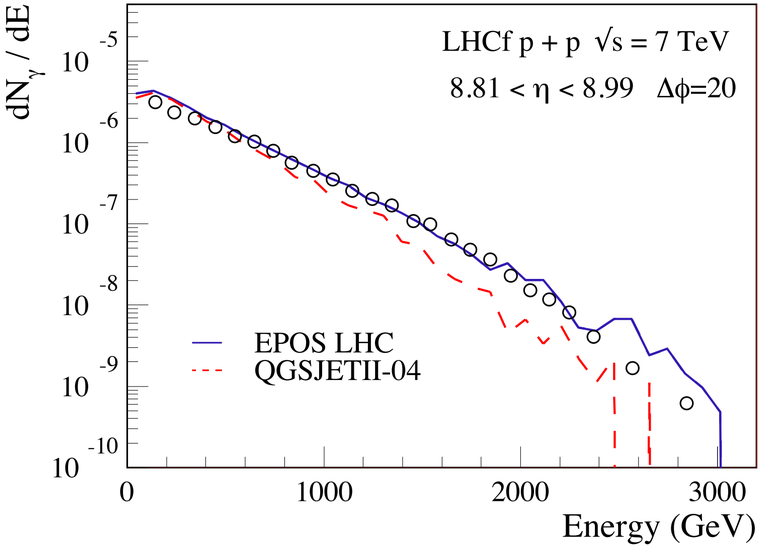

(Pierog 2013, 2014)

Mass composition and cross section measurement

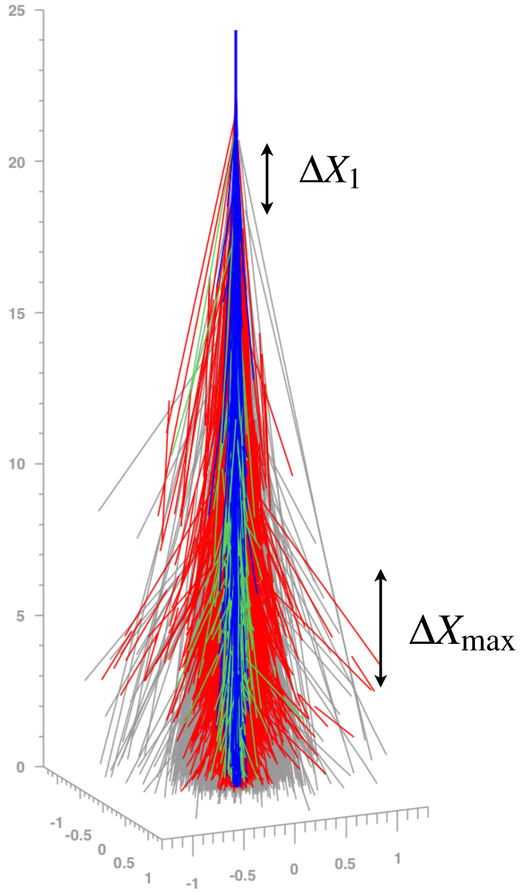

(Auger, PRL 109 (2012) 062002)

$$\frac{dP}{dX_1} = \frac{1}{\lambda_{int}} e^{-X_1/\lambda_{int}}$$

$$\sigma_{p-air} = \frac{\langle m_{air} \rangle}{\lambda_{int}}$$

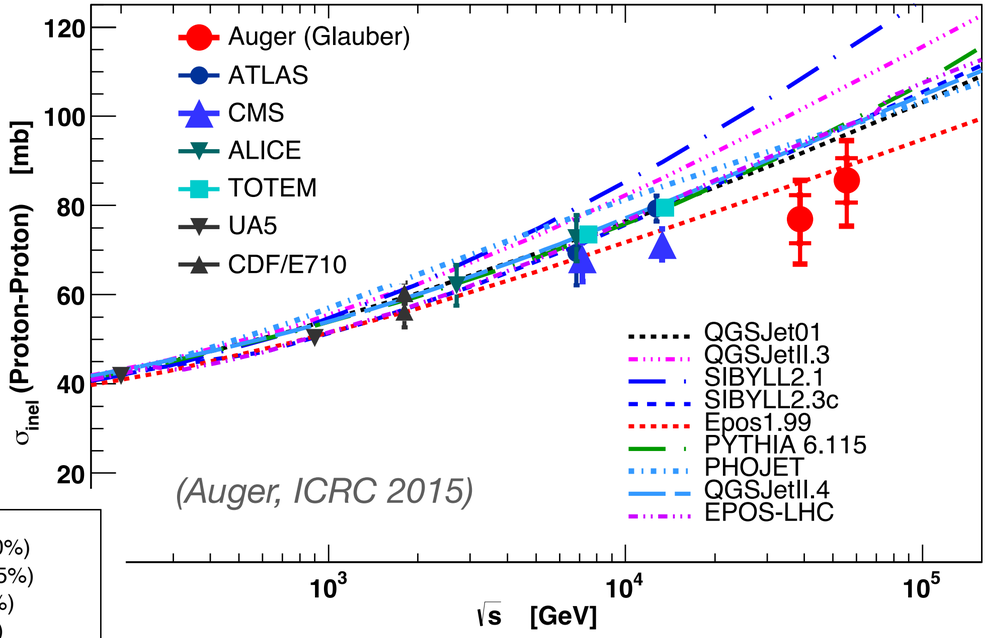

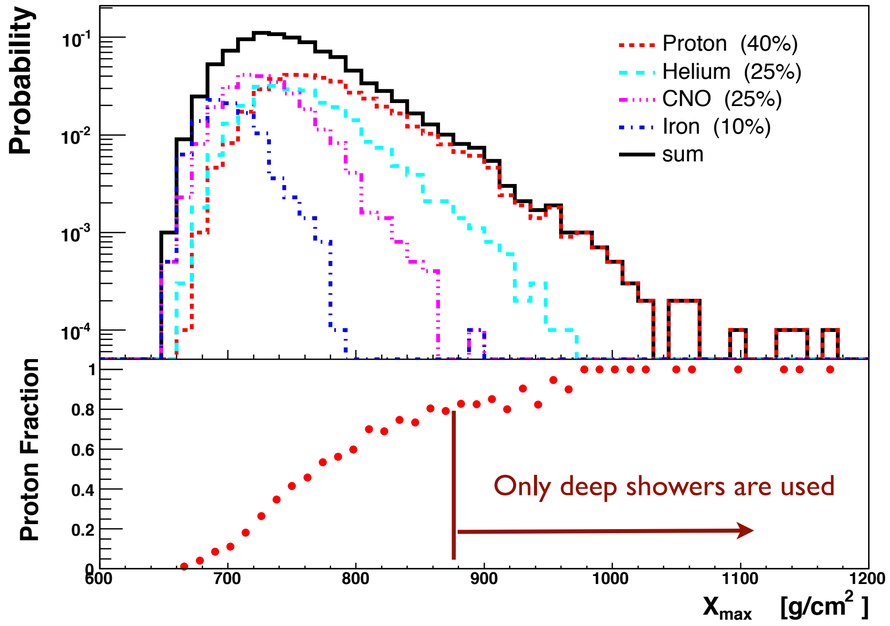

Challenges in analysis

- mass composition
- fluctuations in shower development (model needed for correction)

Elongation rates and model features

Elongation rate theorem

$$D_{10}^{\mathrm{had}} = \ln 10\, X_0 (1 - B_n - B_\lambda)$$

(Linsley, Watson PRL46, 1981)

factor ~ 87 g/cm^2

$$B_n = \frac{d \ln n_{\mathrm{tot}}}{d \ln E}$$

Large if multiplicity of high energy particles rises very fast, **zero in case of scaling**

$$B_\lambda = -\frac{1}{X_0} \frac{d\lambda_{\mathrm{int}}}{d \ln E}$$

Large if cross section rises rapidly with energy

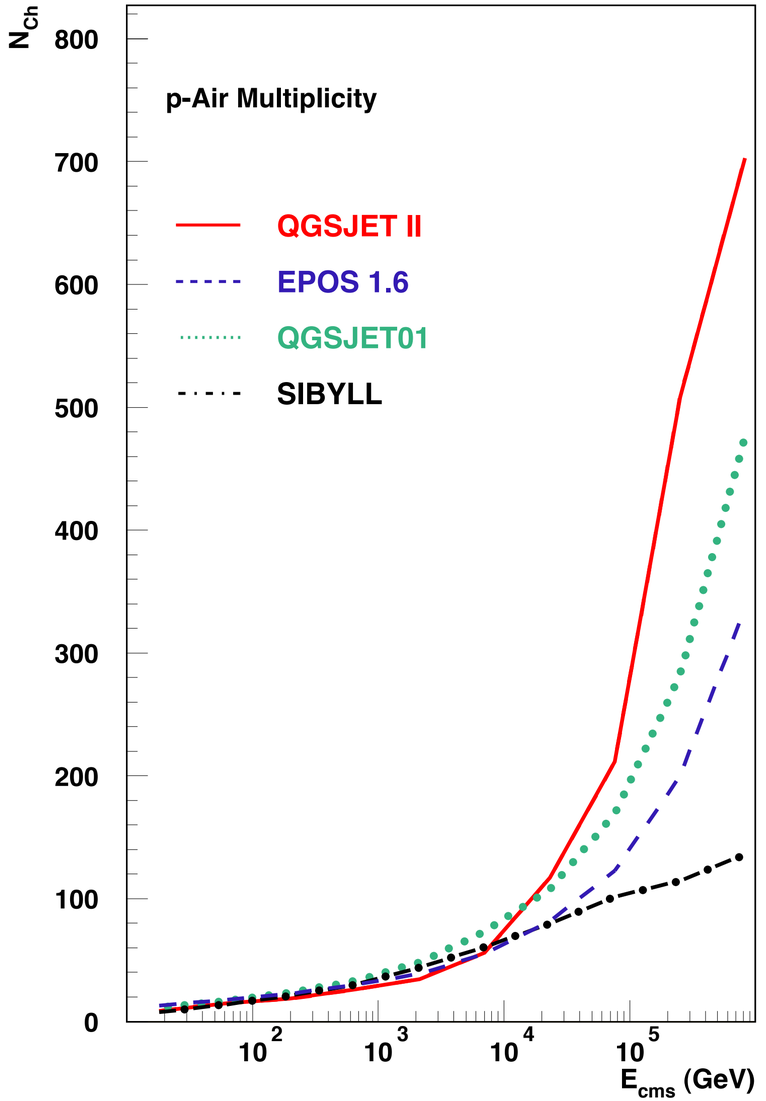

Challenge of limited phase space coverage

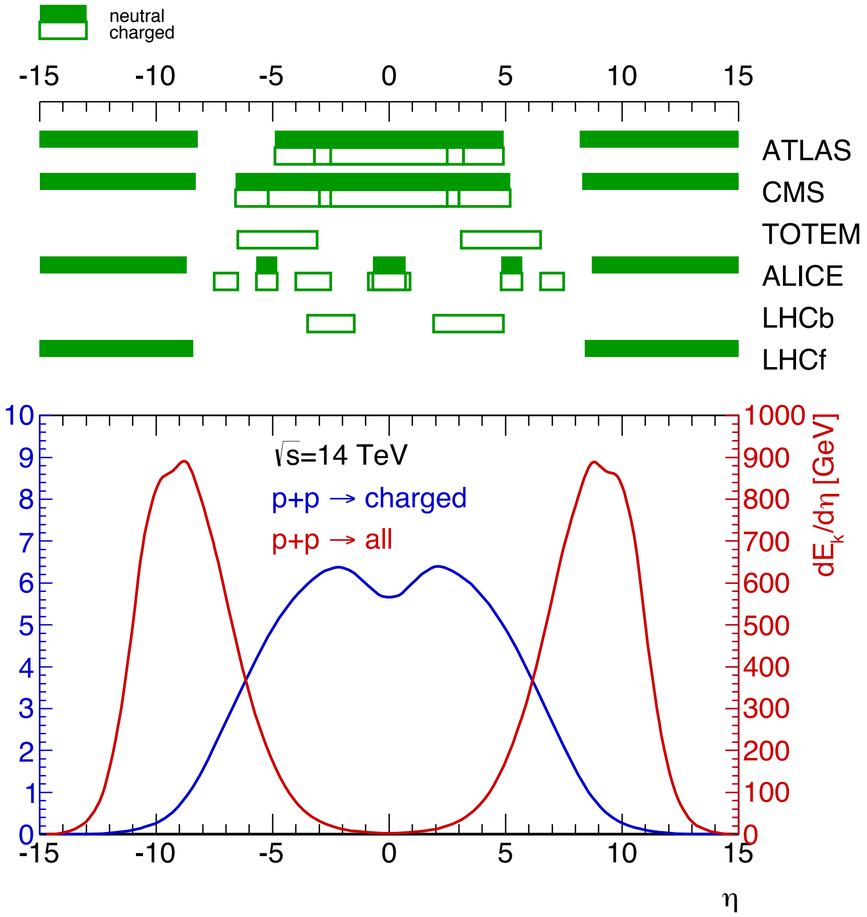

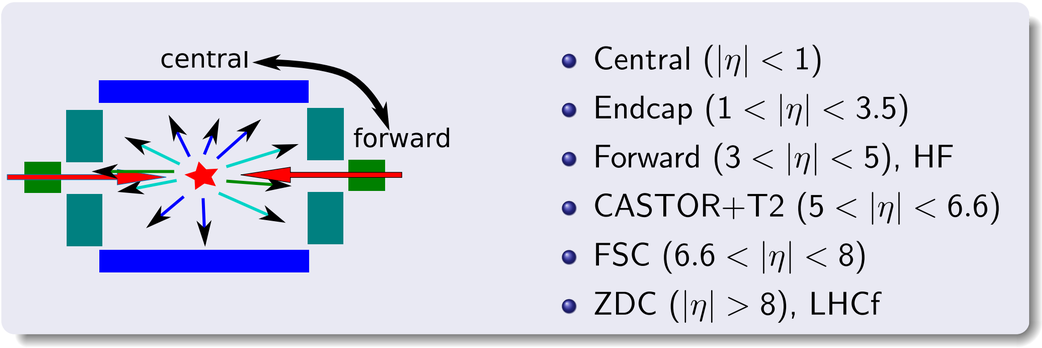

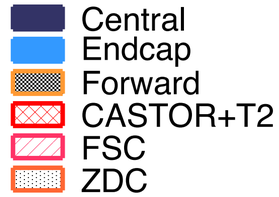

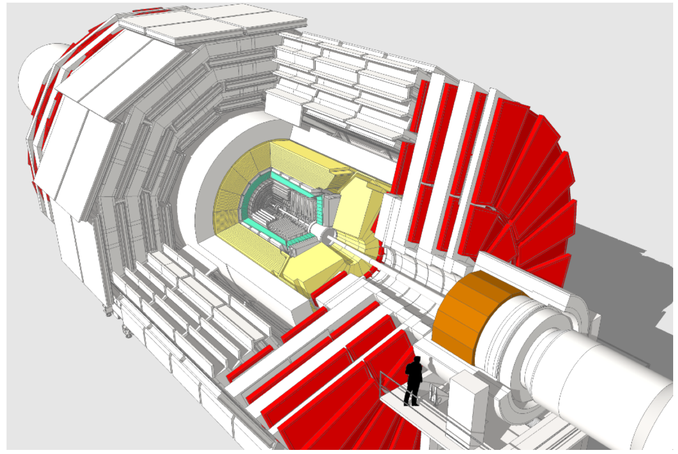

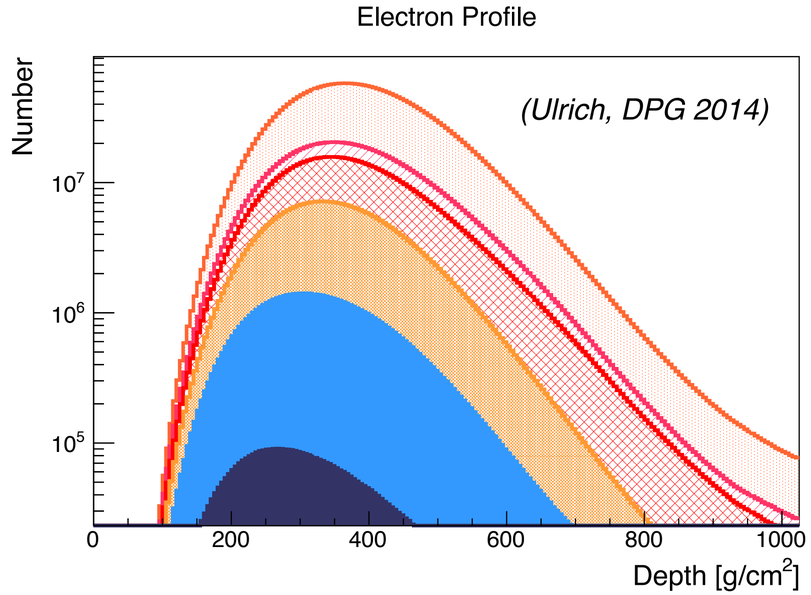

More than 50% of shower from η > 8

(Salek et al., 2014)

(data from all LHC experiments, CMS shown as example)

Mass composition from longitudinal shower profile

Depth of shower maximum as composition-sensitive observable

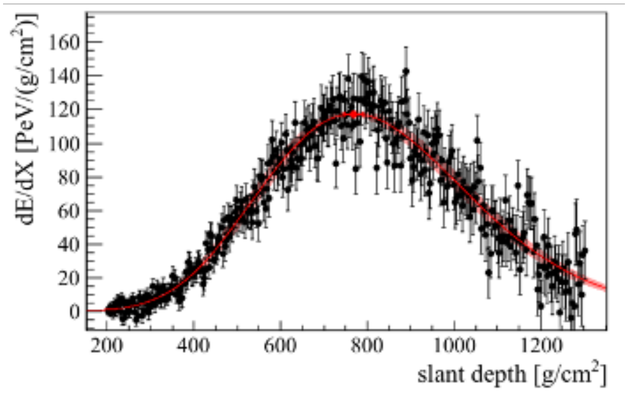

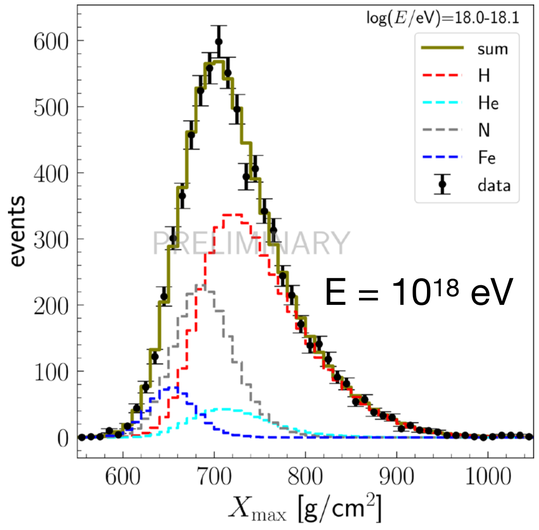

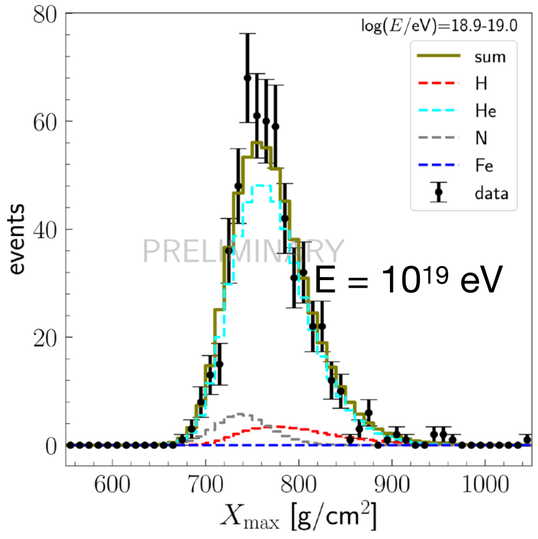

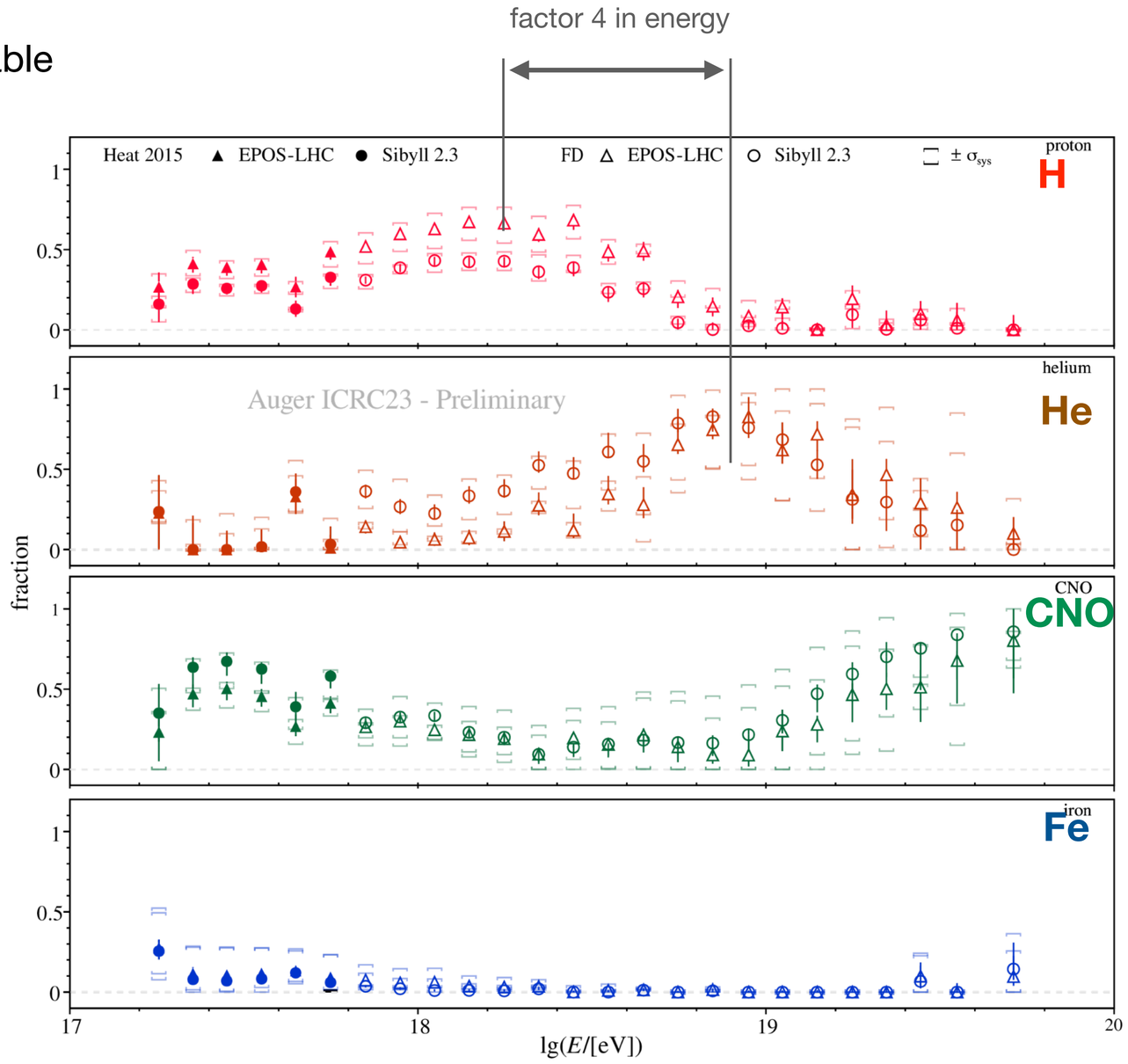

(Auger, Phys. Rev. D90 (2014), 122005 & 122005, ICRC 2023)

Auger-TA comparison of X_{max} distributions (2022)

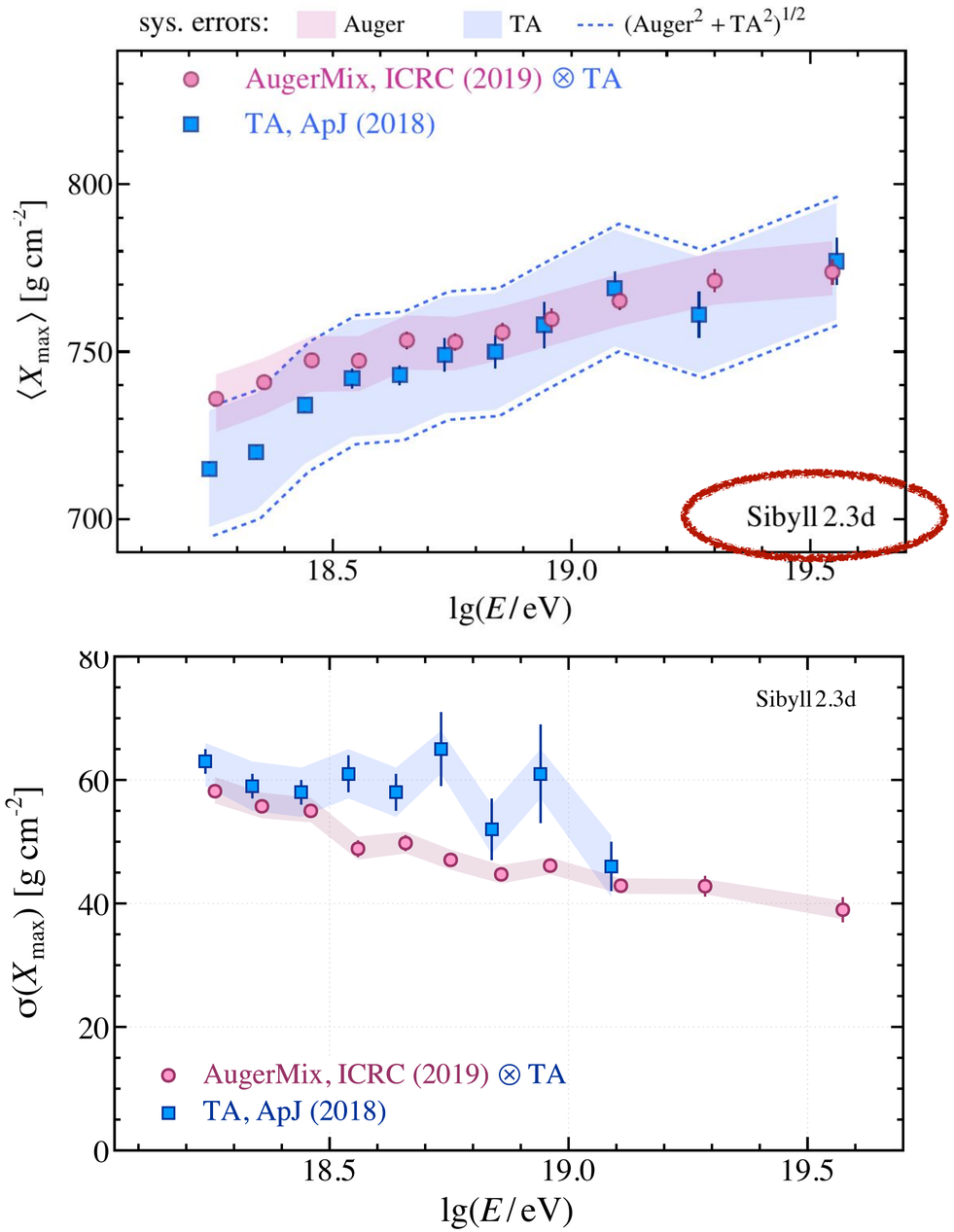

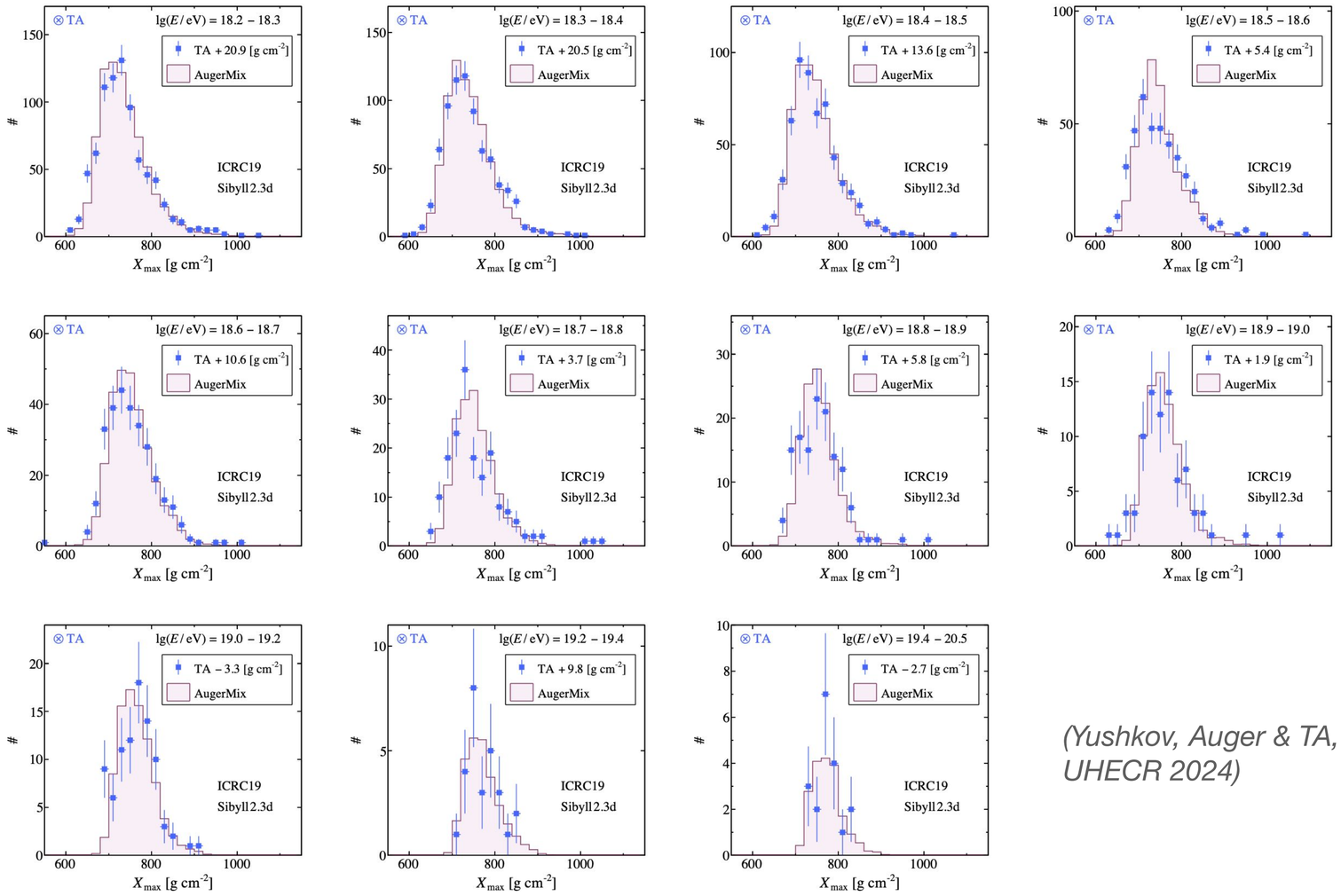

(Yushkov, Auger & TA, UHECR 2024)

Joint working group: no significant difference found

Latest mass composition results of TA

(TA, Gerber, ICRC 2025)

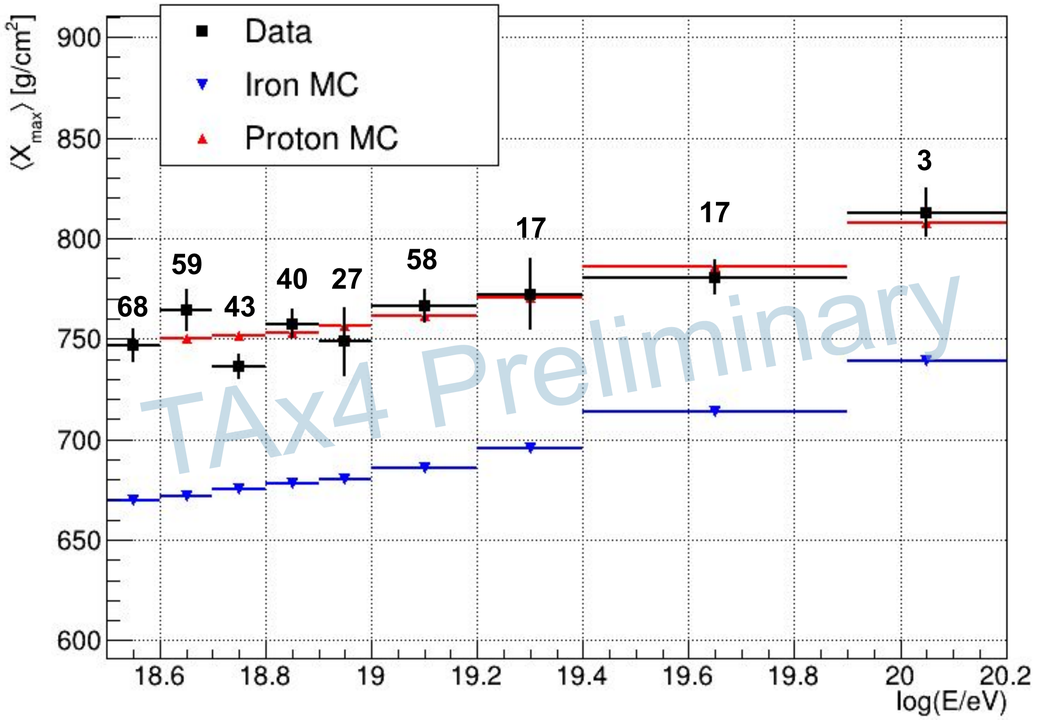

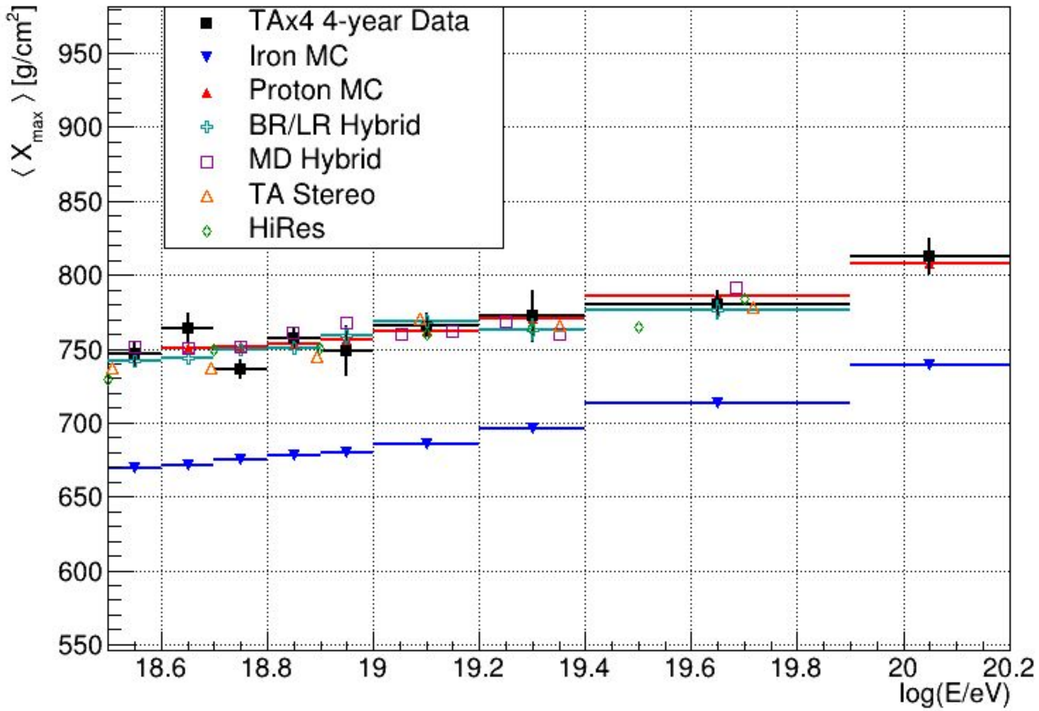

TA data compatible with 100% protons (if QGSjet II.03 is used)
Data compatible with previous TA data and, hence, Auger results

Importance of field-of-view effects and interaction model

(TA, Gerber, ICRC 2025)

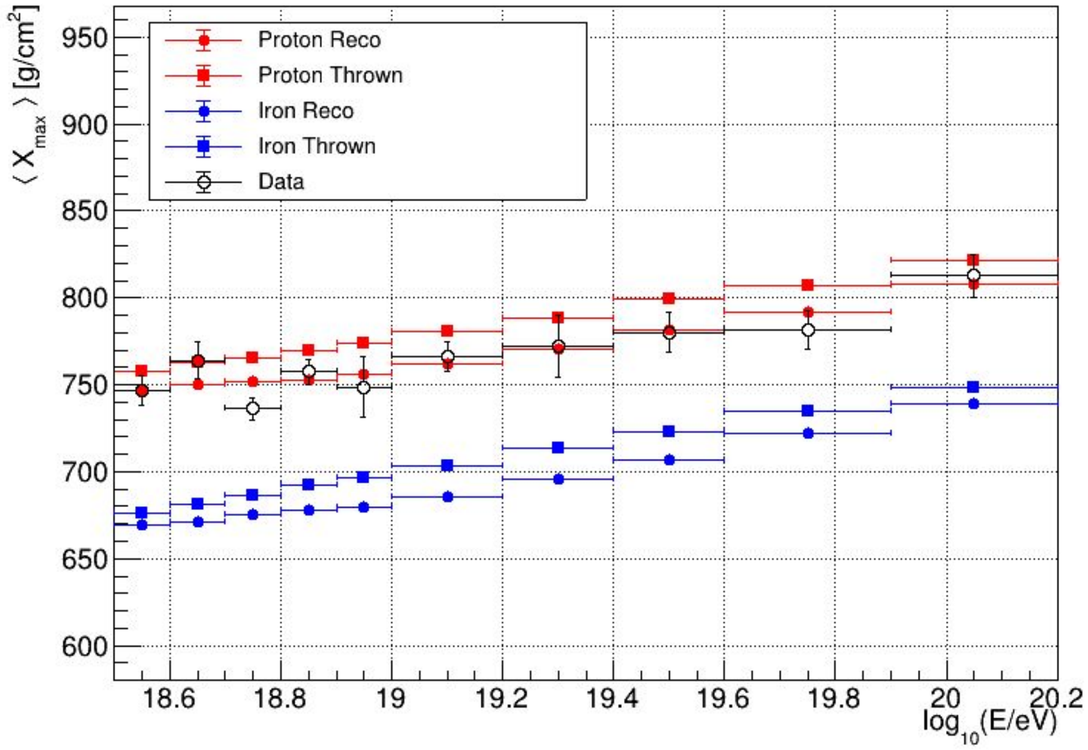

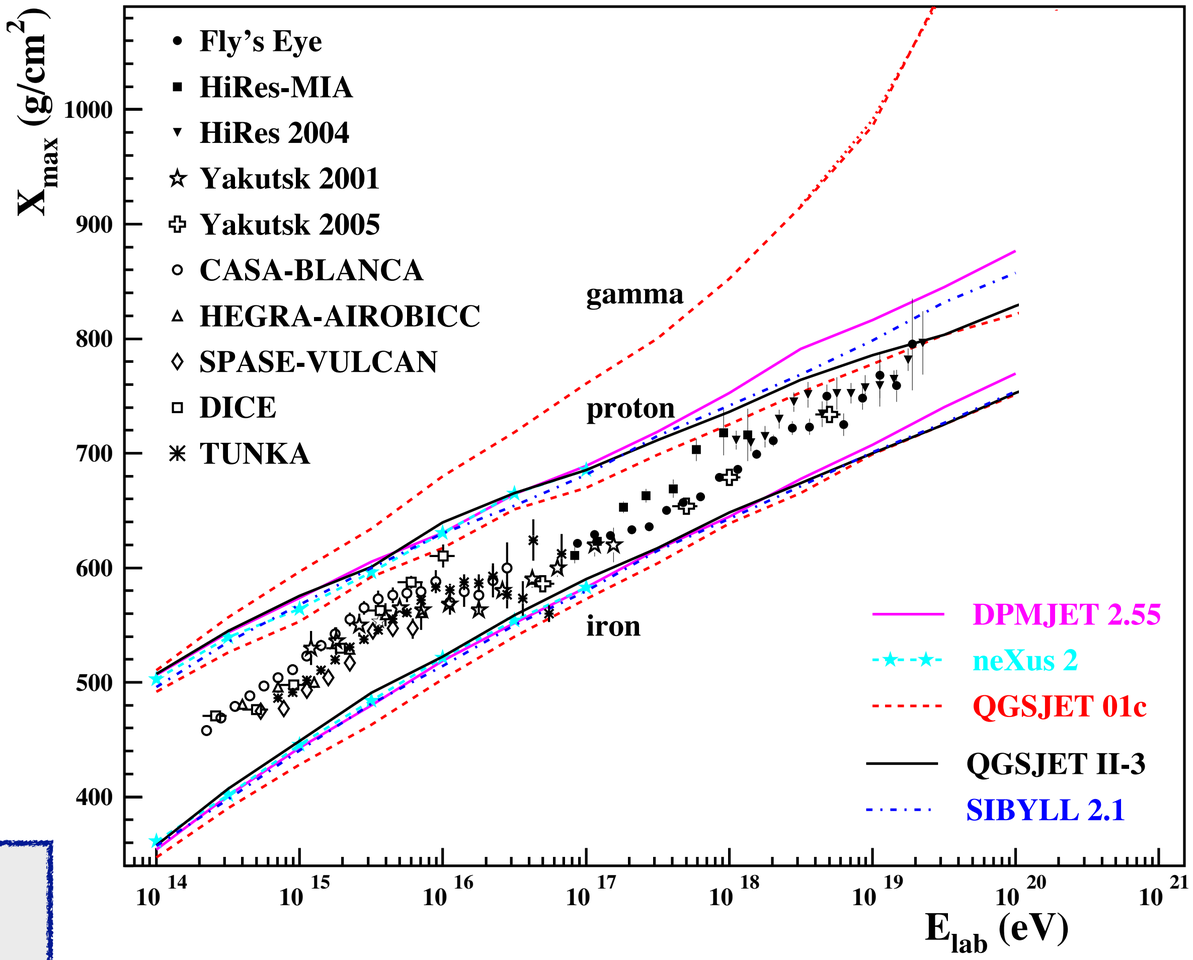

TA data compatible with 100% protons (QGSjet II.03)
Plot with models from 2006, pre-LHC model version

Auger muon measurement – vertical showers

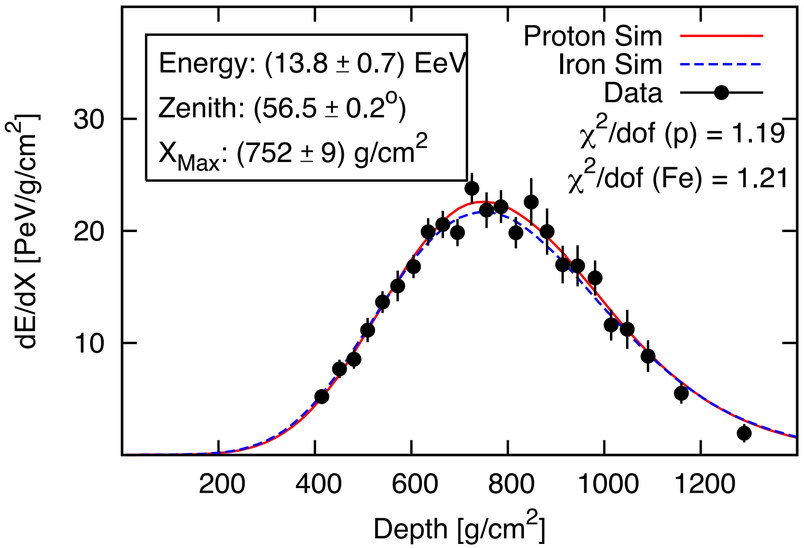

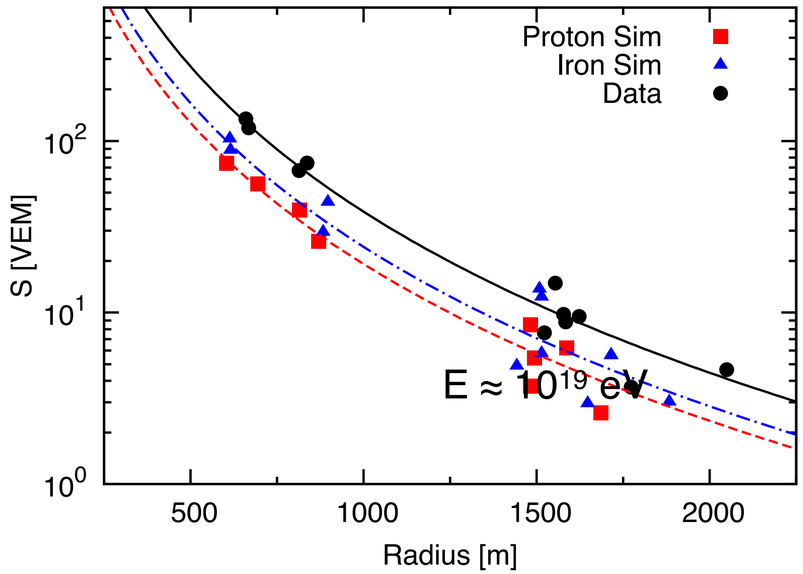

(Auger, PRL 117, 2016)

Energy scaling: em. particles and muons

Muon scaling: hadronically produced muons and muon interaction/decay products

Use showers of different zenith angles

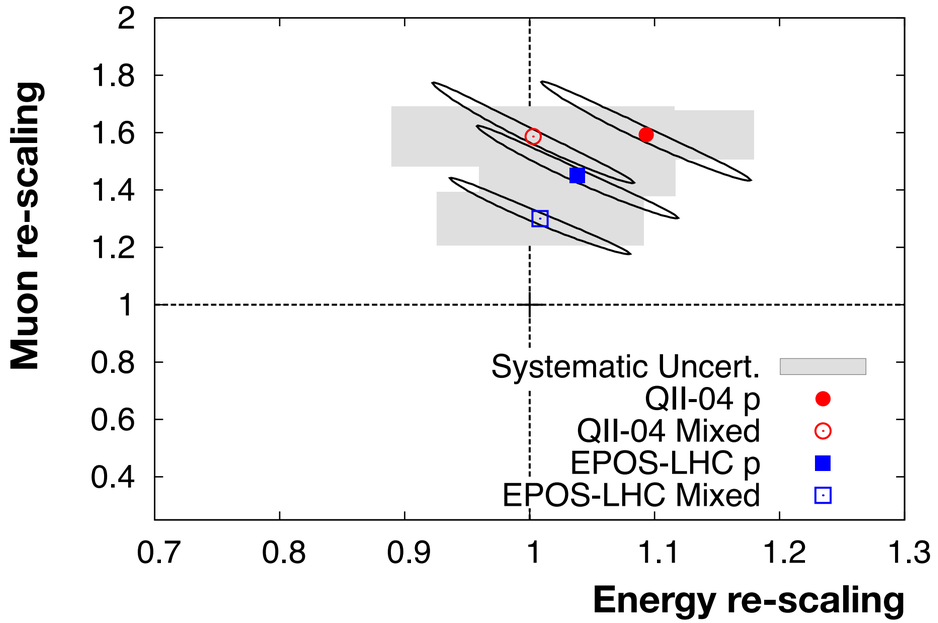

Consistently more muons in data than predicted

The muon problem in ultra-high energy showers

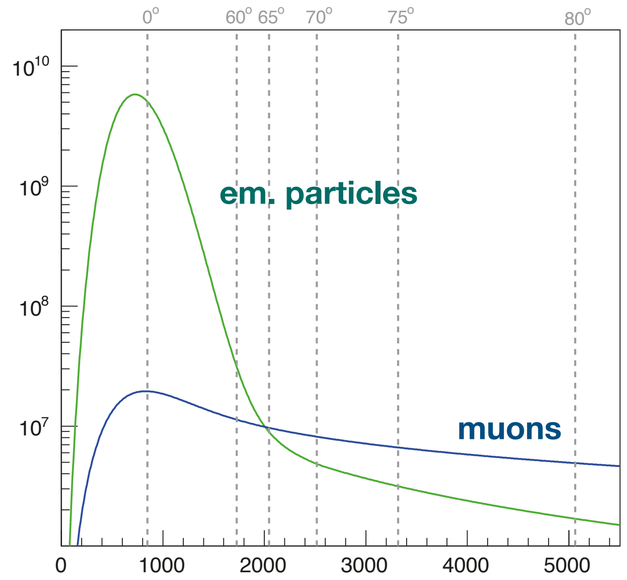

Hybrid events and inclined showers

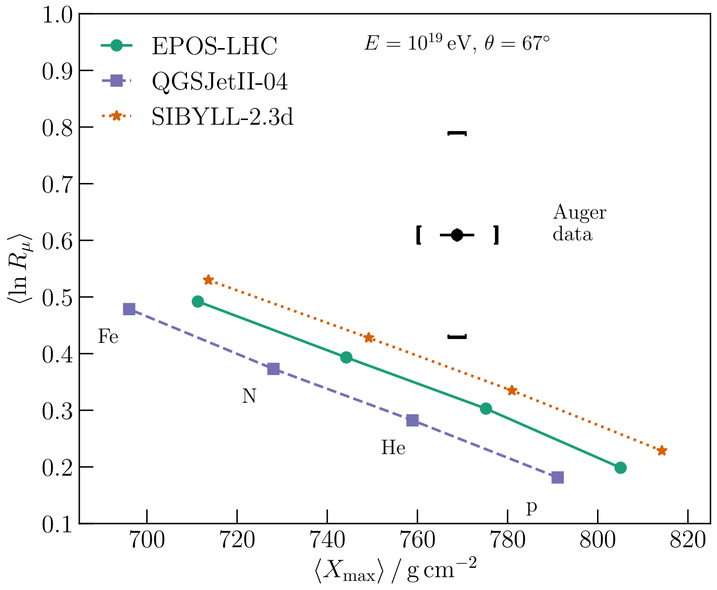

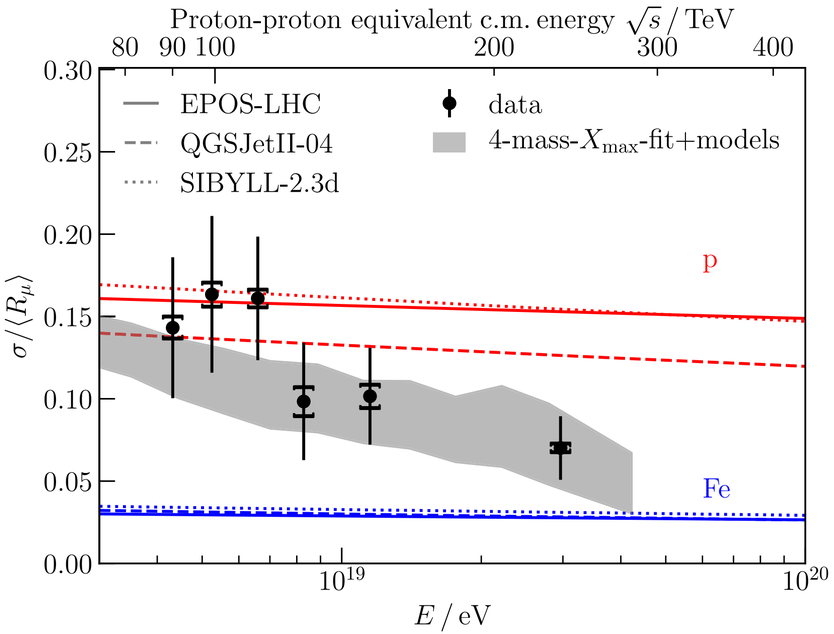

(Phys. Rev. Lett. 117 (2016) 192001, Phys. Rev. D91 (2015) 032003)

Muon counters and vertical showers

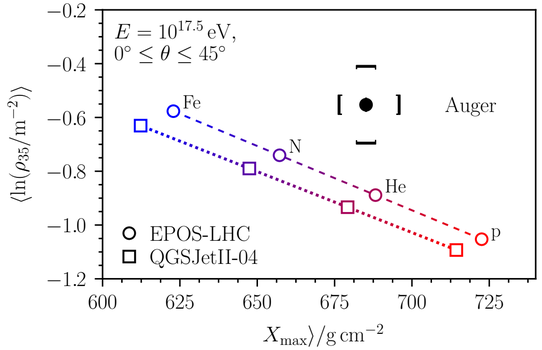

(Eur. Phys. J. C80 (2020) 751)

Discrepancy in number of muons

Relative fluctuations in agreement

PMT analogy of air shower

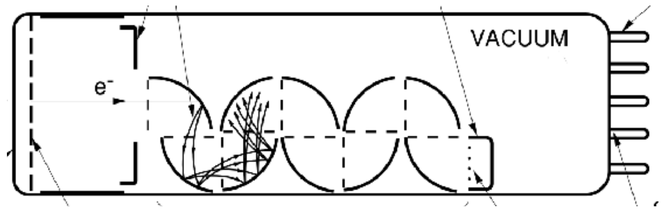

Muon fluctuations driven by first interactions

(Phys. Rev. Lett. 126 (2021) 152002)

Surface detector data and machine learning

Simulated signal of one surface station

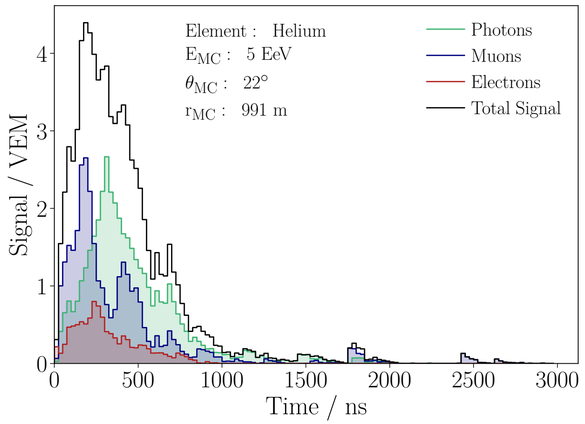

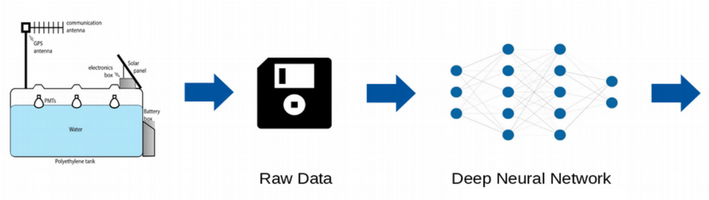

Reconstructing Xmax with DNNs: ultimate check with hybrid data

(Auger, JINST 16 (2021) P07019)

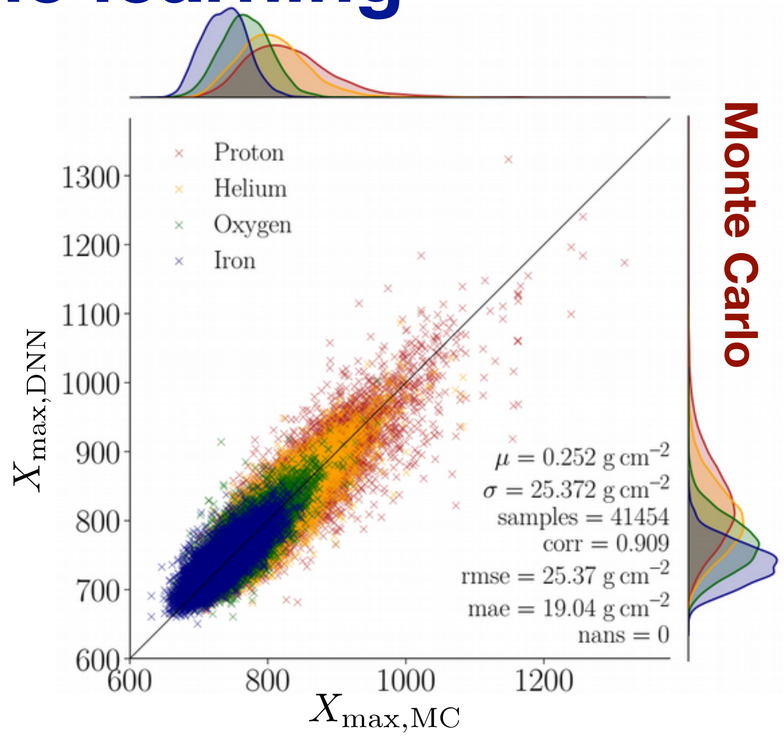

Monte Carlo

Difference in mean Xmax

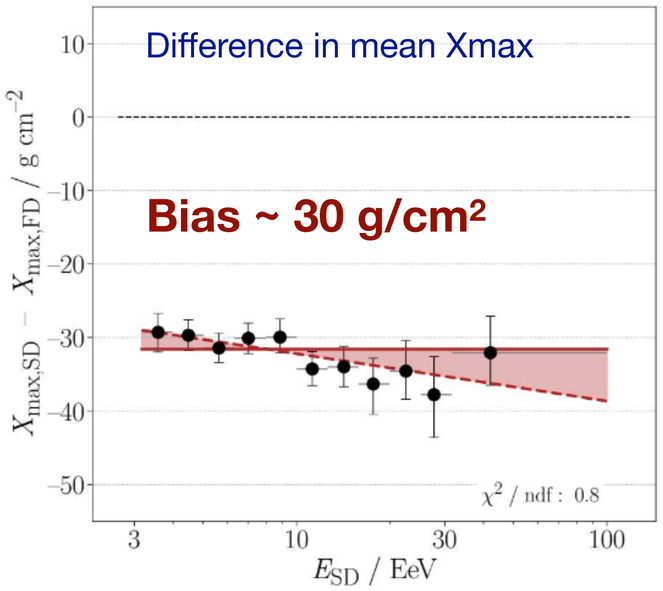

Shower-by shower Xmax resolution

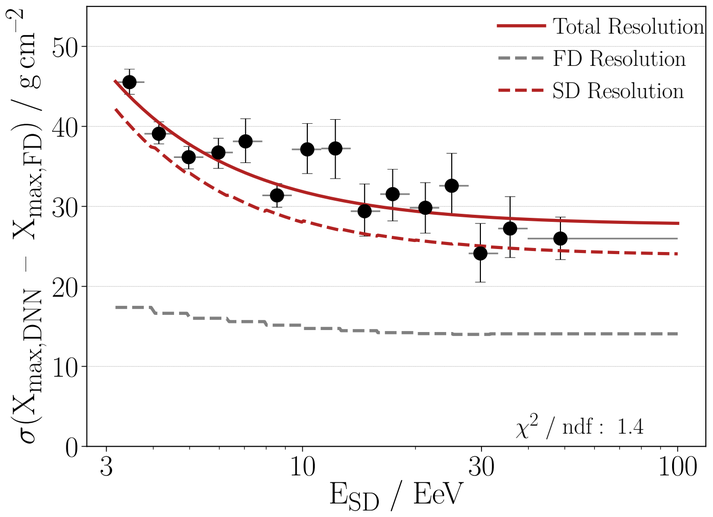

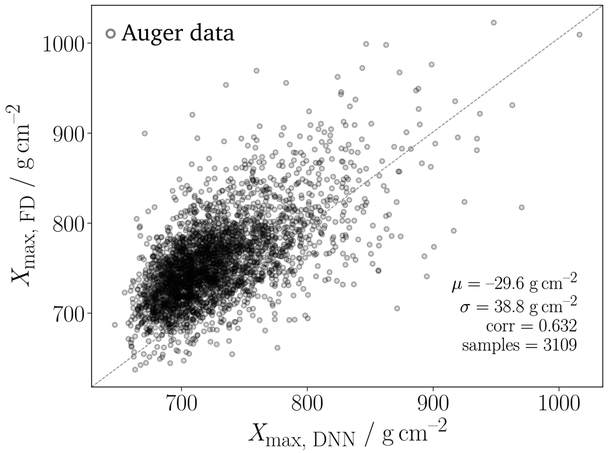

Hybrid data

Muon production depends on hadronic energy fraction

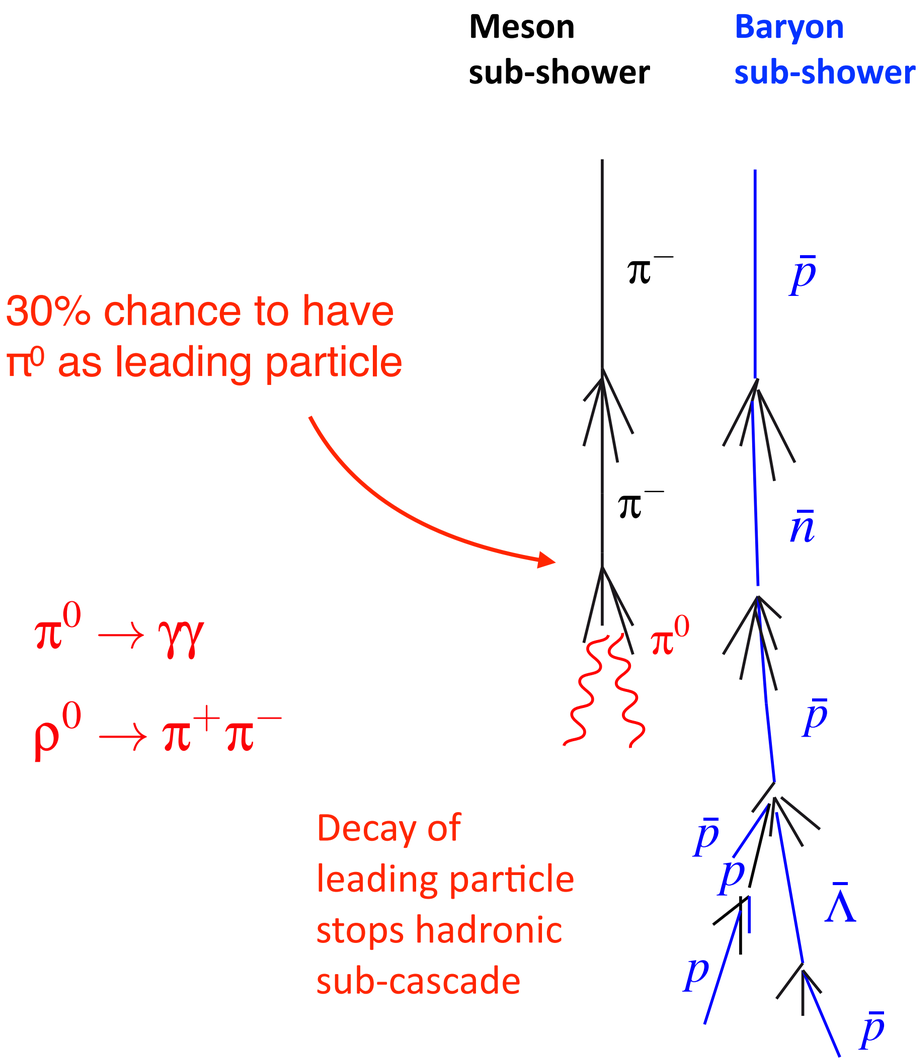

1 Baryon-Antibaryon pair production *(Pierog, Werner 2008)*

- Baryon number conservation
- Low-energy particles: large angle to shower axis
- Transverse momentum of baryons higher
- Enhancement of mainly **low-energy** muons

(Grieder ICRC 1973; Pierog, Werner PRL 101, 2008)

2 Enhanced kaon/strangeness production *(Anchordoqui et al. 2022)*

- Similar effects as baryon pairs
- Decay at higher energy than pions (~600 GeV)

3 Leading particle effect for pions *(Drescher 2007, Ostapchenko 2016)*

- Leading particle for a π could be ρ^0 and not π^0
- Decay of ρ^0 to 100% into two charged pions

4 New hadronic physics at high energy *(Farrar, Allen 2012, Salamida 2009)*

- Inhibition of π^0 decay (Lorentz invariance violation etc.)
- Chiral symmetry restauration

Several of these effects: Core-Corona model (Pierog et al.)

Sensitivity of individual observables

Zenith angle

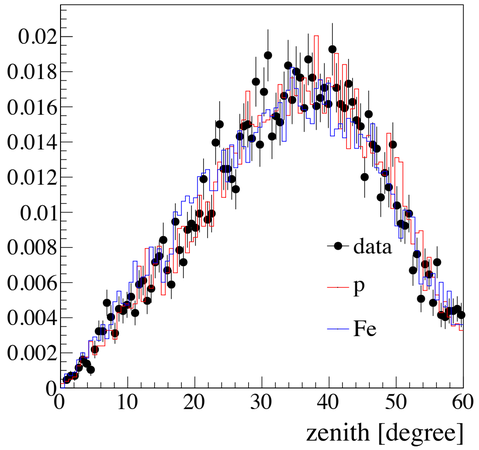

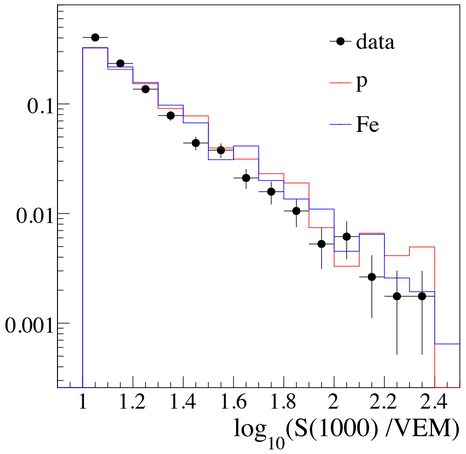

Core distance to closest station (FD)

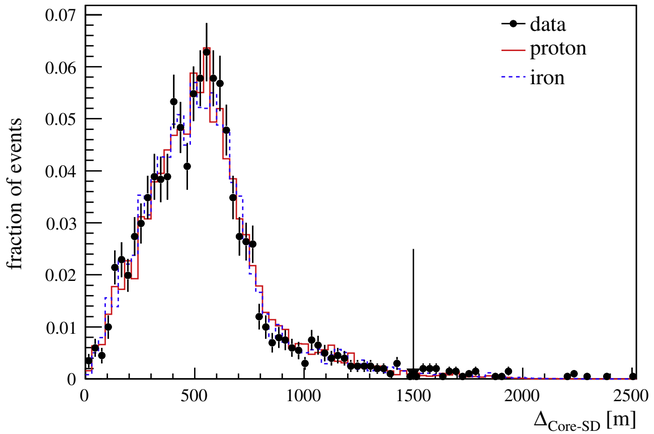

Distance of triggered stations

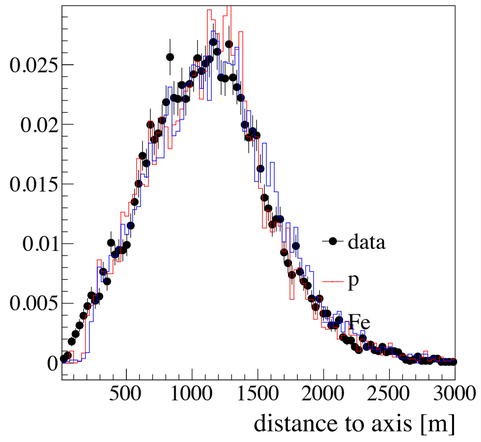

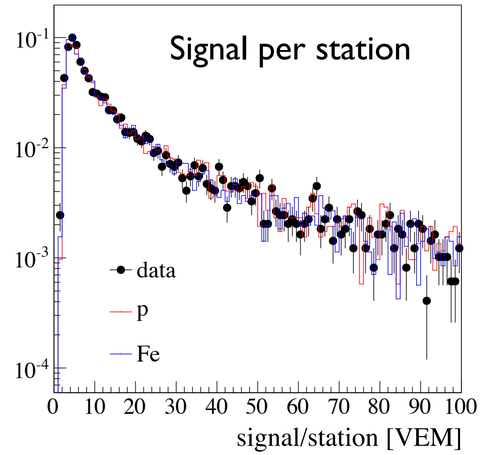

Zenith angle (FD, fluorescence data)

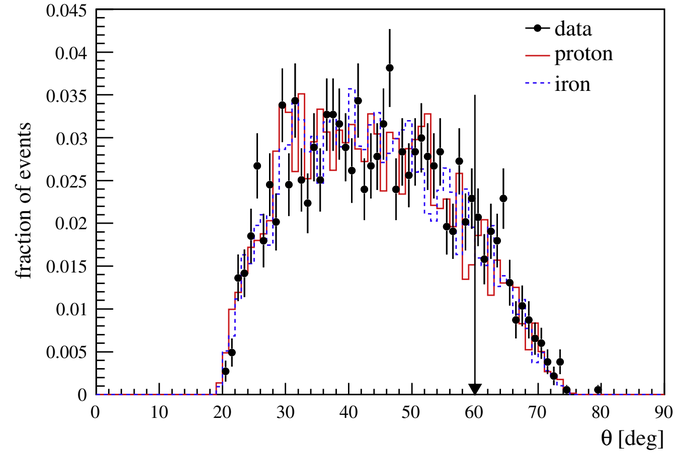

(Auger, Astropart. Phys. 34, 2011)

Data appear fully compatible with MC simulations if only one observable is considered